



ABS Consulting

AN ABS GROUP COMPANY

West Fertilizer Incident Support Services Final Report

U.S. Chemical Safety Board Order No. CSB-15-0022


ABSG Consulting Project No. 3087473

Prepared for:



Prepared by:

ABSG Consulting Inc.
140 Heimer Rd, Suite. 300
San Antonio, TX 78232

For the Public Release version, For Official Use Only (FOUO) data has been redacted and is represented as a solid black bar 

28 August 2015

• ABSG Consulting Inc. • 140 Heimer Rd., Suite 300, San Antonio, TX 78232 USA •
• Tel: 1-210-495-5195 / Fax: 1-210-495-5134 • www.absconsulting.com •

CSB Disclaimer:

The CSB West Fertilizer Company Fire and Explosion investigation report addressed ammonium nitrate as fertilizer grade (FGAN) throughout, and though our contractor did not make a similar distinction, no inference should be presumed regarding the way the material was characterized in this report.

Project No:		3087473			
Project:		West Fertilizer Investigation Support Services			
Client:		U.S. Chemical Safety Board			
Quality Assurance:		x ISO 9001 Program (QMS)			
Client Order No:		CSB-15-0022			
References:		See list of references (Section 6)			
Attachments:		As noted in Table of Contents			
Total Number of Pages (Including Cover Sheet):			210		
Revision Number	Approval Date	Description of Revision	Originator(s)	Checker	Approver
0	02-Apr-14	Original Issue	<i>B. Harrison M. Weinberg N. Duran C. Vergara</i>	<i>B. Harrison M. Weinberg</i>	<i>D. Barker</i>
1	28-Aug-15	Revised For Public Release	<i>B. Harrison M. Weinberg</i>	<i>B. Harrison M. Weinberg</i>	<i>D. Barker</i>

Table of Contents

List of Tables	iv
List of Figures	v
Definitions	ix
1 Background	1-1
1.1 West Fertilizer Co Ammonium Nitrate Properties.....	1-6
1.2 West Fertilizer Co Environmental Conditions.....	1-6
2 Literature Survey	2-1
2.1 Term Disambiguation.....	2-1
2.2 Historical AN Incidents.....	2-3
2.3 Ammonium Nitrate	2-7
2.3.1 General Properties.....	2-7
2.3.2 Decomposition	2-7
2.3.3 Sensitivity and Energy Output	2-8
2.3.3.1 Factors of Interest for Sensitivity and Energy Output.....	2-9
2.3.3.1.1 Physical Properties.....	2-9
2.3.3.1.2 Composition	2-9
2.3.3.1.3 Environmental Factors	2-10
2.3.3.2 Sensitivity.....	2-10
2.3.3.3 Energy Output.....	2-15
2.3.4 Summary	2-25
3 Field Investigation.....	3-1
3.1 West Fertilizer.....	3-2
3.1.1 Anhydrous Ammonia Tanks	3-11
3.2 Community Structures and Facilities	3-14
3.2.1 Rest Haven Nursing Home	3-15
3.2.2 Park	3-24
3.2.3 West Intermediate School	3-27
3.2.4 West High School	3-38

3.2.5	West Middle School	3-50
3.3	Residences	3-57
3.3.1	Single Family Residences	3-57
3.3.2	Apartment Complex.....	3-61
4	Computational Fluid Dynamics Simulation	4-1
4.1	Computational Fluid Dynamics.....	4-1
4.2	CFD vs. Blast Curve Analysis.....	4-1
4.3	Computer Aided Design (CAD) Representation of West	4-3
4.4	Computational Explosion & Blast Assessment Model (CEBAM).....	4-6
4.5	Explosive Size	4-6
4.6	Modeling Explosion.....	4-7
5	Blast Damage Indicator Analysis.....	5-1
5.1	Preliminary Estimate of Explosive Yield.....	5-1
5.1.1	Lightweight Metal Buildings	5-1
5.1.1.1	Observed Damage	5-4
5.1.2	Basketball Goals.....	5-6
5.1.3	Apartment Complex and Nursing Home.....	5-10
5.2	3-D Model of West Community	5-17
5.2.1	Model Methodology	5-17
5.2.2	Single Family Residences	5-20
5.2.3	Community Structures	5-24
5.2.3.1	West Intermediate School.....	5-24
5.2.3.2	West High School.....	5-29
5.2.3.3	West Middle School.....	5-30
5.3	Final Estimate of Explosive Yield Utilizing 3D Model of West	5-31
6	Findings.....	6-1
7	References.....	6-1
Appendix A	Community Structure Damage Survey Summary.....	A-1

List of Tables

Table 1. West Fertilizer Co Ammonium Nitrate Properties [□]	1-6
Table 2. Reported Historical Incidents Involving Ammonium Nitrate	2-4
Table 3. Ammonium Nitrate Decomposition Reactions	2-8
Table 4. Detonation Results for Heated AN from Different Bullet Impacts	2-15
Table 5. TNT Equivalency of Ammonium Nitrate Based on Experimental Factors.....	2-18
Table 6. Summary of Factor Effect on Sensitivity and Energy Output.....	2-25
Table 7. GSA Hazards Classification System.....	3-58
Table 8. Building Damage Level Definition – ABS Consulting	3-59
Table 9. Building Damage Categories – ETL 1110-3-495	3-60
Table 10. Scenarios Modeled.....	4-7
Table 11. Metal Building Damage Assessment.....	5-5
Table 12. Basketball Goal Analysis – TNT _{Eq} Charge Weight	5-10
Table 13. Component Damage Level Definitions ^[57]	5-19
Table 14. Approximate Residential Wall CDL Percentages by ABS Consulting BDL	5-32
Table 15. Summary of Yield Assessment based upon N. Reagan Street Single Family Residence Damage	5-35

List of Figures

Figure 1. USGS Aerial Map of West, TX.....	1-3
Figure 2. Aerial Photo of West Fertilizer (a) Before Event, (b) Post Event	1-4
Figure 3. USGS Map of West, TX with Range from Explosion Source.....	1-5
Figure 4. West Fertilizer Co Fertilizer Production Building Layout	1-7
Figure 5. West Fertilizer Co Fertilizer Production Building Layout	3-2
Figure 6. West Fertilizer Crater on April 23, 2013	3-3
Figure 7. Crater as Viewed from the West on April 25, 2013	3-3
Figure 8. Pump Truck Southeast of Crater on April 23, 2013	3-5
Figure 9. Door from Pump Truck (Pump Truck in the Background)	3-6
Figure 10. Water Tank Truck on Jerry Mashek Drive.....	3-6
Figure 11. Farm Equipment South of Crater Near the Scale House	3-7
Figure 12. Ground Mark from Displacement of Farm Equipment from Blast Overpressure	3-7
Figure 13. Rail Car Loaded with AN Overturned by Explosion.....	3-8
Figure 14. Scale House	3-8
Figure 15. Remains of Chemical Storage / Office Building (Behind Crater in Photo)	3-9
Figure 16. Corn Silo Damage (Composite of Two Photographs)	3-9
Figure 17. Liquid Fertilizer Tank Damage.....	3-10
Figure 18. Liquid Fertilizer Tank Damage (Composite of three photographs)	3-10
Figure 19. Anhydrous Ammonia Tanks Photo of PRVs (CSB Photo 04-19-2013).....	3-12
Figure 20. PRV Valve from Southern Anhydrous Ammonia Tank (Photo 05-28-13)	3-12
Figure 21. Plate on Anhydrous Ammonia Tank	3-13
Figure 22. Pressure Relief Valve Markings.....	3-13
Figure 23. Community Facilities in West, TX.....	3-14
Figure 24. Rest Haven Nursing Home	3-15
Figure 25. Nursing Home Emergency Exit Floor Plan	3-16
Figure 26. East Façade of Rest Haven Nursing Home	3-16
Figure 27. Damage to Reagan St. Entry of Rest Haven Nursing Home	3-17
Figure 28. East Façade of North Wing Rooms at Rest Haven Nursing Home	3-18
Figure 29. East Façade Bedroom in Rest Haven Nursing Home (After FEMA USAR Operations) 3-19	
Figure 30. West Lobby of Rest Haven Nursing Home	3-20
Figure 31. Hallway in Western Portion of Rest Haven Nursing Home Outside of the Chapel .	3-21
Figure 32. Post Incident Aerial View of Rest Haven Nursing Home (Debris Impacts)	3-22
Figure 33. Concrete Crater Debris (West Fertilizer Foundation) that Impacted Nursing Home..	3-22
Figure 34. Typical Glass Fragments on Floor and Into Rooms of Rest haven Nursing Home...	3-23

Figure 35. Typical High Glazing Hazards in Rest Haven Nursing Home	3-23
Figure 36. Playground	3-24
Figure 37. Playground equipment	3-25
Figure 38. Damaged Basketball Goal Post on Basketball Court.....	3-25
Figure 39. Tree Adjacent to Basketball Court	3-26
Figure 40. Map Showing Location of Tree Adjacent to Basketball Court Downwind of Anhydrous Ammonia Tanks.....	3-26
Figure 41. Pre-Explosion Smoke Plume from the Fire (Passing North of Basketball Courts) ...	3-27
Figure 42. West Intermediate School Building Sections.....	3-28
Figure 43. West Intermediate School Room Layout from Evacuation Plan	3-29
Figure 44. West Intermediate School Aerial Photograph (Prior to Event)	3-29
Figure 45. West Intermediate School – Northwest Wing Roof	3-30
Figure 46. West Intermediate School- North Hallway Looking Toward Northeast Exit Door ..	3-31
Figure 47. West Intermediate School Classroom 12.....	3-31
Figure 48. West Intermediate School Glazing Hazard Room 12	3-32
Figure 49. West Intermediate School – Original School Northeast Wing Roof	3-32
Figure 50. West Intermediate School Interior of Northeast Section that Burned	3-33
Figure 51. West Intermediate School – Gymnasium Roof.....	3-34
Figure 52. West Intermediate School Gymnasium	3-34
Figure 53. West Intermediate School Gymnasium Roof Failure.....	3-35
Figure 54. West Intermediate School Cafeteria (Insulate has been picked up and stacked)...	3-35
Figure 55. West Intermediate School – Classroom 20 Nonstructural Debris.....	3-36
Figure 56. West Intermediate School – Typical Failed Classroom Door Latch	3-36
Figure 57. West Intermediate School Library after Shoring and Debris Removal.....	3-37
Figure 58. West Intermediate School Room 22 Interior after Moderate Cleanup.....	3-37
Figure 59. West High School Evacuation Map and Floor Plan.....	3-38
Figure 60. West High School Aerial Photo	3-39
Figure 61. High School Auditorium as Ceiling as Viewed from Below.....	3-39
Figure 62. Auditorium Ceiling Hanger Damage	3-40
Figure 63. Commons Area Ceiling Damage.....	3-40
Figure 64. West High School Band Hall.....	3-41
Figure 65. Joist Girder Damage in Gymnasium 2	3-42
Figure 66. Failed Cross-Bracing Fasteners Gymnasium 2	3-43
Figure 67. Buckled OWSJs in Gymnasium 2	3-43
Figure 68. West Wall of Gymnasium 2.....	3-44
Figure 69. Aerial View of West High School Roof	3-45
Figure 70. West High School Gymnasium 1 Roof Collapse from South Bleachers	3-46

Figure 71. West high School Gymnasium1 Roof Collapse Viewed from Gymnasium Floor Entry 3-46	
Figure 72. Joist Girder Damage in Gymnasium 1.....	3-47
Figure 73. West High School Entrance Lobby	3-48
Figure 74. West High School Library	3-49
Figure 75. West High School Hallway Outside Room 411	3-49
Figure 76. West Middle School Location	3-50
Figure 77. Middle School Campus.....	3-51
Figure 78. West Middle School Practice Gym.....	3-51
Figure 79. West Middle School Practice Gym Buckled Frame.....	3-52
Figure 80. West Middle School Cafeteria / Auditorium.....	3-53
Figure 81. West Middle School – Old High School Classroom Building.....	3-54
Figure 82. West Middle School Original Classroom Building Superficial Damage.....	3-55
Figure 83. Classroom Annex Interior Hallway and Ceiling Damage.....	3-56
Figure 84. Extent of Surveyed Residential Building	3-58
Figure 85. GSA Hazards Classification Diagram	3-59
Figure 86. Apartment Complex East Façade.....	3-62
Figure 87. Apartment Complex after USAR Operations	3-62
Figure 88. Peak Pressure vs. Scaled Distance for Multiple CFD (CEBAM) Simulations and Kingery-Bulmash Curve ¹	4-2
Figure 89. CAD Model of the Area Near the Blast Site (viewed from the Southeast).....	4-3
Figure 90. A View of the Blast Site from the Northwest.....	4-3
Figure 91. Grid Study Results – Peak Free-Field Pressure	4-4
Figure 92. Grid Study Results – Peak Free-Field Scaled Impulse	4-5
Figure 93. Objects modeled in CEBAM	4-5
Figure 94. An Example of Overpressures Along the Ground	4-7
Figure 95. Example of Three-Dimensional Field Data.....	4-8
Figure 96. Typical Resistance-Deflection Curve.....	5-3
Figure 97. Typical Blast Load for High Explosives	5-3
Figure 98. Surveyed Metal Buildings.....	5-4
Figure 99. Undamaged Metal Buildings Indicators.....	5-6
Figure 100. Playground & Basketball Court Plan View – Before and After	5-7
Figure 101. Identified Basketball Goal Locations.....	5-7
Figure 102. Surveyed Basketball Hoops 1 & 2	5-8
Figure 103. Surveyed Basketball Goals 3 & 4	5-8
Figure 104. Basketball Goal Structural Model Analysis	5-9
Figure 105. Apartment Complex Damage.....	5-11
Figure 106. Apartment Complex Damage.....	5-11

Figure 107. Apartment Complex Damage.....	5-12
Figure 108. Apartment Complex Damage Assessment per ETL 1110-3-495	5-13
Figure 109. Rest Haven Nursing Home East Façade Damage	5-15
Figure 110. Nursing Home Damage Assessment per ETL	5-16
Figure 111. Rendering of the West FACET3D Model	5-17
Figure 112. P-I Diagram Example	5-19
Figure 113. Qualitative Building Damage ABS BDL Levels of Surveyed Structures [1/2]	5-20
Figure 114. Qualitative Building Damage ABS BDL Levels of Surveyed Structures [2/2]	5-21
Figure 115. Extent of Observed Window Breakage	5-21
Figure 116. Residential Building Analysis: Wood Stud Wall with Brick Veneer P-I Diagram....	5-22
Figure 117. Residential Building Analysis: Wood Stud Wall with Wood Siding P-I Diagram	5-23
Figure 118. Residential Building Analysis: Roof Wood Truss.....	5-23
Figure 119. Roof Purlin Deformation at Gymnasium	5-25
Figure 120. Roof Beam & Purlin Deformation at Cafeteria	5-26
Figure 121. Deflection of OWSJ at Room 18.....	5-26
Figure 122. Joist Girder Deformation at Library	5-27
Figure 123. West Intermediate School: Gymnasium Roof Purlin P-I Diagram	5-28
Figure 124. West High School: Example OWSJ P-I Diagram	5-29
Figure 125. West Middle School: Gymnasium Roof Purlin P-I Diagram	5-30
Figure 126. West Middle School: Classroom Annex OWSJ P-I Diagram	5-31
Figure 127. 1100 - 1200 Blocks of N. Reagan St. Observed Single Family Dwelling BDLs	5-33
Figure 128. 1400 - 1500 Block of N. Reagan St. Observed Single Family Dwelling BDLs.....	5-34
Figure 129. High School FACET3D Model Response – 20,000-lb _{TNT}	5-36
Figure 130. High School FACET3D Model Response – 25,000-lb _{TNT}	5-37
Figure 131. High School FACET3D Model Response – 30,000-lb _{TNT}	5-37
Figure 132. West Fertilizer Explosion Free-Field K-B Pressure Contours for 25,000 lb _{TNT}	6-2
Figure 133. West Fertilizer Explosion Free-Field K-B Impulse Contours for 25,000 lb _{TNT}	6-3
Figure 134. West High School Applied Pressures (CFD).....	6-4
Figure 135. West Intermediate School Applied Pressures (CFD - Portion that Burned not Included)	6-5
Figure 136. Rest haven Nursing Home Applied Pressures (CFD).....	6-6
Figure 137. Apartment Complex Applied Pressures (CFD)	6-7

Definitions

The following are definitions of several terms used in this document.

- **AG:** Annealed Glass
- **AN:** Ammonium Nitrate, NH_4NO_3
- **BATF:** Bureau of Alcohol Tobacco and Firearms
- **BDL:** Building Damage Level
- **CFD:** Computational Fluid Dynamics
- **CMU:** Concrete Masonry Unit
- **CSB:** Chemical Safety Board
- **Directional Indicator:** A damaged object which has been deformed away from an explosion center and hence indicates the direction of blast wave travel. Direction Indicators may be used to locate explosion centers.
- **Blast Impulse:** The integrated area under the blast associated pressure-time curve.
- **Blast Overpressure:** The peak pressure (above ambient) associated with a blast wave generated by an explosion. See definitions below regarding “Free-Field Blast Overpressure” and “Reflected Blast Overpressure”.
- **Combustion:** A chemical reaction that occurs between a fuel and an oxidizing agent. This reaction can also be described as exothermic decomposition.
- **Consequence Assessment:** Assessment of explosion, fire, and/or toxic hazards associated with a process or unit without assigning specific frequency to the events. Consequence Assessment typically includes defining scenarios based on judgment or past history, modeling the release of flammable or toxic and determining the hazard to occupied buildings. End point criteria are required for blast pressure, thermal exposure, and toxic exposure to determine, if actions are required.
- **Critical Diameter (d_c):** A cross section dimension below which a steady detonation cannot be sustained in the material. If the cross-section is smaller than this value the detonation will slow down or extinguish completely. This value varies with material and can be affected by confinement, density, particle size, and temperature.
- **Critical Impact Pressure (P_{cr}):** The minimum pressure of an incident shock wave which can initiate a detonation process in a mass of explosive material which has a cross section above its critical diameter.
- **Decomposition:** The separation of a chemical compound into elements or simpler compounds. As an example, water (H_2O) can be broken down into hydrogen (H_2) and oxygen (O_2) through electrolysis. Decomposition can be an endothermic or exothermic reaction.

- **Deflagration:** A subsonic combustion propagating through a material via heat transfer. Combusting material (hot) subsequently heats and ignites neighboring material to continue the reaction. An example of deflagration is firing a bullet. The propellant is ignited and a rapid exothermic reaction takes place generating gas. The burning region in the propellant travels at subsonic speeds.
- **Deflagration to Detonation Transition (DDT):** This term describes a reaction in which a deflagration accelerates into a detonation. In this case, a material is initially ignited and it begins to deflagrate. If there is confinement, the combustion products (hot gasses) cannot escape and the overall temperature and pressure increases. This increase in temperature and pressure accelerates the deflagration (chemical reaction) further increasing the temperature and pressure. Eventually, given sufficient time and distance, a shock wave forms and becomes a self-sustaining detonation.
- **Detonation:** A self-sustaining exothermic reaction which propagates through the material at a constant supersonic velocity. An example of a detonation is initiation of TNT.
- **Endothermic Reaction:** A chemical reaction accompanied by the absorption of heat from the surroundings. An example of this type of reaction is the use of instant cold packs. These packs contain water and ammonium nitrate in separate containers. When the two items are mixed together, the packs become cold.
- **Explosion:** A release of mechanical, chemical, or nuclear energy in a sudden manner with the generation of high temperature and typically with the release of gases. For use here, an explosion will refer to the release of chemical energy. While not the same phenomena, combustion and detonation can both be described as explosions by an observer, but are not interchangeable terms.
- **Exothermic Reaction:** A chemical reaction accompanied by the generation of heat.
- **For Official Use Only (FOUO):** FOUO is a DoD dissemination control applied to unclassified information when disclosure to the public of that particular record, or portion thereof, would reasonably be expected to cause a foreseeable harm to an interest protected by one or more of Freedom of Information Act (FOIA) Exemptions (DoDM 5200.01-V4, February 24, 2012, DoD Information Security Program: Controlled Unclassified Information).

- **Free-Field Overpressure:** Often referred to as “Side-on Blast Overpressure.” The peak pressure (above ambient) associated with a blast wave generated by an explosion when measured in an “open field” without the presence of objects such as buildings that would reflect the blast wave. This would be the pressure exerted by the blast wave on the ground surface as it passes over. Many blast contour maps display free-field (or side-on) blast overpressures even though those contours are drawn on a plan with units and buildings present and those contours do not address local reflections that result in pressure enhancements.
- **Free-Field Impulse:** the integrated area under the free-field blast overpressure-time curve.
- **Fixed Building:** A structure that is intended for occupancy and is constructed integral with a permanent foundation (e.g., concrete slab). Such a building is not intended to be moved.
- **Glazing Hazards:** Flying glass fragments produced by blast loading after an explosion.
- **Gravel Ballast:** Small gravel placed upon a built up roof to protect the roof from UV light, heat, and weather and protect the roof membrane from degradation.
- **GSA:** General Services Administration
- **HE:** High Explosive(s)
- **Ideal Detonation:** This occurs when the cross-section of the explosive material is large enough that there are no dimensional effects on the detonation properties (e.g., wave velocity, peak pressure). The charge diameter must equal or exceed the d_c for the material.
- **Ideal Explosive:** These materials have a uniform density and support a uniform reaction front. Typically these materials have small values of d_c and undergo ideal detonation.
- **IGU:** Insulating glass unit
- **Joist Girder:** A primary horizontal joist carrying loads from other joists and slabs connected to it
- **Net Explosive Weight (NEW):** The total weight of all explosives substances, expressed in lbs.
- **Non-ideal Detonation:** This occurs when the cross-section of the explosive material has a significant effect on detonation properties (e.g., wave velocity, peak pressure). This type of detonation will occur when the charge diameter is smaller than the critical diameter (d_c).
- **Non-ideal Explosive:** These materials have an irregular shape or density resulting in non-uniform shock wave expansion. Typically these materials have large values of d_c and undergo non-ideal detonation.
- **Open Webbed Steel Joist:** A lightweight steel truss consisting, in the standard form, of parallel chords and a triangulated web system, proportioned to span between bearing points.
- **OWSJ:** Open Webbed Steel Joist


- **PRV:** Pressure Relief Valve.
- **Reflected Overpressure:** An amplification of local blast overpressure (over the free-field value) due to interaction of the blast front with a surface or object, such as a building wall. An upper limit occurs for an infinite rigid wall aligned normal to the path of the blast wave. There, the wave fully stagnates at the wall and reverses course. Oblique reflections occur when the interaction is off-normal angle of incidence and typically result in less pressure enhancement over the free-field value than does a true normal reflection.
- **Reflected Impulse:** The integrated area under the associated reflected blast overpressure-time curve.
- **Run Distance:** This is the distance required to develop a steady state detonation. When a material is shocked, by detonator, impact, or deflagration build-up, the shock must travel a specific distance to achieve a steady state detonation. This value varies with material and is a function of the peak shock pressure of the reaction front. Higher shock pressures require shorter run distances.
- **Shock Wave:** A rapid pressure (compression) disturbance which moves through a medium (e.g., solid, liquid, or gas). The velocity of the shock wave is greater than the speed of sound for the current medium.
- **Side-on Overpressure:** See “Free-Field Blast Overpressure.”
- **Side-on Impulse** See “Free-Field Impulse
- **SBEDS:** A computer program, distributed by the U.S. Army Corps of Engineers Protective Design Center, which performs SDOF analysis.
- **SDOF:** Single-Degree-of-Freedom, a common dynamic structural analysis method used in blast analysis.
- **TNT:** Trinitrotoluene, a high explosive commonly used in quantifying blast loads.
- **TNT Equivalence (TNT_{eq}):** TNT equivalency is a “rough” approximation correlating a material’s explosive energy output (pressure and impulse) to a specific mass of TNT (for a given density). The pressure and impulse equivalency values are not typically the same for a material. TNT equivalency is not a perfect correlation, and will produce results (pressure and impulse vs. distance) of varying quality when compared to the actual explosive material. However, due to the historical use of TNT equivalency and extensive existing data, it is a common method for performing general comparisons between different explosives and predicting their impact. TNT is highly studied explosive and most computational models are able to properly evaluate TNT.
- **TTG:** Thermally Tempered Glass

1 Background

On April 17, 2013, a fire and explosion occurred at the West Fertilizer Co. which resulted in the deaths of 15 people, injuries to members of the community, and extensive damage to the facility, surrounding homes, and community facilities. West Fertilizer was a fertilizer storage and distribution facility located in the town of West, TX. The source of the explosion was firmly established by the CSB, prior to ABS Consulting's arrival on site of West Fertilizer, as a catastrophic explosion of Ammonium Nitrate within the Production Building. The explosion projected many pieces of the Process Building and a substantial amount of crater ejecta. The explosion also generated a blast wave that swept across the surrounding area causing significant structural damage to homes and community structures.

ABSG Consulting Inc. (ABS Consulting) was contracted by the U.S. Chemical Safety Board (CSB) to perform a site survey,^{[1],[2]} collect data pertaining to structural damage and to perform analyses^[3] to develop an estimate of the explosion severity and resulting overpressure and impulse contours. The objectives of the ABS Consulting work included:

1. Provide preliminary opinions of explosion characteristics including but not limited to potential fuel source(s), blast pressures and fuel source configurations.
2. Perform a field investigation in order to document damage to the community and measure structural damage.
3. Conduct a literature review of Ammonium Nitrate (AN) including review of the following information:
 - a. AN-TNT explosive equivalence with various contaminants, physical states, particle size and AN pile geometry.
 - b. Percentage of AN quantity present that would be expected to detonate from review of previous incidents and testing.
4. Perform a Computational Fluid Dynamics (CFD) analysis of the West community to simulate the blast wave expansion and interaction with structures to confirm the estimated Net Explosive Weight (NEW) required to cause the observed damage.
5. Perform a detailed assessment of explosive yield based upon blast damage indicators.

For the Public Release version, FOUO data has been redacted and is represented as a solid black bar 

¹ CSB Contract CSB-13-022, GSA order number GS—10F-0242L. 04/19/2013.

² CSB Contract CSB-13-025, GSA order number GS—10F-0242L, 04/23/2013.

³ CSB Contract CSB-13-026, GSA order number GS—10F-0242L, 08/19/2013.

The town of West, TX is located approximately 20 miles north of Waco, TX on Interstate 35. A USGS map of West is shown in Figure 1. The West Fertilizer Co. site is highlighted yellow and prominent community structures are also noted including:

- West Intermediate School
- West High School
- West Middle School
- Rest Haven Nursing Home
- Apartment complex
- Playground

In addition, photographs of the West Fertilizer Co. site, that were provided to ABS Consulting by the CSB, with key features of the West Fertilizer Co. property labeled is provided for reference in Figure 2. An additional USGS map is provided in Figure 3 that has radii centered on the approximate location of the crater to provide reference on the distances to the center of the explosion (ground zero).

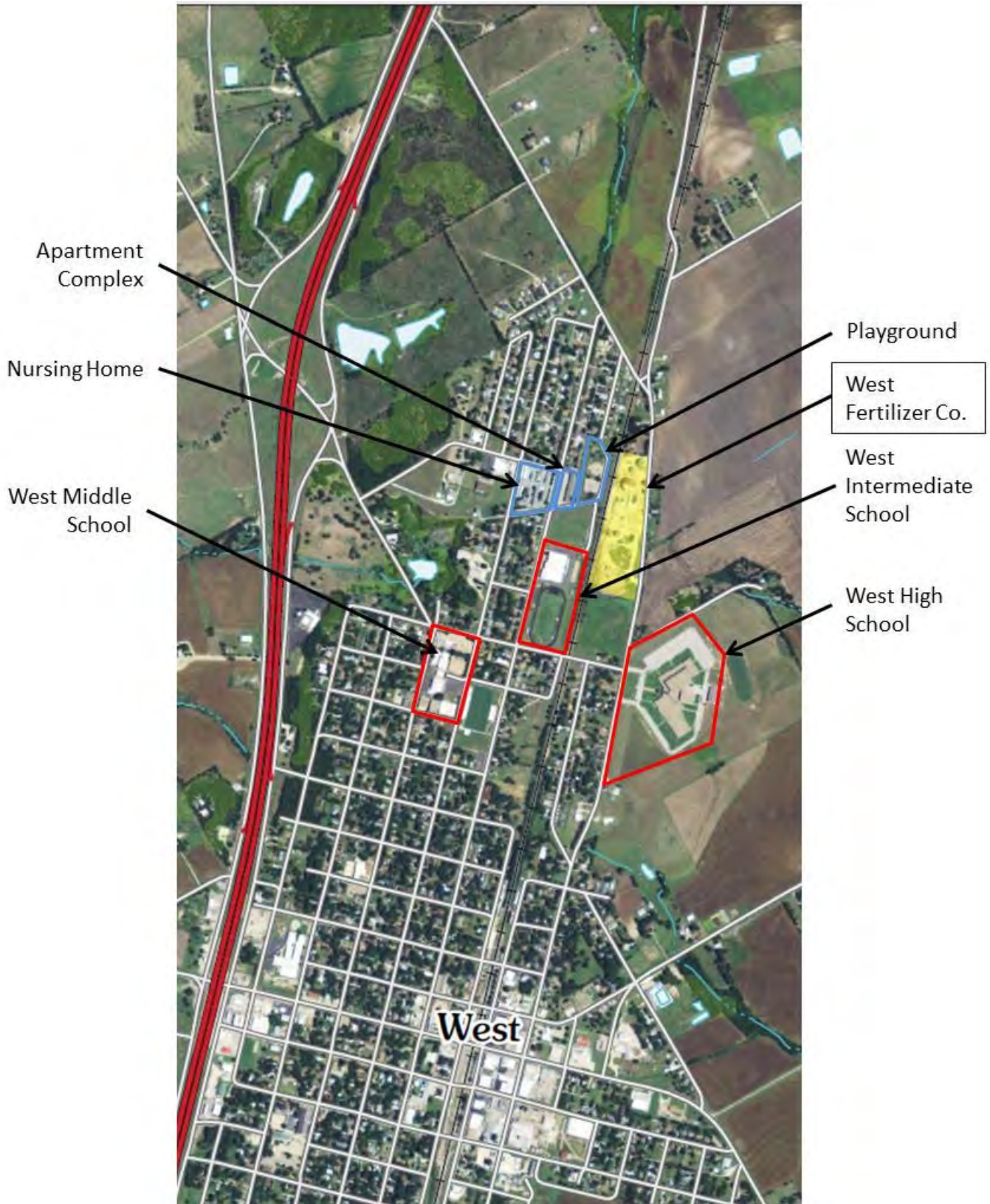


Figure 1. USGS Aerial Map of West, TX

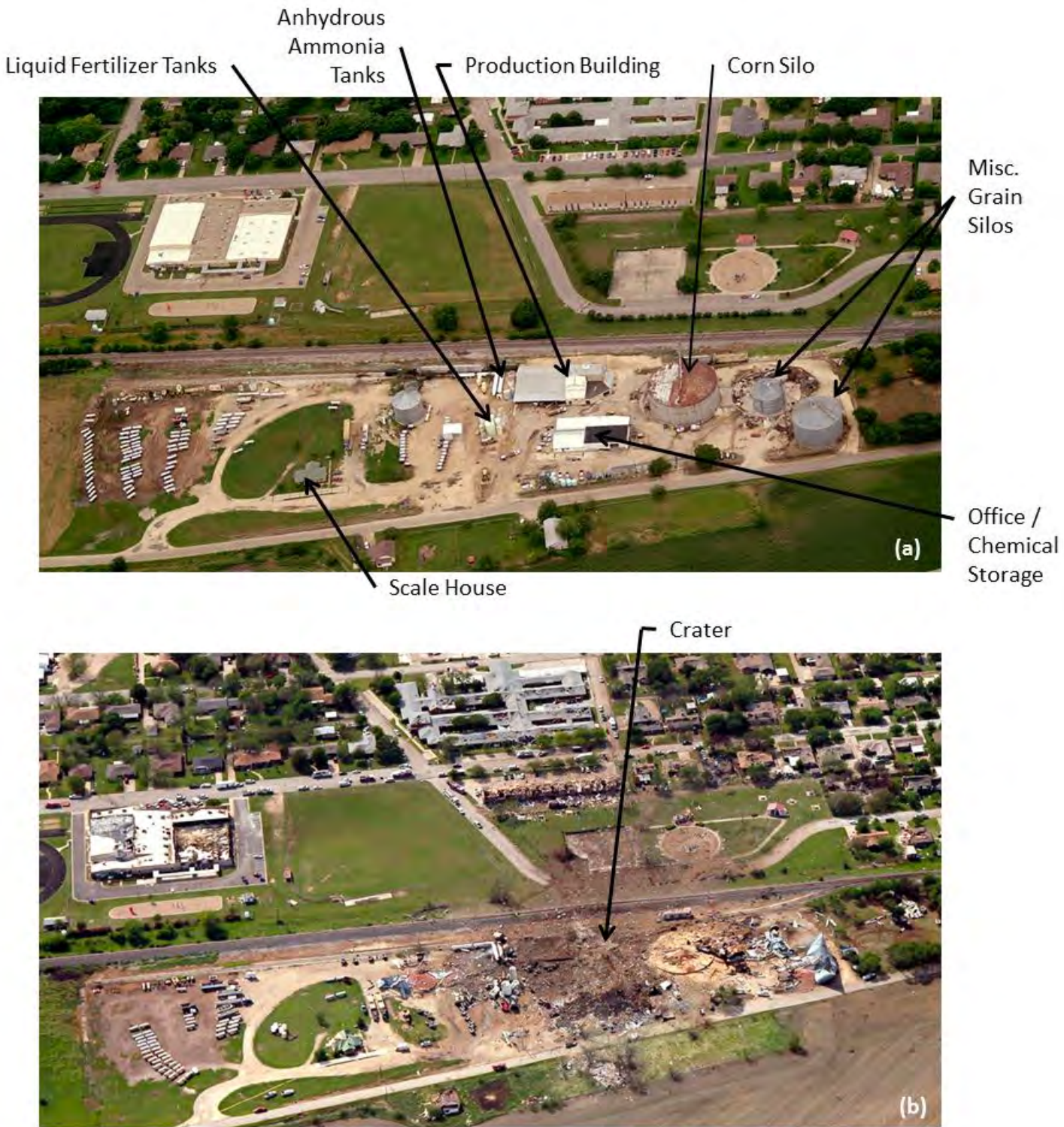


Figure 2. Aerial Photo of West Fertilizer (a) Before Event, (b) Post Event

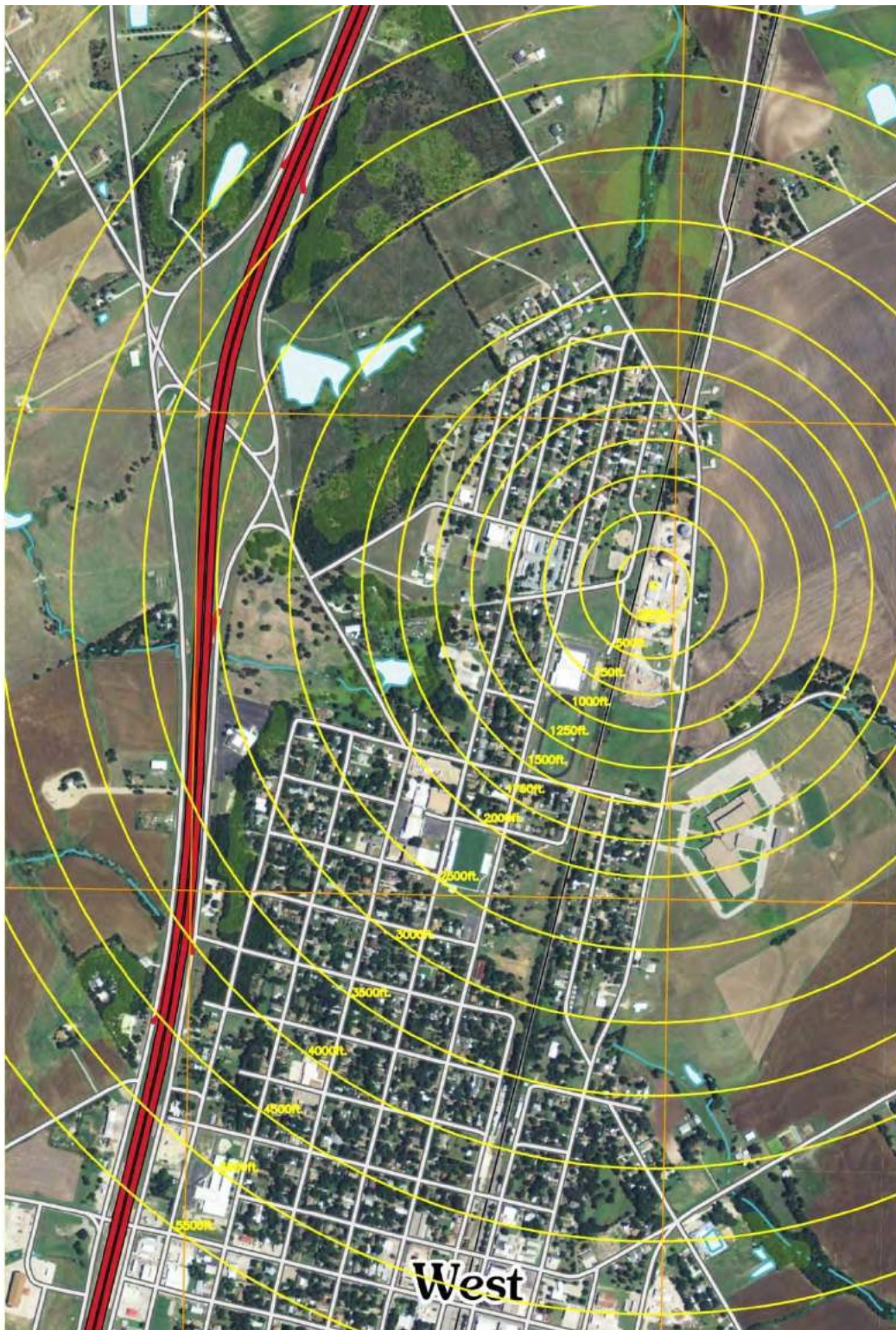


Figure 3. USGS Map of West, TX with Range from Explosion Source

1.1 West Fertilizer Co Ammonium Nitrate Properties

Based on information provided by the Chemical Safety Board (CSB), the AN onsite had the properties shown in Table 1.

Table 1. West Fertilizer Co Ammonium Nitrate Properties ^[4]

Property	Value
Composition	AN = 98-100 wt% Conditioning Agent = 0-0.2 wt%
Physical Form	Solid prills or granules
Particle Size	Not specified
% Fines (-12 Tyler Mesh)	1.0%
Bulk Density	0.93-0.99 g/cm ³
Melting Point	155-169 C
Melting Point/Decomposition	210 C

1.2 West Fertilizer Co Environmental Conditions

A layout of the WFC facility is shown in Figure 4. WFC was reported to have 40 to 60 tons of AN with the Main AN Bin containing 50%-100% of the total with the remainder in the southern overflow bin. The AN was stored in bulk (no bags or barrels) in each of the bins. Based on the provided layout, the distance from the AN overflow bins to the main AN bin was ~20 ft. Among the AN stored in the building, K-Mag (potassium magnesium), potash (potassium chloride), diammonium phosphate, and ammonium sulfate was also stored in the fertilizer building. A variety of seeds were stored in the northeast area of the building.

The details describing the building and bin construction, as well as typical loading, unloading, and housekeeping procedures is provided in the CSB document ^[5].

⁴ Chemical MSDSs and Spec Sheets, received from CSB via e-mail on 10-30-2013.

⁵ Production Process and Materials of Construction, received from CSB via e-mail on 10-30-2013.

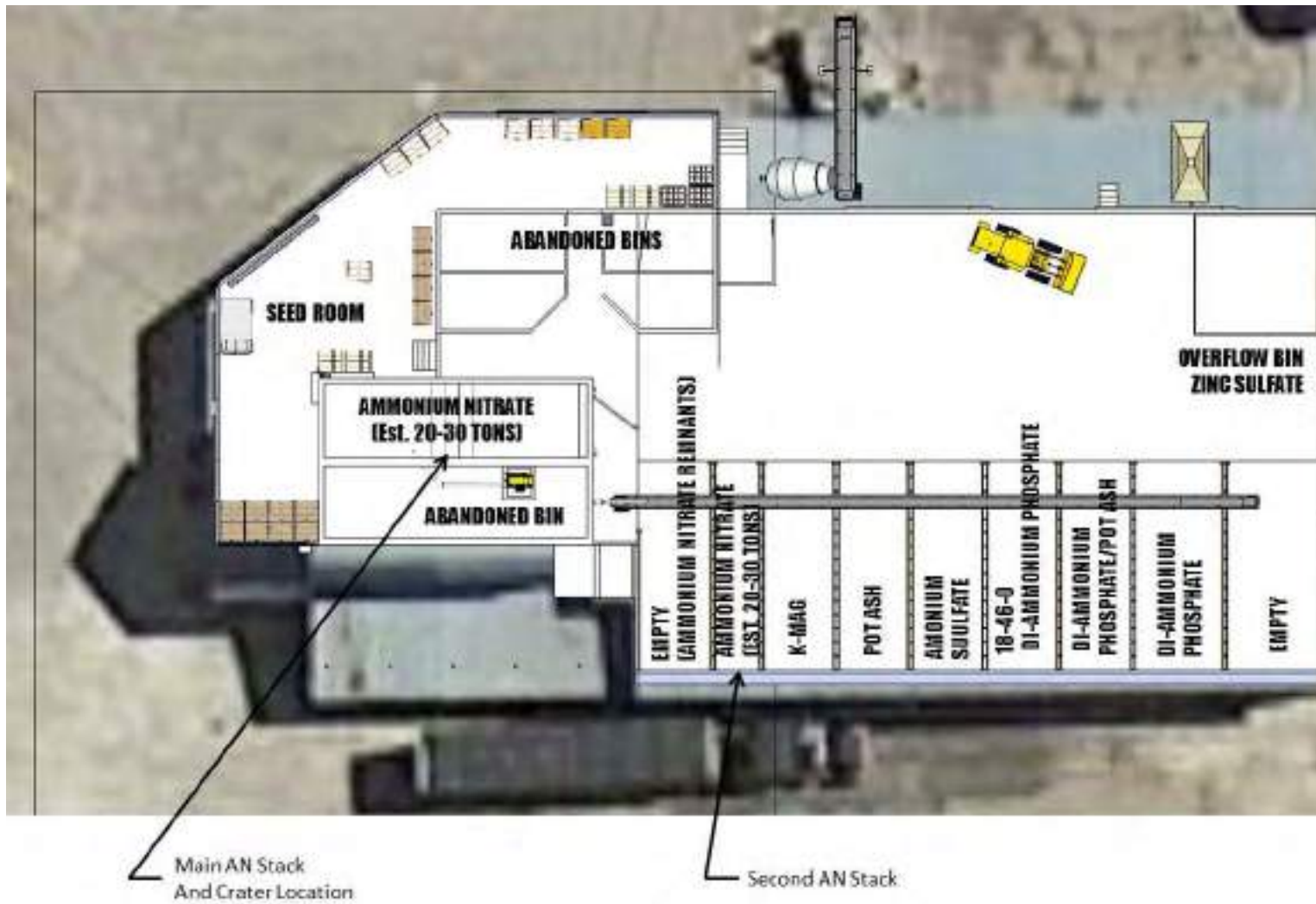


Figure 4. West Fertilizer Co Fertilizer Production Building Layout

2 Literature Survey

This literature survey reviewed approximately 50 references including books and journal articles. The references were identified by text/subject matching incorporating terms such as, but not limited to: ammonium nitrate, detonation, thermal decomposition, critical diameter, molten AN, shock initiation, and sensitivity. These searches utilized several academic libraries (e.g., University of Texas), research libraries (Los Alamos National Library), government libraries (Defense Technical Information Center) as well as educational and research based textbooks. As the information was organized, the searches were refined to focus on specific characteristics reported to alter the sensitivity and energy output of ammonium nitrate. This report provides an overall general summary of factors that influence ammonium nitrate sensitivity and energy output based on literature experiments as well as events. References used under the “For Official Use Only” (FOUO) designation are indicated by red text.

2.1 Term Disambiguation

When reviewing literature concerning this topic matter, it is common to encounter several terms that may have been used interchangeably or incorrectly. In order to facilitate a consistent review of the information gathered in this literature survey, a list of commonly used and pertinent terms are defined and briefly discussed. The terms are presented in a progression, as several terms build upon one another.

Endothermic Reaction: A chemical reaction accompanied by the absorption of heat from the surroundings. An example of this type of reaction is the use of instant cold packs. These packs contain water and ammonium nitrate in separate containers. When the two items are mixed together, the packs become cold.

Exothermic Reaction: A chemical reaction accompanied by the generation of heat. An example of this type of reaction is the use of instant hot packs. These packs contain water and calcium chloride in separate containers. When the two items are mixed together, the packs become hot.

Decomposition: The separation of a chemical compound into elements or simpler compounds. As an example, water (H₂O) can be broken down into hydrogen (H₂) and oxygen (O₂) through electrolysis. Decomposition can be an endothermic or exothermic reaction.

Explosion: A release of mechanical, chemical, or nuclear energy in a sudden manner with the generation of high temperature and typically with the release of gases. For use here, an explosion will refer to the release of chemical energy. While not the same phenomena, combustion and detonation can both be described as explosions by an observer, but are not interchangeable terms.

Combustion: A chemical reaction that occurs between a fuel and an oxidizing agent. This reaction can also be described as exothermic decomposition.

Deflagration: A subsonic combustion propagating through a material via heat transfer. Combusting material (hot) subsequently heats and ignites neighboring material to continue the reaction. An example of deflagration is firing a bullet. The propellant is ignited and a rapid exothermic reaction takes place generating gas. The burning region in the propellant travels at subsonic speeds.

Shock Wave: A rapid pressure (compression) disturbance which moves through a medium (e.g., solid, liquid, or gas). The velocity of the shock wave is greater than the speed of sound for the current medium.

Detonation: A self-sustaining exothermic reaction which propagates through the material at a constant supersonic velocity. An example of a detonation is initiation of TNT.

Deflagration to Detonation Transition (DDT): This term describes a reaction in which a deflagration accelerates into a detonation. In this case, a material is initially ignited and it begins to deflagrate. If there is confinement, the combustion products (hot gasses) cannot escape and the overall temperature and pressure increases. This increase in temperature and pressure accelerates the deflagration (chemical reaction) further increasing the temperature and pressure. Eventually, given sufficient time and distance, a shock wave forms and becomes a self-sustaining detonation.

Run Distance: This is the distance required to develop a steady state detonation. When a material is shocked, by detonator, impact, or deflagration build-up, the shock must travel a specific distance to achieve a steady state detonation. This value varies with material and is a function of the peak shock pressure of the reaction front. Higher shock pressures require shorter run distances.

Critical Diameter (d_c): A cross section dimension below which a steady detonation cannot be sustained in the material. If the cross-section is smaller than this value the detonation will slow down or extinguish completely. This value varies with material and can be affected by confinement, density, particle size, and temperature.

Critical Impact Pressure (P_{cr}): The minimum pressure of an incident shock wave which can initiate a detonation process in a mass of explosive material which has a cross section above its critical diameter.

Ideal Detonation: This occurs when the cross-section of the explosive material is large enough that there is no dimensional effects on the detonation properties (e.g., wave

velocity, peak pressure). The charge diameter must equal or exceed the d_c for the material.

Non-ideal Detonation: This occurs when the cross-section of the explosive material has a significant effect on detonation properties (e.g., wave velocity, peak pressure). This type of detonation will occur when the charge diameter is smaller than the critical diameter (d_c).

Ideal Explosive: These materials have a uniform density and support a uniform reaction front. Typically these materials have small values of d_c and undergo ideal detonation.

Non-ideal Explosive: These materials have an irregular shape or density resulting in non-uniform shock wave expansion. Typically these materials have large values of d_c and undergo non-ideal detonation.

TNT Equivalence (TNT_{eq}): TNT equivalency is a “rough” approximation correlating a material’s explosive energy output (pressure and impulse) to a specific mass of TNT (for a given density). The pressure and impulse equivalency values are not typically the same for a material. TNT equivalency is not a perfect correlation, and will produce results (pressure and impulse vs. distance) of varying quality when compared to the actual explosive material. However, due to the historical use of TNT equivalency and extensive existing data, it is a common method for performing general comparisons between different explosives and predicting their impact. TNT is highly studied explosive and most computational models are able to properly evaluate TNT.

2.2 Historical AN Incidents

Table 2 provides a list of reported accidents involving AN from the sources included in the survey. A brief description is provided for each event as well as an indication whether a fire and/or explosion was reported. An estimate of the mass of AN involved in the accident is also included.

Seventy incidents involving AN are compiled in Table 2. Of those events, 40 involved a fire being reported and 51 resulted in an explosion. However, only 21 of the events resulted in an explosion following a reported fire. Roughly 50% of the reported incidents involving fire progressing to an explosion. This indicates that fire, while an indicator of a potential explosion, does not ensure that an explosion is imminent.

Table 2. Reported Historical Incidents Involving Ammonium Nitrate

Date	Location	Description	Fire	Explosion	Quantity of AN	Reference
[REDACTED]	[REDACTED]	[REDACTED]			[REDACTED]	[6]
21-Sep-1911	Brescia, Italy	Explosives manufacture		x		[7]
[REDACTED]	[REDACTED]	[REDACTED]			[REDACTED]	[7, 6, 8, 9]
[REDACTED]	[REDACTED]	[REDACTED]			[REDACTED]	[6, 10]
[REDACTED]	[REDACTED]	[REDACTED]			[REDACTED]	[7, 6, 9]
[REDACTED]	[REDACTED]	[REDACTED]			[REDACTED]	[6, 9]
[REDACTED]	[REDACTED]	[REDACTED]			[REDACTED]	[6, 10, 11, 9]
26-Jul-1920	Kriewald, Germany	Blasting caked AN		x	2 car loads	[9]
[REDACTED]	[REDACTED]	[REDACTED]			[REDACTED]	[6, 11]
[REDACTED]	[REDACTED]	[REDACTED]			[REDACTED]	[7, 6]
[REDACTED]	[REDACTED]	[REDACTED]			[REDACTED]	[7, 6]
10-Sep-1922	Sinnemahonig, PA	Fire in Pan of AN	x		4,300 lbs	[9]
1-Mar-1924	New Brunswick or Nixon NJ, USA	AN exploded in vacuum grainer and sympathetic detonation occurred in a nearby hot pile of prills		x	44,800 lbs	[7]
[REDACTED]	[REDACTED]	[REDACTED]			[REDACTED]	[6, 11, 9]
[REDACTED]	[REDACTED]	[REDACTED]			[REDACTED]	[6]
[REDACTED]	[REDACTED]	[REDACTED]			[REDACTED]	[6]
[REDACTED]	[REDACTED]	[REDACTED]			[REDACTED]	[6]
[REDACTED]	[REDACTED]	[REDACTED]			[REDACTED]	[6]
[REDACTED]	[REDACTED]	[REDACTED]			[REDACTED]	[6]
27-Jan-1938	Ardeer, Scotland	Explosion during mixing of AN for explosives		x	~4,500	[7]
27-Mar-1940	England	Explosion in mixture of explosives containing AN		x		[7]
c. 1940	Gibbstown NJ, USA	Uncoated AN was consumed in a warehouse fire	x		147,000 lbs	[11]
c. 1941	Sankt Lambrecht, Austria	Ammonium nitrate mill exploded		x		[7]
[REDACTED]	[REDACTED]	[REDACTED]			[REDACTED]	[7, 6, 8, 9]
[REDACTED]	[REDACTED]	[REDACTED]			[REDACTED]	[6, 9]
2-Dec-1944	Benson, AZ USA	AN explosion in drying pan		x	8,500 lbs	[7, 9]
26-Feb-1946	Bobeoka, Japan	AN spilled onto RDX		x	400 kg	[7]
16-Apr-1947	Texas City, TX, USA	AN catches fire in hold of a liberty ship (Grandcamp and highflyer) and detonates	x	x	~3,300 tons	[7, 8, 9]

⁶ Clancey, V.J., *The Explosive and fire hazard characteristics of ammonium nitrate fertilisers: Part 1. Introduction and critical literature survey.* 1963.

⁷ Biasutti, G.S., *History of Accidents in the Explosives Industry.* 1985: Corbaz.

⁸ Khan, F.I. and S.A. Abbasi, *Major accidents in process industries and an analysis of causes and consequences.* Journal of Loss Prevention in the Process Industries, 1999. **12**(5): p. 361-378.

⁹ Oxley, J.C., et al., *Ammonium nitrate: thermal stability and explosivity modifiers.* Thermochemica Acta, 2002. **384**(1-2): p. 23-45.

¹⁰ Munroe, C.E., *The Explosivity of Ammonium nitrate.* Chemical & Metallurgical Engineering, 1922. **26**: p. 535-542.

¹¹ Greiner, M., *Ammonium Nitrate Fertilizer--exploding the myth.* Ammonia Plant Safety (Environmental Sciences & Pollution Management), 1985. **25**: p. 1-8.

Table 2. Reported Historical Incidents Involving Ammonium Nitrate

Date	Location	Description	Fire	Explosion	Quantity of AN	Reference
28-Jul-1947	Brest, France	AN on fire in hold of S.S. Liberty, explosion form gas products and later explosion from AN	x	x	3,300 tons	[7, 8, 9]
						[6, 11]
						[6]
						[6, 11]
c. 1949	Independence, KS	Fire started in a storage building of AN and went out of control after several hours.	x		1,400 tons	[11]
25-Aug-1951	Avigliana, Italy	Mixing of explosives with AN		x		[7]
28-Dec-1956	New Castle, PA	Explosion in evaporator		x	5,200 lbs	[9]
7-Aug-1959	Roseburg OR, USA	Dynamite and AN (Car Prill explosive aka ANFO) were initiated by nearby fire	x	x	4.5 tons AN, 2 tons dynamite	[7]
						[6]
c. 1960	Boron, CA	Prilled AN destroyed in burning warehouse	x		20 tons	[11]
27-Dec-1961	Norton VA USA	Fire in bucket conveyor to an ANFO manufacturing/storage site resulting in detonation	x	x	20 ton AN, 30 ton ANFO	[7]
						[6]
9-Apr-1962	Saint-Marcel D'ardeche, France	Explosion occurred in explosive's manufacture where AN was mixed with explosives	x	x		[7]
9-Jan-1963	Oulu, Finland	Molten AN detonated in an AN manufacturing facility		x	10 tons	[7]
9-Jan-1963	Typpi, Oy, Finland	Thermal runaway to detonation		x	8-10 ton	[9]
23-Jun-1963	England	Milling of AN with TNT and aluminum resulted in explosion and then fire		x		[7]
c. 1967	US	A screw conveyor shaft for FGAN burst after a welding operation	x	x		[7]
c. 1967	Potosi, WI	A boxcar loaded with AN catches fire and consumes some AN	x		50 tons	[11]
5-Jul-1968	La Manjoya, Spain	Crushing mill exploded while milling AN		x		[7]
23-May-1969	Arequipa, Peru	Dynamite factory exploded by accident when hand mixing AN with explosive		x		[7]
13-May-1972	Rourkela, India	Manufacture of slurry type explosive composed of AN and nitric acid, fire caused by nitric acid caused primers to detonate, followed by slurry	x	x		[7]
c. 1972	Taroon, Australia	Transport of AN catches on fire then explodes	x	x		[12]
17-Jan-1973	Prior OK, USA	Fire in AN storage building led to detonation of 4-5 tons of 14,000 tons	x	x	4 to 5 tons	[7]
c. 1973	Cheerokee, OK USA	Severe fire in storage area of AN, small quantity of total exploded	x	x	10 tons	[12]
1-Oct-1975	Beloelil, Canada	Slurry explosives manufacture plant batch exploded, made with AN		x		[7]
1-Mar-1976	Tahawas, NY	AN catches fire	x		100 lbs	[9]
c. 1977	Delaware City, DE	Thermal runaway to detonation		x		[9]
7-Jul-1978	Manouba, Tunisia	AN store spontaneously ignites and explodes at an Explosives factory, (fire is implied by author but not stated)	x	x	80 tons	[7]
c. 1978	Rocky Mountain, NC	A storage facility containing AN was destroyed by fire	x		500 tons	[11]
c. 1979	Moreland, ID	Fire started on a conveyor belt unloading AN from rail cars	x		200 tons	[11]
						[13]

¹² Marlair, G. and M.-A. Kordek, *Safety and security issues relating to low capacity storage of AN-based fertilizers*. Journal of Hazardous Materials, 2005. **123**(1–3): p. 13-28.

¹³ Ivanov, Y.A., *Fire and Explosion Hazards of Ammonium Nitrate*. Foreign Technology Division, 1990: p. 7.

Table 2. Reported Historical Incidents Involving Ammonium Nitrate

Date	Location	Description	Fire	Explosion	Quantity of AN	Reference
19-Dec-1994	Sioux City, IA	An explosion occurred in the Port Neal complex in the AN plant.		x	18,000 gallons AN solution	[14]
c. 1997	Brazil	Truck carrying AN exposed to fire from a Tanker truck explodes	x	x		[12]
c. 2000	Florida, USA	Collision between AN truck and Gasoline tanker	x			[12]
21-Sep-2001	Toulouse, France	Explosion in warehouse containing AN		x	390-450 tons	[15,16]
2-Oct-2003	Saint-Romain-en-Jarez, France	Fire on Farm/warehouse storing several tons of AN explodes	x	x		[12]
18-Feb-2004	Neyshabur, Iran	A fire resulted from the derailment of a train carrying fuel, cotton, sulfur, and fertilizer. Firefighters nearly had the blaze out when an explosion occurred.	x	x	~ 280,000 to 560,000 lbs	[17]
22-Apr-2004	Ryongchon, North Korea	A train carrying fuel collided with a train carrying AN, an explosion resulted		x	88 tons	[17]
24-May-2004	Mihailesti, Romania	A truck carrying AN overturned and caught fire. It later exploded	x	x	22 tons	[17, 12]
c. Feb-2004	Barracas, Spain	Transport of AN catches on fire then explodes	x	x	25 tons	[12]
12-Sep-2005	Shengangzhai, China	A truck carrying AN exploded in the village.		x	18 tons	[17]
16-Jun-2006	Mesa, AZ	A fire occurred on a semi-truck hauling liquid AN, dynamite, and electric blasting caps	x		22,050 lbs	[17]

¹⁴ Thomas, M.J., *TERRA CHEMICAL ACCIDENT INVESTIGATION REPORT*. U.S. Environmental Protection Agency, 1996: p. 114.

¹⁵ Hengel, E.I.V.v.d., et al., *Ammonium nitrate behaviour in a fire*. Loss Prevention Bulletin, 2008(202): p. 19.

¹⁶ Dechy, N., et al., *First lessons of the Toulouse ammonium nitrate disaster, 21st September 2001, AZF plant, France*. Journal of Hazardous Materials, 2004. **111**(1-3): p. 131-138.

¹⁷ Mainiero, R.J. and J.H. Rowland, *A review of recent accidents involving explosives transport*. 2008: National Institute for Occupational Safety and Health.

2.3 Ammonium Nitrate

2.3.1 General Properties

Ammonium nitrate under normal conditions is a white solid. The chemical formula for AN is NH_4NO_3 (N:Nitrogen, H:Hydrogen, O:Oxygen). It is highly soluble in water and extremely hygroscopic. Hygroscopic materials actively adsorb water from their surroundings. The melting point of AN is ~ 170 C. The Department of Transportation classifies AN as an oxidizer. Oxidizing materials enhance the combustion properties of other materials. This can manifest as lowering the necessary temperature for a material to combust and increasing the burning rate and temperature of materials. Ammonium nitrate is considered to be a non-ideal explosive, due to its large critical diameter.

The primary use of AN is in the agriculture industry as a fertilizer. Ammonium nitrate is typically supplied in the form of prills. The prills can vary in purity, size, and density. A protective coating is also applied to the prills to prevent water absorption. Ammonium nitrate also has a large use in the mining industry as an explosive. When used directly as an explosive, ammonium nitrate is commonly mixed with a fuel. Due to the large amounts used by these two industries it is common for them to store these large quantities in bins, piles, and stacks of bags.

2.3.2 Decomposition

The literature review identified the following potential thermal decomposition reactions for pure AN as a function of temperature (Table 3)^[18,19]. It has been shown that over many temperatures ranges several different decomposition reactions may occur. However, individual reactions may be more prevalent at certain temperatures. Several of these reactions as well others (not listed here) may occur depending on the presence of other materials (e.g., catalysts, contaminants). All of the listed reactions, except for Equation 1, are exothermic. For events involving AN detonation, Equation 3 is considered the reaction of complete (ideal) detonation. When Equation 3 occurs, calculations show a large gas evolution generating temperatures around 1500 C and pressures around 159,000 psi.

¹⁸ Fedoroff, B.T., *The Encyclopedia of Explosives and Related Items*. Picatinny Arsenal, 1960. **1**: p. A311-A340.

¹⁹ Shaffer, H.B., *Studies in comparative detonation sensitivities*. Fertilizer research, 1987. **14**(3): p. 265-273.

Table 3. Ammonium Nitrate Decomposition Reactions

Thermal Decomposition Equation	Temperature Range	Equation
$NH_4NO_3(s) \xrightarrow{\text{yields}} HNO_3(g) + NH_3(g)$	> 100 C	Equation 1
$NH_4NO_3(s \text{ or } l) \xrightarrow{\text{yields}} N_2O(g) + 2H_2O(g)$	180-200 C	Equation 2
$2NH_4NO_3(s) \xrightarrow{\text{yields}} 2N_2(g) + 2O_2(g) + 4H_2O(g)$	-	Equation 3
$2NH_4NO_3(s) \xrightarrow{\text{yields}} 2NO(g) + 2N_2(g) + 4H_2O(g)$	200-230 C	Equation 4
$3NH_4NO_3(s) \xrightarrow{\text{yields}} 2N_2(g) + N_2O_3(g) + 6H_2O(g)$	-	Equation 5
$4NH_4NO_3(s) \xrightarrow{\text{yields}} 2NO_2(g) + 3N_2(g) + 8H_2O(g)$	-	Equation 6
$5NH_4NO_3(s) \xrightarrow{\text{yields}} 2HNO_3(g) + 4N_2(g) + 9H_2O(g)$	-	Equation 7
$8NH_4NO_3(s) \xrightarrow{\text{yields}} 2NO_2(g) + 5N_2(g) + 16H_2O(g) + 4NO(g)$	260-300 C	Equation 8
$4NH_4NO_3(s) \xrightarrow{\text{yields}} 2NH_3(g) + 3NO_2(g) + NO(g) + N_2(g) + 5H_2O(g)$	260-300 C	Equation 9

2.3.3 Sensitivity and Energy Output

When considering potential AN events, it is desirable to attempt to identify circumstances that either increase the likelihood of an event and/or increase the severity of the event. While AN is traditionally classified as an oxidizer, there is no shortage of historical events where AN detonated with severe consequences. For the purposes discussed here, any factors that encourage AN to deflagrate, self-heat, or reduce the energy needed to potentially transition to a detonation, will be considered to increase AN sensitivity. In literature, common terms which are useful for sensitivity comparisons include, critical diameter, burning rate, and reaction rate. Temperature and pressure are base factors used to describe the two basic mechanisms explored to evaluate the effect of other factors on sensitivity. The two mechanisms are:

1. Heating the AN to the point that it decomposes, self-heats, and progresses to a detonation. This is typically a slow process. It takes time to initially heat the AN to the point that it self-heats. The general time-frame for this event can vary greatly; from minutes to hours depending on the initial AN sensitivity factors.
2. Shocking the AN or composition to the point that it decomposes, self-heats, and progresses to a detonation. This is a fast time-frame event, since it is caused by pressure waves moving at a velocity near the speed of sound. This event is effectively instantaneous.

Detonation velocity is a common indicator of the overall energy/power of an explosive. Higher denotation velocities result in greater energy output. For the purposes discussed here, any factors that enhance the detonation velocity of AN will be considered to increase AN energy output.

2.3.3.1 Factors of Interest for Sensitivity and Energy Output

Through the history of AN, when evaluating accidents and experiments it is clear that the conditions necessary for detonation and the factors affecting the sensitivity and severity of an event are complex and have complex relationships with each other. However, the general consensus is that the primary factors are physical properties (e.g., particle size, porosity, density), composition (e.g., contaminants, stabilizers, moisture) and environmental factors (e.g., confinement, temperature and pressure).

As seen in the review of past accidents (typically large-scale events) AN detonation is not certain, even in the event of a fire. Post-accident details regarding the primary factors can be very approximate, if known at all. Scientific experiments (typically small-scale) have attempted to isolate and evaluate the contribution of these primary factors to predict the outcome of an AN event. These experiments have had some success in terms of evaluating and eliminating some accident mechanisms (e.g., vapor explosion initiation), but rarely document every primary factor so a complete causation map has not yet been generated. Laboratory experiments are also designed to be repeatable, but not all small-scale conclusions can be applied to large-scale events.

2.3.3.1.1 Physical Properties

The physical properties of AN and AN mixtures includes items like particle structure, particle size, porosity, bulk density and phase. Particle structure types range from powdered AN to AN prills (similar to rice grains). The particle size is typically reported as various percentages for a range of sizes relating to the particle diameter in millimeters (mm). However, particle size can also be described as a Tyler mesh size. This indicates the size of the mesh used to sift the particles. Porosity and void fraction are terms describing the same attribute. It is the fraction of a particle that contains air (voids). This can most easily be visualized by considering a block of Swiss cheese. The volume of the holes (voids) when compared to the entire volume is the porosity. Also related to porosity is the surface area. In most cases, the surface area increases as the porosity increases. Bulk density is similar to the porosity except that it is considering the solid portion (as opposed to voids) and is a bulk property. One way the bulk density can be altered is by compacting the material (increasing density). The phase of AN is a physical property that is also linked to environmental factors. Due to the interest in AN involved with fires, the phase (solid or liquid) of AN is frequently considered.

2.3.3.1.2 Composition

The composition of AN can potentially have wide variation depending on its use case. Typical information regarding AN composition can be specified by the grade, stabilizers, contaminants, and moisture content. A variety of terms exist describing the grade of AN e.g., pure, American Chemical Society (ACS), technical, industrial, explosives, or fertilizer. This designation refers to

the AN as it is provided (to a distributor/seller), but before a potential secondary mixture is made (e.g., use in experiments, or other specialized applications). The grade will commonly indicate the purity of the AN, the physical properties (size), non-AN composition, and moisture content. Most non-AN composition components are stabilizers added to the AN for manufacturing or transportation purposes. These stabilizers can prevent caking of AN in process equipment and/or provide a moisture barrier against excessive water absorption. Contaminants can refer to material that was introduced intentionally (e.g., fuel oil, aluminum) or unintentionally (e.g., grain dust, metal oxides, roof tar). These materials, depending on their quantity, may suppress or enhance AN sensitivity and/or energy output.

2.3.3.1.3 Environmental Factors

Environmental factors that can affect the sensitivity and energy output of AN include confinement, temperature, and pressure. Confinement is the isolation of material in one or more dimensions to inhibit movement or expansion. Examples of confinement include a trench (material is allowed to move/expand in two directions) or a vessel (material cannot move/expand beyond specified volume). Confinement can also be represented in storage arrangement (e.g. pile size, bag stacking arrangement) Temperature and pressure are generally well understood concepts, but it bears reiterating that these two conditions, as well as confinement, can have considerable inter-dependent relationships. Depending on the level of confinement, an increase in pressure will also force an increase in temperature. However, there are some special forms of the pressure condition that are worth explaining in more detail. These pressure conditions are forms of a compression (shock) wave. There are three different mechanisms which are frequently mentioned in literature. The mechanisms are shock due to explosives, vapor cloud explosions, and physical impacts. Shock due to explosives refers to an inducted shock wave generated by a conventional explosive either in physical contact (sympathetic) or from an air shock. An example would be a TNT booster charge placed against/inside an ANFO charge. Vapor cloud explosions shock generation is similar to a conventional explosive, except that is due to a flammable vapor and the shock propagates solely through the air. An example of would be the ignition of a leaking natural gas line. Impact is due to the striking of one object on another. Depending on the impact conditions, this can cause localized sharp pressure (shock wave) in the material. An example would be a bullet or piece of shrapnel hitting a steel plate.

2.3.3.2 Sensitivity

As previously mentioned, factors which encourage AN to deflagrate, self-heat, or transition to a detonation will be considered to increase AN sensitivity. Facilitating or encouraging AN decomposition, self-heating, or even increased burning rates does not ensure detonation. However, it does increase the likelihood of a transition to detonation. Too little research (with narrow focus compared to all of the primary factors) has been performed to date to address

the interactions of the various factors with each other to enhance or suppress AN sensitivity. It is also common to find conflicting statements in literature regarding some of these factors. However based on the current literature available, one can make some qualitative assessments of individual factors on AN sensitivity.

In the base case of very pure (ACS, or technical grade) AN, regardless of particle size, at ambient conditions (atmospheric pressure, and 25 C), and with no confinement, the sensitivity is very low [20, 21, 15]. For reference with other reported critical diameters, the critical diameter for this AN base case is less than 1160 mm [45.7 in] [22]. King [23] reports a critical diameter for prills (0.9 g/cm³) to be ~1000 mm [39.3 in]. In a similar case, pure AN dust has a low sensitivity (dust explosion hazard) [11]. Pure AN is reported to have a run-away decomposition onset at ~300 C (does not ensure DDT). In general, sensitivity is increased as the particle size is reduced [24,25]. The influence of particle size appears to be a minor contributor to sensitivity, when compared to other factors.

When discussing AN grade (aside from pure, ACS, or technical), one can expect the introduction of measurable additives, contaminants, and/or moisture (water). For the conclusions expressed here, it is assumed the additives/contaminants are of comparable size to the AN and mixed homogeneously. Materials that are mixed in (but easily visible) or laying on an AN pile do not have a significant influence on sensitivity [15,26]. Additives are usually materials that assist in the manufacture, transportation, and storage of the AN. However, some additives are “use based”, as in the case of fertilizer grades. Due to the wide variety of potential additives and contaminants, specific results will require individual testing, however some conclusions regarding general categories can be made. [REDACTED]

[REDACTED] [11,27, 20,28, 15,29]. This is primarily due to essentially the addition of a fuel

²⁰ Izato, Y.-i., A. Miyake, and S. Date, *Combustion Characteristics of Ammonium Nitrate and Carbon Mixtures Based on a Thermal Decomposition Mechanism*. Propellants, Explosives, Pyrotechnics, 2013. **38**(1): p. 129-135.

²¹ Dolah, R.W.V., *Explosion Hazards of ammonium nitrate under fire exposure*. U.S. Dept. of Interior, Bureau of Mines, 1966: p. 79.

²² Nygaard, E.C., *Large scale testing of ammonium nitrate*. The 4th EFEE World Conf. of Explosives and Blasting, 2007. **4**(1).

²³ King, D.A.W., *Threshold Shock Initiation Parameters of Liquid Phase Ammonium Nitrate*. 2008: p. 26.

²⁴ Winning, C.H., *Detonation characteristics of prilled ammonium nitrate*. Fire Technology, 1965. **1**(1): p. 23-31.

²⁵ Miyake, A., et al., *Detonation characteristics of ammonium nitrate and activated carbon mixtures*. Journal of Loss Prevention in the Process Industries, 2007. **20**(4-6): p. 584-588.

²⁶ Marshall, A., *Explosibility of ammonium nitrate*. Nature, 1949. **164**(4165): p. 348-349.

²⁷ Ermolaev, B.S., et al., *Initial stage of the explosion of ammonium nitrate and its powder mixtures*. Russian Journal of Physical Chemistry B, 2010. **5**(4): p. 640-649.

²⁸ Ottoson, K.G., *Investigation of Sensitivity of fertilizer grade ammonium nitrate to explosion. Explosibility of Cal-Nitro and uraform-ammonium nitrate fertilizers*. Picatinny arsenal Technical Division, 1948: p. 8.

²⁹ Macy, P.F., *Investigation of Sensitivity of Fertilizer Grade Ammonium Nitrate to Explosion*. Picatinny arsenal Technical Division Chemical Branch, 1947(1658): p. 1-49.

(organic compound) to a strong oxidizer (AN) which encourages combustion. For example, one fertilizer grade (0.4% organic coating) mixture showed no increase in sensitivity when compared to pure. [REDACTED]

[REDACTED] [30]. [REDACTED] [20, 28,31]. [REDACTED] [28]. [REDACTED] [16,19, 11, 20,32,33, 14,34, 6, 13,35]. [REDACTED]

[REDACTED] [6]. In some accident cases, it was presumed that compounds from stainless steel corrosion (e.g., chlorides, chromates, nickel) was sufficient to significantly increase AN sensitivity [33]. Solution acidity also has a strong influence on AN sensitivity. AN sensitivity increases (encourages decomposition) as acidity increases [36, 11, 33, 14,37]. In AN manufacturing it is common to inject ammonia into the AN solution to keep the pH of the solution higher than 4 (neutral to basic) [33]. Since AN is hygroscopic, it is common for coatings to be added to prevent excessive water absorption. The amount of water in a particular batch of AN will vary with grade and time. Experiments with 1% water, or more, with AN has shown to reduce sensitivity [38]. AN mixtures with 0.15% water have shown to decompose slower vs. those without any water [26]. However, it has also been noted that while the presence of water has a de-sensitizing effect, the evaporation of water (during accelerated decomposition or other event) will take ammonia with it, subsequently increasing the solution acidity (decrease pH). Adding compounds to AN can have a wide range of influence on the overall AN mixture sensitivity. Water and inorganic compounds in small to large quantities can have a de-sensitizing effect. Organic compounds over ~1% range can increase sensitivity. Metal powders, metal salts, chloride and chromate compounds even in the smallest amount (0.1%) can significantly increase sensitivity.

³⁰ Verrato, P., *Investigation of Sensitivity of Fertilizer Grade Ammonium nitrate to Explosion-Relative sensitivity of pure, Wax-Coated and Fertilizer Grade Ammonium Nitrate*. Picatinny arsenal Technical Division, 1949(1720): p. 26.

³¹ Clancey, V.J., *The Explosive and fire hazard characteristics of ammonium nitrate fertilizers: Part 2 Assessment of the fire hazard*. Royal Armament Research and Development Establishment, 1966. **Explosives Division**(1/66).

³² Oommen, C. and S.R. Jain, *Ammonium nitrate: a promising rocket propellant oxidizer*. Journal of Hazardous Materials, 1999. **67**(3): p. 253-281.

³³ Ettouney, R.S. and M.A. El-Rifai, *Explosion of ammonium nitrate solutions, two case studies*. Process Safety and Environmental Protection, 2012. **90**(1): p. 1-7.

³⁴ Sinditskii, V.P., et al., *Ammonium Nitrate: Combustion Mechanism and the Role of Additives*. Propellants, Explosives, Pyrotechnics, 2005. **30**(4): p. 269-280.

³⁵ Jahrestagung, F.-I.f.C.T.I., et al., *Energetic Materials : Performance and Safety: 36th International Annual Conference of ICT & 32nd International Pyrotechnics Seminar : June 28-July 1, 2005, Karlsruhe, Federal Republic of Germany*. 2005: Fraunhofer-Institut für Chemische Technologie.

³⁶ Turcotte, R., et al., *Thermal hazard assessment of AN and AN-based explosives*. Journal of Hazardous Materials, 2003. **101**(1): p. 1-27.

³⁷ Little, A.D., *Study of Ammonium Nitrate Materials*. 1952: p. 1-49.

³⁸ Munroe, C.E., *The Explosivity of Ammonium nitrate*. Chemical & Metallurgical Engineering, 1922. **26**: p. 535-542.

Confinement is a difficult factor to quantify, and as mentioned previously, it does have relationships with temperature and pressure. However, the consensus in the literature is quite clear that sensitivity increases as confinement increases ^[14]. [REDACTED]

[REDACTED] ^[20, 32, 14, 21, 28, 26, 15]. For example, AN near its melting point (~170 C) has a critical diameter of 102-127 mm (4-5 in) with light* confinement. Under heavy* confinement, the critical diameter reduces to ~51 mm (2 in) ^[21]. Large piles or bags of AN can create self-imposed confinement for the inner material, which can increase sensitivity if other enhancing factors exist (e.g., elevated temperature/fire, hot penetrating projectiles). [REDACTED] ^[21, 28]. Bagged AN can allow fire to penetrate the pile to encourage confined heating. Several experiments have indicated that surface burning of combustible material on AN piles has not lead to detonation ^[21, 15]. As confinement for AN is increased, the sensitivity is increased.

The phase of AN and AN mixtures as well as the density are primarily evaluated as a function of temperature. Considering AN in solid form (at room temperature), the maximum theoretical density is 1.7 g/cm³ ^[39]. [REDACTED]

[REDACTED] ^[6, 15]. A significant portion of AN experimentation deals with molten AN (liquid phase). [REDACTED]

[REDACTED] ^[16, 11, 23, 33, 21, 13, 15]. The critical diameter for molten AN at 220 C is 76-114 mm (3-4.5 in) ^[21] At temperatures above the melting point of AN (~170 C) decomposition reactions are taking place (Equation 2) that produce gas phase materials. These gas bubbles reduce the overall density and increase the number of “hot spots,” which are potential start points for a run-away decomposition or detonation. Tests have been performed which show that molten AN (190 C) with glass micro-balloons to simulate the density of AN at 260 C produced the same sensitivity results as AN truly at 260 C ^[23]. A considerable number of references state the increased danger in molten AN in confined areas ^[11, 32, 21]. As the AN temperature is increased, especially at and beyond the molten phase, the sensitivity increases.

Pressure in the form of a static load (inside of an enclosure) or a dynamic load (shock wave) can also influence and/or be a measure of AN sensitivity. Static loading is more akin to confinement situation. Experiments with a closed vessel show that sensitivity is increased (onset temperature lowered) when the vessel is pressurized to over 27.5 MPa. The reaction’s onset temperature shows no change in the 0-27.5 MPa range. In order to evaluate the effect of projectile impact or other methods of applying shock waves to AN, it is important to define the

* This terminology used but not defined by the author of the source material

³⁹ Presles, H.-N., P. Vidal, and B. Khasainov, *Experimental study of the detonation of technical grade ammonium nitrate*. *Comptes Rendus Mécanique*, 2009. **337**(11–12): p. 755-760.

critical pressure. The critical pressure is the pressure needed to ensure a transition to detonation from a shock wave .

The following critical pressures were presented for AN at different temperatures, which shows that the shock pressure necessary to initiate detonation decreases with increasing temperature. In the data provided by King ^[23], the critical pressure for molten AN decreases exponentially as temperature increases. This further reinforces that sensitivity increases as temperature increases.

- 25 C $P_{cr} = 2,027$ MPa (estimated) ^[21]
- 230 C $P_{cr} = 12,500$ MPa (extrapolated) ^[23]
- 250 C $P_{cr} = 350-510$ MPa ^[15]
- [REDACTED] ^[11, 23, 13]
- 300 C $P_{cr} = 600$ MPa ^[15]

In the explosives industry, it is relatively common knowledge that a powerful booster is need to detonate AN (even with a combustible additive, such as fuel oil). When using a booster charge (e.g., TNT, PETN), the booster is in direct contact with the AN explosive. For example TNT (1.6 g/cm³) generates a shock wave with a peak pressure of 18,000 MPa ^[40]. This concept is important when considering storage of AN near other material. In 1942 a 200 ton AN pile detonated, but failed to initiate a neighboring 60 ton pile of AN located 80 ft away ^[7]. The potential for sympathetic detonation from vapor cloud explosions (e.g. propane tanks) is a commonly considered event in accident situations. The most severe vapor cloud detonations are acetylene/oxygen mixtures. These mixtures have been experimentally shown to generate a maximum shock wave of 10 MPa ^[21]. Several experiments have been performed, and all of the results have indicated that AN (even sensitized from elevated temperatures) has an extremely small likelihood of initiation ^[21, 37]. When considering the effect of physical impact on AN, the impact pressure and the critical diameter are of interest. The increased/decreased sensitivity of the AN dictates the size, weight, and velocity of the projectile necessary to initiate a detonation. The experimental results are mixed in terms of reported conditions. Ideally, the reported values would be the condition of the AN (temperature, composition, etc.) and the critical pressure. The data based on bullet impact really only provide a general sense of sensitivity, since bullets have impact surfaces with special geometries. With the data that is reported (Table 4) in the literature, the observation can be made that AN, near and above its melting point, can be realistically be initiated by bullet/projectile impact.

⁴⁰ Cooper, P.W., *Explosives Engineering*. 2009: John Wiley & Sons, Incorporated.

Table 4. Detonation Results for Heated AN from Different Bullet Impacts

AN Temperature (C)	Weight (grain)	Diameter (caliber)	Velocity (m/s)	Detonation	Reference
140	110	0.3	1,080	Yes	[21]
220	110	0.3	1,080	Yes	[21]
260	-	150 mm	190	Yes (estimate)	[23]
260	-	0.3	823	Yes	[21]

Since bullet impact is shown to initiate AN, more detailed experiments were performed using flyer plates. Flyer plate impact experiments provide more consistent and controllable conditions for evaluating the sensitivity of different conditions. For AN at 260 C, a 2 inch impact surface can initiate detonation between 180 and 190 m/s [23]. For AN at 260 C, a 6 inch impact surface can initiate detonation between 122 and 190 m/s [23]. This illustrates that both the critical diameter and critical pressure must be achieved for the AN, in order for a detonation to occur.

While experimental impacts (e.g. bullets, flyer plates) are instructive on the sensitivity to projectile impact, accident scenarios (e.g. rupturing vessels, falling debris) contain a wide range of impact geometries and velocities. [REDACTED]

[REDACTED] [11, 21, 29, 15]. However, in certain conditions, it does seem possible that the impact of a sufficiently large and high velocity projectile into sensitized AN may be sufficient to transition to detonation [11, 21]. While most projectile impacts will likely not initiate due to shock, it should be considered that hot projectile may be able to penetrate the pile. Since the thermal conductivity of AN is low (thermal insulator), a hot projectile may locally sensitize AN (on a thermal basis) inside the pile [37].

2.3.3.3 Energy Output

As previously mentioned, detonation velocity is a common indicator for the overall energy/power of an explosive. The various experimental parameters and results, for the references evaluated, are collated in Table 5. In many cases, several of the experimental parameters were not reported and methods can vary greatly, so only general conclusions can be drawn from the available data. Experimental results for the most part are also performed with near perfect initiation mechanisms (not representative of unintentional events), so the conclusions should be considered to be conservative. Assuming AN was perfectly initiated and exhibited an ideal detonation, the maximum calculated detonation velocity is ~5.4 km/s (60%

TNT_{eq}). The US Army Field Manual ^[41] (AN < 0.5% water, 1.12 g/cm³) suggests an equivalency factor of 23% (3.35 km/s). The highest TNT_{eq} for pure AN at room temperature in the reviewed literature was 15% (2.7 km/s) ^[42, 18]. However, the average TNT_{eq} for pure AN (all grades) at ambient conditions was 4.3%.

Some conclusions can be made with organic additives/contaminants, but it is recommended that individual studies be performed, due to the wide range of possibilities. Using the data provided by Miyake ^[25], for AN with 7% activated carbon (organic additive) the TNT_{eq} increased from 20% to 22.5% by changing from prilled AN (size 1.15 mm, 0.865 g/cm³) to powdered AN (size 0.14 mm, 0.92 g/cm³, respectively. The same dataset for AN with 10% activated carbon (organic additive), shows a TNT_{eq} increase from 17% to 23% for prilled AN and powdered AN, respectively. This illustrates that in lieu of other sensitizing factors, smaller particle size (powdered vs. prilled) results in an increased TNT_{eq}. Interestingly, increasing the amount of activated carbon for prilled AN decreased the TNT_{eq}, while for powdered AN, increasing the amount of activated carbon generally increased the TNT_{eq}. However, this result is likely due to limited data, since it is expected that there is an optimal concentration (maximum TNT_{eq}) for each additive given a specific AN state; increases above this amount will reduce the energy output. [29]

. The particle size of AN seems to have a small influence on increasing the energy output, especially when combined with other factors. Generally, organic compounds do increase the energy output of AN. However, in the 10-20% range the maximum additive limit is reached and the energy output can drop significantly.

Some conclusions can be made with inorganic additives/contaminants, but it is recommended that individual studies be performed, due to the wide range of possibilities. While chloride compounds have a significant impact on sensitivity, no experiments were found that presented detonation data. The addition of powdered aluminum (10%) indicated a marked increase in TNT_{eq} (65%) over pure AN ^[43]. This equivalence increases to 70% as the aluminum composition increases to 20%. As seen with organic compounds, there is a limit for additives where the energy output is at a maximum and increasing the additive composition beyond this will reduce the TNT_{eq}. Increasing the aluminum composition to 30% dropped the TNT_{eq} to 60%. Experiments with ammonium carbonate show a decrease in TNT_{eq} (13% to 9%) as the additive is

⁴¹ United States. Headquarters, D.o.t.a., *Explosives and demolitions: FM 5-25*. 1994: Paladin Press.

⁴² Shvedov, K.K., A.I. Kazakov, and Y.I. Rubtsov, *Shock-wave sensitivity and self-propagating explosive processes in binary mixtures on the basis of ammonium nitrate with exo- and endothermic transformations of the components*. Russian Journal of Physical Chemistry B, 2007. 1(6): p. 553-562.

⁴³ Keshavarz, M.H., *Simple correlation for predicting detonation velocity of ideal and non-ideal explosives*. Journal of Hazardous Materials, 2009. 166(2-3): p. 762-769.

increased (20% to 30%) [42]. [REDACTED]
[REDACTED]
[REDACTED] [28, 42]. The experiments from Miyake [25], include a series of prilled AN at ambient conditions with a constant composition of potassium nitrate (inorganic) and varying amounts of activated carbon (organic). The potassium nitrate composition was kept constant at 10%. The TNT_{eq} saw an increase from 5% to 17% as the activated carbon was increased from 1% to 10%. When the organic compound was increased to 20%, the TNT_{eq} dropped to 8%. For metals (aluminum specifically), the energy output is increased as the metal content is increased. The energy gains, in general, for metals are significantly large when compared to organic additives. In the 20-30% range the maximum metal additive limit is reached and the energy output can drop. Chloride compounds aside, inorganic compounds appear to have a small increase (less than organic additives) on TNT_{eq}. While the current data does not indicate at which point the maximum contribution is reached, compositions up to ~40% can significantly increase detonation resistance.

The data provided by Winning [24] implies that for AN in prill form, the TNT_{eq} (12-26%) increases linearly for increasing density (0.52-1.02 g/cm³). King [23] provides 14 data points for liquid AN (assuming no contaminants) for a temperature range of 220-262 C. At the ends of the evaluated spectrum the TNT_{eq} is 16% (2.8 km/s) and 7% (1.8 km/s) for 219 C and 263 C, respectively. The trend of the data shows that the detonation velocity decreases as temperature increases for AN in liquid form.

Table 5. TNT Equivalency of Ammonium Nitrate Based on Experimental Factors

Reference	Name	Type of AN	AN Particle Diameter	AN Pore Diameter	Contaminants	Contaminant size	Contaminant %	Bulk Density	Confinement Material	Confinement Shape	Charge Diameter (mm)	Phase	Temperature C	Initiator	Detonation Velocity (km/s)	TNT Eq (%)
[28]	[REDACTED]	[REDACTED]	[REDACTED]	[REDACTED]	[REDACTED]	[REDACTED]	[REDACTED]	[REDACTED]	[REDACTED]	[REDACTED]	[REDACTED]	[REDACTED]	[REDACTED]	[REDACTED]	[REDACTED]	[REDACTED]
[28]	[REDACTED]	[REDACTED]	[REDACTED]	[REDACTED]	[REDACTED]	[REDACTED]	[REDACTED]	[REDACTED]	[REDACTED]	[REDACTED]	[REDACTED]	[REDACTED]	[REDACTED]	[REDACTED]	[REDACTED]	[REDACTED]
[28]	[REDACTED]	[REDACTED]	[REDACTED]	[REDACTED]	[REDACTED]	[REDACTED]	[REDACTED]	[REDACTED]	[REDACTED]	[REDACTED]	[REDACTED]	[REDACTED]	[REDACTED]	[REDACTED]	[REDACTED]	[REDACTED]
[28]	[REDACTED]	[REDACTED]	[REDACTED]	[REDACTED]	[REDACTED]	[REDACTED]	[REDACTED]	[REDACTED]	[REDACTED]	[REDACTED]	[REDACTED]	[REDACTED]	[REDACTED]	[REDACTED]	[REDACTED]	[REDACTED]
[44]	[REDACTED]	[REDACTED]	[REDACTED]	[REDACTED]	[REDACTED]	[REDACTED]	[REDACTED]	[REDACTED]	[REDACTED]	[REDACTED]	[REDACTED]	[REDACTED]	[REDACTED]	[REDACTED]	[REDACTED]	[REDACTED]
[44]	[REDACTED]	[REDACTED]	[REDACTED]	[REDACTED]	[REDACTED]	[REDACTED]	[REDACTED]	[REDACTED]	[REDACTED]	[REDACTED]	[REDACTED]	[REDACTED]	[REDACTED]	[REDACTED]	[REDACTED]	[REDACTED]
[44]	[REDACTED]	[REDACTED]	[REDACTED]	[REDACTED]	[REDACTED]	[REDACTED]	[REDACTED]	[REDACTED]	[REDACTED]	[REDACTED]	[REDACTED]	[REDACTED]	[REDACTED]	[REDACTED]	[REDACTED]	[REDACTED]
[44]	[REDACTED]	[REDACTED]	[REDACTED]	[REDACTED]	[REDACTED]	[REDACTED]	[REDACTED]	[REDACTED]	[REDACTED]	[REDACTED]	[REDACTED]	[REDACTED]	[REDACTED]	[REDACTED]	[REDACTED]	[REDACTED]
[44]	[REDACTED]	[REDACTED]	[REDACTED]	[REDACTED]	[REDACTED]	[REDACTED]	[REDACTED]	[REDACTED]	[REDACTED]	[REDACTED]	[REDACTED]	[REDACTED]	[REDACTED]	[REDACTED]	[REDACTED]	[REDACTED]
[44]	[REDACTED]	[REDACTED]	[REDACTED]	[REDACTED]	[REDACTED]	[REDACTED]	[REDACTED]	[REDACTED]	[REDACTED]	[REDACTED]	[REDACTED]	[REDACTED]	[REDACTED]	[REDACTED]	[REDACTED]	[REDACTED]
[44]	[REDACTED]	[REDACTED]	[REDACTED]	[REDACTED]	[REDACTED]	[REDACTED]	[REDACTED]	[REDACTED]	[REDACTED]	[REDACTED]	[REDACTED]	[REDACTED]	[REDACTED]	[REDACTED]	[REDACTED]	[REDACTED]
[44]	[REDACTED]	[REDACTED]	[REDACTED]	[REDACTED]	[REDACTED]	[REDACTED]	[REDACTED]	[REDACTED]	[REDACTED]	[REDACTED]	[REDACTED]	[REDACTED]	[REDACTED]	[REDACTED]	[REDACTED]	[REDACTED]
[44]	[REDACTED]	[REDACTED]	[REDACTED]	[REDACTED]	[REDACTED]	[REDACTED]	[REDACTED]	[REDACTED]	[REDACTED]	[REDACTED]	[REDACTED]	[REDACTED]	[REDACTED]	[REDACTED]	[REDACTED]	[REDACTED]
[44]	[REDACTED]	[REDACTED]	[REDACTED]	[REDACTED]	[REDACTED]	[REDACTED]	[REDACTED]	[REDACTED]	[REDACTED]	[REDACTED]	[REDACTED]	[REDACTED]	[REDACTED]	[REDACTED]	[REDACTED]	[REDACTED]
[44]	[REDACTED]	[REDACTED]	[REDACTED]	[REDACTED]	[REDACTED]	[REDACTED]	[REDACTED]	[REDACTED]	[REDACTED]	[REDACTED]	[REDACTED]	[REDACTED]	[REDACTED]	[REDACTED]	[REDACTED]	[REDACTED]
[44]	[REDACTED]	[REDACTED]	[REDACTED]	[REDACTED]	[REDACTED]	[REDACTED]	[REDACTED]	[REDACTED]	[REDACTED]	[REDACTED]	[REDACTED]	[REDACTED]	[REDACTED]	[REDACTED]	[REDACTED]	[REDACTED]
[44]	[REDACTED]	[REDACTED]	[REDACTED]	[REDACTED]	[REDACTED]	[REDACTED]	[REDACTED]	[REDACTED]	[REDACTED]	[REDACTED]	[REDACTED]	[REDACTED]	[REDACTED]	[REDACTED]	[REDACTED]	[REDACTED]
[44]	[REDACTED]	[REDACTED]	[REDACTED]	[REDACTED]	[REDACTED]	[REDACTED]	[REDACTED]	[REDACTED]	[REDACTED]	[REDACTED]	[REDACTED]	[REDACTED]	[REDACTED]	[REDACTED]	[REDACTED]	[REDACTED]
[44]	[REDACTED]	[REDACTED]	[REDACTED]	[REDACTED]	[REDACTED]	[REDACTED]	[REDACTED]	[REDACTED]	[REDACTED]	[REDACTED]	[REDACTED]	[REDACTED]	[REDACTED]	[REDACTED]	[REDACTED]	[REDACTED]
[44]	[REDACTED]	[REDACTED]	[REDACTED]	[REDACTED]	[REDACTED]	[REDACTED]	[REDACTED]	[REDACTED]	[REDACTED]	[REDACTED]	[REDACTED]	[REDACTED]	[REDACTED]	[REDACTED]	[REDACTED]	[REDACTED]
[44]	[REDACTED]	[REDACTED]	[REDACTED]	[REDACTED]	[REDACTED]	[REDACTED]	[REDACTED]	[REDACTED]	[REDACTED]	[REDACTED]	[REDACTED]	[REDACTED]	[REDACTED]	[REDACTED]	[REDACTED]	[REDACTED]
[44]	[REDACTED]	[REDACTED]	[REDACTED]	[REDACTED]	[REDACTED]	[REDACTED]	[REDACTED]	[REDACTED]	[REDACTED]	[REDACTED]	[REDACTED]	[REDACTED]	[REDACTED]	[REDACTED]	[REDACTED]	[REDACTED]
[32]	None	Pure	Unknown	Unknown	None	Unknown	0	1.725	Unknown	Unknown	Unknown	Solid	Unknown	Unknown	4.65	44.8%
[43]	Amatex-20	Pure	Unknown	Unknown	RDX/TNT	Unknown	20%/38%	1.66	Unknown	Unknown	Unknown	Solid	Unknown	Unknown	7.55	118.0%

⁴⁴ Akst, I., *EXPLOSIVE PERFORMANCE MODIFICATION BY COSOLIDIFICATION OF AMMONIUM NITRATE WITH FUELS*. US ARMY Picatinny Arsenal, 1976(4987): p. 59.

Table 5. TNT Equivalency of Ammonium Nitrate Based on Experimental Factors

Reference	Name	Type of AN	AN Particle Diameter	AN Pore Diameter	Contaminants	Contaminant size	Contaminant %	Bulk Density	Confinement Material	Confinement Shape	Charge Diameter (mm)	Phase	Temperature C	Initiator	Detonation Velocity (km/s)	TNT Eq (%)
[43]	Amatex-40	Pure	Unknown	Unknown	RDX/TNT	Unknown	41%/38%	1.61	Unknown	Unknown	Unknown	Solid	Unknown	Unknown	7.01	101.7%
[43]	Amatol-60/40	Pure	Unknown	Unknown	TNT	Unknown	40%	1.6	Unknown	Unknown	Unknown	Solid	Unknown	Unknown	5.76	68.7%
[43]	Amatol-80/20	Pure	Unknown	Unknown	TNT	Unknown	20%	1.6	Unknown	Unknown	Unknown	Solid	Unknown	Unknown	5.2	56.0%
[43]	AN	Pure	Unknown	Unknown	None	Unknown	0%	1.05	Unknown	Unknown	Unknown	Solid	Unknown	Unknown	4.5	41.9%
[43]	90/10 AN/AI	Pure	Unknown	Unknown	Aluminum	Unknown	10%	1.05	Unknown	Unknown	Unknown	Solid	Unknown	Unknown	5.6	64.9%
[43]	80/20 AN/AI	Pure	Unknown	Unknown	Aluminum	Unknown	20%	1.05	Unknown	Unknown	Unknown	Solid	Unknown	Unknown	5.8	69.6%
[43]	70/30 AN/AI	Pure	Unknown	Unknown	Aluminum	Unknown	30%	1.05	Unknown	Unknown	Unknown	Solid	Unknown	Unknown	5.4	60.4%
[43]	ANFO-6/94	Pure	Unknown	Unknown	Fuel Oil	Unknown	94%	0.88	Unknown	Unknown	Unknown	Solid	Unknown	Unknown	5.5	62.6%
[39]	Technical Grade AN	Technical Grade	1-2 mm	Unknown	None	None	0%	0.66	Steel	Cylinder	53	Solid	Unknown	Pentrite (FORMEX)	1.9	7.3%
[39]	Technical Grade AN	Technical Grade	1-2 mm	Unknown	None	None	0%	0.66	Steel	Cylinder	41	Solid	Unknown	Pentrite (FORMEX)	1.7	5.8%
[39]	Technical Grade AN	Technical Grade	1-2 mm	Unknown	None	None	0%	0.66	Steel	Cylinder	36	Solid	Unknown	Pentrite (FORMEX)	1.5	4.8%
[39]	Technical Grade AN	Technical Grade	1-2 mm	Unknown	None	None	0%	0.66	Steel	Cylinder	27	Solid	Unknown	Pentrite (FORMEX)	1.3	3.3%
[39]	Technical Grade AN	Technical Grade	1-2 mm	Unknown	None	None	0%	0.66	Steel	Cylinder	21	Solid	Unknown	Pentrite (FORMEX)	1.2	2.9%
[39]	Technical Grade AN	Technical Grade	1-2 mm	Unknown	None	None	0%	0.66	Steel	Cylinder	15	Solid	Unknown	Pentrite (FORMEX)	1.1	2.7%
[39]	Technical Grade AN	Technical Grade	1-2 mm	Unknown	None	None	0%	0.66	Steel	Cylinder	12	Solid	Unknown	Pentrite (FORMEX)	1.2	2.9%
[39]	Technical Grade AN	Technical Grade	1-2 mm	Unknown	None	None	0%	0.66	PVC	Cylinder	81	Solid	Unknown	Pentrite (FORMEX)	1.6	5.0%
[23]	CIL LD	Prill	Unknown	Unknown	None	None	0%	0.8	None	Hemisphere	6 ft	Solid	Unknown	50/50 pentolite or TNT	3.3	22.4%
[23]	Genstar XP	Prill	Unknown	Unknown	None	None	0%	0.74	None	Hemisphere	6 ft	Solid	Unknown	50/50 pentolite or TNT	3.2	21.2%
[23]	Cyanamid LD	Prill	Unknown	Unknown	None	None	0%	0.8	None	Hemisphere	6 ft	Solid	Unknown	50/50 pentolite or TNT	3.2	21.3%
[23]	Cyanamid MD	Prill	Unknown	Unknown	None	None	0%	0.86	None	Hemisphere	6 ft	Solid	Unknown	50/50 pentolite or TNT	2.7	14.8%

Table 5. TNT Equivalency of Ammonium Nitrate Based on Experimental Factors

Reference	Name	Type of AN	AN Particle Diameter	AN Pore Diameter	Contaminants	Contaminant size	Contaminant %	Bulk Density	Confinement Material	Confinement Shape	Charge Diameter (mm)	Phase	Temperature C	Initiator	Detonation Velocity (km/s)	TNT Eq (%)
[23]	Unknown	Unknown	N/A	Unknown	Unknown	None	0%	Unknown	Steel	Cylinder	5 in	Liquid	220	Unknown	2.5	13.4%
[23]	Unknown	Unknown	N/A	Unknown	Unknown	None	0%	Unknown	Steel	Cylinder	5 in	Liquid	220	Unknown	2.8	16.0%
[23]	Unknown	Unknown	N/A	Unknown	Unknown	None	0%	Unknown	Steel	Cylinder	5 in	Liquid	220	Unknown	2.5	13.3%
[23]	Unknown	Unknown	N/A	Unknown	Unknown	None	0%	Unknown	Steel	Cylinder	5 in	Liquid	225	Unknown	2.4	12.1%
[23]	Unknown	Unknown	N/A	Unknown	Unknown	None	0%	Unknown	Steel	Cylinder	5 in	Liquid	230	Unknown	2.4	11.5%
[23]	Unknown	Unknown	N/A	Unknown	Unknown	None	0%	Unknown	Steel	Cylinder	5 in	Liquid	234	Unknown	2.2	10.0%
[23]	Unknown	Unknown	N/A	Unknown	Unknown	None	0%	Unknown	Steel	Cylinder	5 in	Liquid	236	Unknown	2.2	9.8%
[23]	Unknown	Unknown	N/A	Unknown	Unknown	None	0%	Unknown	Steel	Cylinder	5 in	Liquid	240	Unknown	2.2	9.7%
[23]	Unknown	Unknown	N/A	Unknown	Unknown	None	0%	Unknown	Steel	Cylinder	5 in	Liquid	241	Unknown	2.1	8.9%
[23]	Unknown	Unknown	N/A	Unknown	Unknown	None	0%	Unknown	Steel	Cylinder	5 in	Liquid	250	Unknown	2.0	8.1%
[23]	Unknown	Unknown	N/A	Unknown	Unknown	None	0%	Unknown	Steel	Cylinder	5 in	Liquid	252	Unknown	1.9	7.8%
[23]	Unknown	Unknown	N/A	Unknown	Unknown	None	0%	Unknown	Steel	Cylinder	5 in	Liquid	254	Unknown	2.0	8.5%
[23]	Unknown	Unknown	N/A	Unknown	Unknown	None	0%	Unknown	Steel	Cylinder	5 in	Liquid	260	Unknown	2.0	8.0%
[23]	Unknown	Unknown	N/A	Unknown	Unknown	None	0%	Unknown	Steel	Cylinder	5 in	Liquid	262	Unknown	2.0	8.0%
[25]	Prilled AN	Prill	1.15 mm	Unknown	Activated Carbon	3.41 um	7%	0.865	Steel	Cylinder	35.5 mm	Solid	Unknown	C-4 and RDX	3.1	19.9%
[25]	Prilled AN	Prill	1.15 mm	Unknown	Activated Carbon	3.41 um	10%	0.815	Steel	Cylinder	35.5 mm	Solid	Unknown	C-4 and RDX	2.9	16.8%
[25]	Phase-stablized AN	Prill	0.13 mm	Unknown	Potassium Nitrate/Activated Carbon	AC 3.41 um	10%/1%	0.985	Steel	Cylinder	35.5 mm	Solid	Unknown	C-4 and RDX	1.6	5.3%
[25]	Phase-stablized AN	Prill	0.13 mm	Unknown	Potassium Nitrate/Activated Carbon	AC 3.41 um	10%/8%	0.945	Steel	Cylinder	35.5 mm	Solid	Unknown	C-4 and RDX	2.4	11.4%
[25]	Phase-stablized AN	Prill	0.13 mm	Unknown	Potassium Nitrate/Activated Carbon	AC 3.41 um	10%/10%	0.885	Steel	Cylinder	35.5 mm	Solid	Unknown	C-4 and RDX	2.9	16.8%
[25]	Phase-stablized AN	Prill	0.13 mm	Unknown	Potassium Nitrate/Activated Carbon	AC 3.41 um	10%/20%	0.715	Steel	Cylinder	35.5 mm	Solid	Unknown	C-4 and RDX	2.0	7.9%
[25]	Powdered AN	Powdered	0.14 mm	Unknown	Activated Carbon	3.41 um	0.1%	1.010	Steel	Cylinder	35.5 mm	Solid	Unknown	C-4 and RDX	1.25	3.2%

Table 5. TNT Equivalency of Ammonium Nitrate Based on Experimental Factors

Reference	Name	Type of AN	AN Particle Diameter	AN Pore Diameter	Contaminants	Contaminant size	Contaminant %	Bulk Density	Confinement Material	Confinement Shape	Charge Diameter (mm)	Phase	Temperature C	Initiator	Detonation Velocity (km/s)	TNT Eq (%)
[25]	Powdered AN	Powdered	0.14 mm	Unknown	Activated Carbon	3.41 um	0.3%	1.010	Steel	Cylinder	35.5 mm	Solid	Unknown	C-4 and RDX	1.60	5.3%
[25]	Powdered AN	Powdered	0.14 mm	Unknown	Activated Carbon	3.41 um	0.5%	0.980	Steel	Cylinder	35.5 mm	Solid	Unknown	C-4 and RDX	1.75	6.3%
[25]	Powdered AN	Powdered	0.14 mm	Unknown	Activated Carbon	3.41 um	1%	0.965	Steel	Cylinder	35.5 mm	Solid	Unknown	C-4 and RDX	2.05	8.7%
[25]	Powdered AN	Powdered	0.14 mm	Unknown	Activated Carbon	3.41 um	3%	0.960	Steel	Cylinder	35.5 mm	Solid	Unknown	C-4 and RDX	2.95	18.0%
[25]	Powdered AN	Powdered	0.14 mm	Unknown	Activated Carbon	3.41 um	5%	0.915	Steel	Cylinder	35.5 mm	Solid	Unknown	C-4 and RDX	3.40	23.9%
[25]	Powdered AN	Powdered	0.14 mm	Unknown	Activated Carbon	3.41 um	7%	0.920	Steel	Cylinder	35.5 mm	Solid	Unknown	C-4 and RDX	3.30	22.5%
[25]	Powdered AN	Powdered	0.14 mm	Unknown	Activated Carbon	3.41 um	10%	0.900	Steel	Cylinder	35.5 mm	Solid	Unknown	C-4 and RDX	3.35	23.2%
[25]	Powdered AN	Powdered	0.14 mm	Unknown	Activated Carbon	3.41 um	13%	0.840	Steel	Cylinder	35.5 mm	Solid	Unknown	C-4 and RDX	3.35	23.2%
[25]	Powdered AN	Powdered	0.14 mm	Unknown	Activated Carbon	3.41 um	15%	0.840	Steel	Cylinder	35.5 mm	Solid	Unknown	C-4 and RDX	2.95	18.0%
[25]	Powdered AN	Powdered	0.14 mm	Unknown	Activated Carbon	3.41 um	20%	0.745	Steel	Cylinder	35.5 mm	Solid	Unknown	C-4 and RDX	2.60	14.0%
[45]	A-1	Unknown	1.46 mm	15.1 um	Decane	N/A	94%	0.845	Steel	Cylinder	35.5 mm	Solid	Unknown	No. 6 electric detonator	2.85	16.8%
[45]	A-2	Unknown	1.46 mm	15.1 um	Decane	N/A	94%	0.845	Steel	Cylinder	35.5 mm	Solid	Unknown	No. 6 electric detonator	2.95	18.0%
[45]	A# (Aged)	Unknown	1.46 mm	15.1 um	Decane	N/A	94%	0.855	Steel	Cylinder	35.5 mm	Solid	Unknown	No. 6 electric detonator	2.90	17.4%
[45]	B-1	Unknown	1.40 mm	8.2 um	Decane	N/A	94%	0.870	Steel	Cylinder	35.5 mm	Solid	Unknown	No. 6 electric detonator	3.35	23.2%
[45]	B-2	Unknown	1.40 mm	8.2 um	Decane	N/A	94%	0.870	Steel	Cylinder	35.5 mm	Solid	Unknown	No. 6 electric detonator	3.20	21.2%
[45]	B# (Aged)	Unknown	1.40 mm	8.2 um	Decane	N/A	94%	0.865	Steel	Cylinder	35.5 mm	Solid	Unknown	No. 6 electric detonator	3.20	21.2%
[45]	C-1	Unknown	1.35 mm	4.5 um	Decane	N/A	94%	0.850	Steel	Cylinder	35.5 mm	Solid	Unknown	No. 6 electric detonator	3.30	22.5%
[45]	C-2	Unknown	1.35 mm	4.5 um	Decane	N/A	94%	0.850	Steel	Cylinder	35.5 mm	Solid	Unknown	No. 6 electric detonator	3.50	25.4%
[45]	C# (Aged)	Unknown	1.35 mm	4.5 um	Decane	N/A	94%	0.875	Steel	Cylinder	35.5 mm	Solid	Unknown	No. 6 electric detonator	3.25	21.9%
[45]	D-1	Unknown	> 1.40 mm	7.6 um	Decane	N/A	94%	0.840	Steel	Cylinder	35.5 mm	Solid	Unknown	No. 6 electric detonator	2.90	17.4%
[45]	D-2	Unknown	> 1.40 mm	7.6 um	Decane	N/A	94%	0.840	Steel	Cylinder	35.5 mm	Solid	Unknown	No. 6 electric detonator	2.95	18.0%
[45]	D# (Aged)	Unknown	> 1.40 mm	7.6 um	Decane	N/A	94%	0.825	Steel	Cylinder	35.5 mm	Solid	Unknown	No. 6 electric detonator	3.05	19.3%
[45]	E-1	Unknown	1.14 mm	4.6 um	Decane	N/A	94%	0.850	Steel	Cylinder	35.5 mm	Solid	Unknown	No. 6 electric detonator	3.40	23.9%
[45]	E-2	Unknown	1.14 mm	4.6 um	Decane	N/A	94%	0.850	Steel	Cylinder	35.5 mm	Solid	Unknown	No. 6 electric detonator	3.45	24.6%
[45]	E# (Aged)	Unknown	1.14 mm	4.6 um	Decane	N/A	94%	0.860	Steel	Cylinder	35.5 mm	Solid	Unknown	No. 6 electric detonator	3.30	22.5%

⁴⁵ Miyake, A., et al., *Influence of physical properties of ammonium nitrate on the detonation behavior of ANFO*. Journal of Loss Prevention in the Process Industries, 2001. 14(6): p. 533-538.

Table 5. TNT Equivalency of Ammonium Nitrate Based on Experimental Factors

Reference	Name	Type of AN	AN Particle Diameter	AN Pore Diameter	Contaminants	Contaminant size	Contaminant %	Bulk Density	Confinement Material	Confinement Shape	Charge Diameter (mm)	Phase	Temperature C	Initiator	Detonation Velocity (km/s)	TNT Eq (%)
[45]	F-1	Unknown	> 0.85 mm	4.6 um	Decane	N/A	94%	0.860	Steel	Cylinder	35.5 mm	Solid	Unknown	No. 6 electric detonator	3.75	29.1%
[45]	F-2	Unknown	> 0.85 mm	4.6 um	Decane	N/A	94%	0.865	Steel	Cylinder	35.5 mm	Solid	Unknown	No. 6 electric detonator	3.85	30.7%
[45]	F# (Aged)	Unknown	> 0.85 mm	4.6 um	Decane	N/A	94%	0.885	Steel	Cylinder	35.5 mm	Solid	Unknown	No. 6 electric detonator	3.65	27.6%
[24]	A	Unknown	~ 1.48 mm	Unknown	Insoluble Inert	Unknown	0.7%	0.82	Fiber tube with earth-cover	Cylinder	20 in	Solid	Unknown	98/2 prill/oil booster	3.20	21.2%
[24]	A	Unknown	~ 1.48 mm	Unknown	Insoluble Inert	Unknown	0.7%	0.82	Fiber tube with earth-cover	Cylinder	18 in	Solid	Unknown	98/2 prill/oil booster	3.10	19.9%
[24]	A	Unknown	~ 1.48 mm	Unknown	Insoluble Inert	Unknown	0.7%	0.82	Fiber tube with earth-cover	Cylinder	15.25 in	Solid	Unknown	98/2 prill/oil booster	2.80	16.2%
[24]	A	Unknown	~ 1.48 mm	Unknown	Insoluble Inert	Unknown	0.7%	0.82	Fiber tube with earth-cover	Cylinder	15.25 in	Solid	Unknown	98/2 prill/oil booster	2.70	15.1%
[24]	A	Unknown	~ 1.48 mm	Unknown	Insoluble Inert	Unknown	0.7%	0.82	Fiber tube with earth-cover	Cylinder	15.25 in	Solid	Unknown	98/2 prill/oil booster	2.75	15.7%
[24]	A	Unknown	~ 1.48 mm	Unknown	Insoluble Inert	Unknown	0.7%	0.82	Fiber tube with earth-cover	Cylinder	12.75 in	Solid	Unknown	98/2 prill/oil booster	2.40	11.9%
[24]	B	Unknown	~ 1.88 mm	Unknown	Insoluble Inert	Unknown	2.3%	0.81	Fiber tube with earth-cover	Cylinder	20 in	Solid	Unknown	98/2 prill/oil booster	2.80	16.2%
[24]	B	Unknown	~ 1.88 mm	Unknown	Insoluble Inert	Unknown	2.3%	0.81	Fiber tube with earth-cover	Cylinder	15.25 in	Solid	Unknown	98/2 prill/oil booster	2.40	11.9%
[24]	C	Unknown	~ 1.66 mm	Unknown	Insoluble Inert	Unknown	0.0%	0.98	Fiber tube with earth-cover	Cylinder	20 in	Solid	Unknown	98/2 prill/oil booster	2.90	17.4%
[24]	D	Unknown	~ 1.65 mm	Unknown	Insoluble Inert	Unknown	3.1%	0.88	Fiber tube with earth-cover	Cylinder	20 in	Solid	Unknown	98/2 prill/oil booster	2.15	9.6%
[24]	E	Unknown	~ 1.54 mm	Unknown	Insoluble Inert	Unknown	0.7%	0.8	Fiber tube	Cylinder	20 in	Solid	Unknown	98/2 prill/oil booster	3.00	18.6%
[24]	E	Unknown	~ 1.54 mm	Unknown	Insoluble Inert	Unknown	0.7%	0.8	Fiber tube	Cylinder	15 in	Solid	Unknown	98/2 prill/oil booster	2.70	15.1%
[24]	E	Unknown	~ 1.54 mm	Unknown	Insoluble Inert	Unknown	0.7%	0.8	Fiber tube	Cylinder	15 in	Solid	Unknown	98/2 prill/oil booster	2.70	15.1%
[24]	E	Unknown	~ 1.54 mm	Unknown	Insoluble Inert	Unknown	0.7%	0.8	Fiber tube	Cylinder	12 in	Solid	Unknown	98/2 prill/oil booster	2.25	10.5%
[24]	E'	Unknown	~ 1.54 mm	Unknown	Insoluble Inert	Unknown	4.7%	0.8	Fiber tube	Cylinder	30 in	Solid	Unknown	98/2 prill/oil booster	3.00	18.6%

Table 5. TNT Equivalency of Ammonium Nitrate Based on Experimental Factors

Reference	Name	Type of AN	AN Particle Diameter	AN Pore Diameter	Contaminants	Contaminant size	Contaminant %	Bulk Density	Confinement Material	Confinement Shape	Charge Diameter (mm)	Phase	Temperature C	Initiator	Detonation Velocity (km/s)	TNT Eq (%)
[24]	F	Unknown	~ 1.95 mm	Unknown	Insoluble Inert	Unknown	0.0%	1.02	Fiber tube	Cylinder	40 in	Solid	Unknown	98/2 prill/oil booster	3.60	26.8%
[24]	F	Unknown	~ 1.95 mm	Unknown	Insoluble Inert	Unknown	0.0%	1.02	Fiber tube	Cylinder	30 in	Solid	93.3	Flake TNT	3.70	28.3%
[42]	AN2	Granulated, porous	~ 0.135 mm	Unknown	None	N/A	0%	0.83	Steel	Cylinder	Unknown	Solid	Unknown	Shock-wave generator (square profile with varying durations) 2.2 GPa	2.25	10.5%
[42]	AHP	None	N/A	Unknown	Ammonium hydrogen phosphate	Unknown	100%	0.83	Steel	Cylinder	Unknown	Solid	Unknown	Shock-wave generator (square profile with varying durations) 2.2 GPa	1.55	5.0%
[42]	AC	None	N/A	Unknown	Ammonium carbonate	Unknown	100%	0.92	Steel	Cylinder	Unknown	Solid	Unknown	Shock-wave generator (square profile with varying durations) 2.2 GPa	1.88	7.3%
[42]	AN2/AHP	Granulated, porous	~ 0.135 mm	Unknown	Ammonium hydrogen phosphate	Unknown	30%	0.93	Steel	Cylinder	Unknown	Solid	Unknown	Shock-wave generator (square profile with varying durations) 2.2 GPa	2.13	9.4%
[42]	AN2/AC	Granulated, porous	~ 0.135 mm	Unknown	Ammonium carbonate	Unknown	30%	0.83	Steel	Cylinder	Unknown	Solid	Unknown	Shock-wave generator (square profile with varying durations) 2.2 GPa	2.06	8.8%
[42]	AN2	Granulated, porous	~ 0.135 mm	Unknown	None	N/A	0%	0.84	Steel	Cylinder	Unknown	Solid	Unknown	Shock-wave generator (square profile with varying durations) 3.8 GPa	2.73	15.4%
[42]	AP	None	N/A	Unknown	Ammonium phosphate	Unknown	100%	0.99	Steel	Cylinder	Unknown	Solid	Unknown	Shock-wave generator (square profile with varying durations) 3.8 GPa	2.27	10.7%
[42]	AC	None	N/A	Unknown	Ammonium carbonate	Unknown	100%	0.88	Steel	Cylinder	Unknown	Solid	Unknown	Shock-wave generator (square profile with varying durations) 3.8 GPa	2.27	10.7%
[42]	CC	None	N/A	Unknown	Calcium carbonate	Unknown	100%	1.22	Steel	Cylinder	Unknown	Solid	Unknown	Shock-wave generator (square profile with varying durations) 3.8 GPa	2.10	9.1%
[42]	AN2/AP	Granulated, porous	~ 0.135 mm	Unknown	Ammonium phosphate	Unknown	30%	0.84	Steel	Cylinder	Unknown	Solid	Unknown	Shock-wave generator (square profile with varying durations) 3.8 GPa	2.72	15.3%
[42]	AN2/AC	Granulated, porous	~ 0.135 mm	Unknown	Ammonium carbonate	Unknown	20%	0.87	Steel	Cylinder	Unknown	Solid	Unknown	Shock-wave generator (square profile with varying durations) 3.8 GPa	2.52	13.1%
[42]	AN2/CC	Granulated, porous	~ 0.135 mm	Unknown	Calcium carbonate	Unknown	20%	0.91	Steel	Cylinder	Unknown	Solid	Unknown	Shock-wave generator (square profile with varying durations) 3.8 GPa	2.52	13.1%
[29]	FGAN	Fertilizer Grade	Unknown	Unknown	Wax/clay	Unknown	0.75%/3.5%	0.90	Steel	Cylinder	1.25 in	Solid	Unknown	50 gm Composition A-3	1.37	3.9%
[29]																
[29]																

Table 5. TNT Equivalency of Ammonium Nitrate Based on Experimental Factors

Reference	Name	Type of AN	AN Particle Diameter	AN Pore Diameter	Contaminants	Contaminant size	Contaminant %	Bulk Density	Confinement Material	Confinement Shape	Charge Diameter (mm)	Phase	Temperature C	Initiator	Detonation Velocity (km/s)	TNT Eq (%)
[18]	AN	Pure	Unknown	Unknown	None	N/A	0%	0.705	Unknown	Cylinder	26.2	Solid	15	75 g Tetryl	1.14	2.7%
[18]	AN	Pure	Unknown	Unknown	None	N/A	0%	0.705	Unknown	Cylinder	26.2	Solid	71	75 g Tetryl	1.56	5.0%
[18]	AN	Pure	Unknown	Unknown	None	N/A	0%	0.69	Steel	Cylinder	50	Solid	Room	100 g PA	1.23	3.1%
[18]	AN	Pure	Unknown	Unknown	None	N/A	0%	0.84	Steel	Cylinder	25	Solid	Room	50 g Tetryl	1.31	3.6%
[18]	AN	Pure	Unknown	Unknown	None	N/A	0%	0.83	Steel	Cylinder	26	Solid	Room	60 g Tetryl	1.47	4.5%
[18]	AN	Pure	Unknown	Unknown	None	N/A	0%	0.79	Steel	Cylinder	80	Solid	Room	100 g PA	1.53	4.8%
[18]	AN	Pure	Unknown	Unknown	None	N/A	0%	0.88	Steel	Cylinder	80	Solid	Room	100 g PA	1.55	5.0%
[18]	AN	Pure	Unknown	Unknown	None	N/A	0%	0.84	Steel	Cylinder	100	Solid	Room	100 g PA	1.82	6.9%
[18]	AN	Pure	Unknown	Unknown	None	N/A	0%	82	Unknown	Cylinder	26.2	Solid	Room	100 g Tetryl	1.85	7.1%
[18]	AN	Pure	Unknown	Unknown	None	N/A	0%	0.64	Steel	Cylinder	100	Solid	Room	100 g PA	1.92	7.6%
[18]	AN	Pure	Unknown	Unknown	None	N/A	0%	Unknown	Lead	Cylinder	50	Solid	Room	100 g PA	2.44	12.3%
[18]	AN	Pure	Unknown	Unknown	None	N/A	0%	0.98	Steel	Cylinder	80	Solid	Room	250 Tetryl	2.70	15.1%
[18]	AN + 1% Nitrostar ch	Pure	Unknown	Unknown	Nitrostarch	Unknown	1%	0.82	Unknown	Cylinder	26.2	Solid	Room	100 g PA	1.94	7.8%
[18]	AN + 5% Nitrostar ch	Pure	Unknown	Unknown	Nitrostarch	Unknown	5%	0.82	Unknown	Cylinder	26.2	Solid	Room	100 g PA	2.06	8.8%
[18]	AN + 10% Nitrostar ch	Pure	Unknown	Unknown	Nitrostarch	Unknown	10%	0.82	Unknown	Cylinder	26.2	Solid	Room	100 g PA	2.47	12.6%
[18]	FGAN	Fertilizer Grade	Unknown	Unknown	Unknown	Unknown	0%	0.9	Paper	Cylinder	114.3	Solid	Room	225 g Comp C	1.11	2.5%
[18]	FGAN	Fertilizer Grade	Unknown	Unknown	Unknown	Unknown	0%	0.91	Steel	Cylinder	31.7	Solid	Room	50 g Comp A3	1.35	3.8%
[18]	FGAN	Fertilizer Grade	Unknown	Unknown	Unknown	Unknown	0%	1.4	Glass	Cylinder	30	Solid	> 169	50 g Com A3	2.11	9.2%
[41]	AN	Unknown	Unknown	Unknown	Unknown	Unknown	Unknown	1.12	Unknown	Unknown	Unknown	Solid	Room	Unknown	2.55	13.5%

2.3.4 Summary

A summary of the effect of the examined factors on the sensitivity and energy output of AN is shown in Table 6. The table presents the general effect (e.g., increase, decrease), but the specific effect of studied factors can be found in Section 2.3.3.2 and 2.3.3.3. A collection of the experimental data from the reviewed literature can be found in Table 5. The table includes the TNT equivalence calculations based on reported detonation velocities and tabulate factors such as particle size, temperature, contaminants, etc. As discussed in Section 2.3.3.3, the theoretical maximum TNT_{eq} for AN is 60%. Assuming significant amounts of fuel oil or metal powders are not homogenously mixed in with the AN, a realistic TNT_{eq} encompassing most factors is approximately 0% to 23%.

Table 6. Summary of Factor Effect on Sensitivity and Energy Output

As Factor Increases ...	Sensitivity	Energy Output
Particle Size	↑	↓
Solution Acidity	↑	Δ
Contaminant (Organic)	↑	↑
Contaminant (Inorganic)	↓	↑
Contaminant (Metal/Chloride)	↑	↑
Water	↓	Δ
Confinement	↑	Δ
Temperature	↑	↓
Static Pressure	↑	Δ

- ↑ Increasing Effect
- Δ Unknown/No Effect
- ↓ Decreasing Effect

3 Field Investigation

A field investigation was performed by ABS Consulting (project 3008473^{[1],[2]}). ABS Consulting engineers were on site in West, TX on the following dates:

- April 21 – April 27 2013
- May 15, 2013
- May 28 – 29, 2013

Activities April 21- April 27 were predominantly spent off of the West Fertilizer property surveying damage to the community homes, community structures and damaged metal buildings.

On May 28th ABS Consulting conducted a survey of the basketball court area and the surrounding vegetation for evidence of burning from flammable vapors that could have been released by the on-site ammonia storage tanks. This investigation included inspection of the ammonia tanks and the pressure relief valves. A summary of the field observations pertaining to the ammonia Tanks is provided in Section 3.1.1 below; however, no additional investigation of a potential ammonia release or any contribution to the event at West, TX was conducted by ABS Consulting.

A detailed damage survey of West Intermediate School was conducted on May 29th. This school is located at a distance of approximately 700 feet from ground zero.

ABS Consulting documented the damage in the community of West, TX and performed analyses of blast damage indicators in order to make an estimate of the explosive yield based upon the observed damage to the community. The blast damage indicator analysis is summarized in Section 5 of this report. The field observations are summarized in this section to provide a better understanding of the damaged caused by the explosion on the West Fertilizer property to the surrounding community. A summary of each of the field observations is provided in the following sections.

3.1 West Fertilizer

ABS Consulting was able to perform a photographic survey of the West Fertilizer Co. property South and East of the crater on April 23rd. A second photographic survey was performed on April 25th which included the portion of the facility north of the crater including the corn silo. The visible location of the crater demonstrates that the explosion only involved the northern stack of Ammonium Nitrate and that the Ammonium Nitrate bin along the west wall across from the office did not contribute to the explosive yield. A layout of the Production Building is provided in Figure 5. This conclusion is apparent because the crater was located directly under the northern bin and did not extend to the additional bin along the west wall. The crater was measured by BATF to be approximately 93 ft. in diameter and 10 feet deep from the top of the slab and 7 feet below grade as reported by BATF during a team debriefing on April 22, 2013. Crater photographs taken on April 23rd and April 25th are shown below in Figure 6 and Figure 7, respectively.

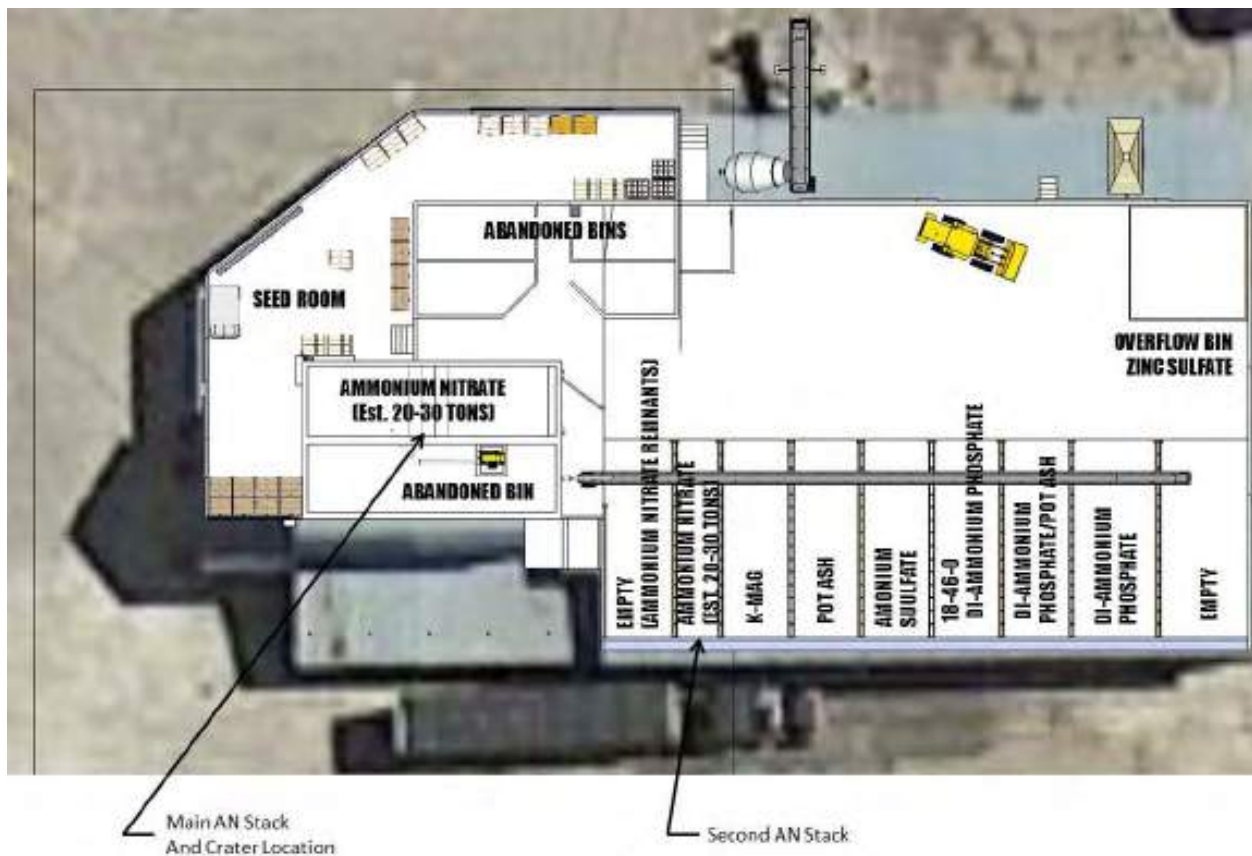


Figure 5. West Fertilizer Co Fertilizer Production Building Layout



Figure 6. West Fertilizer Crater on April 23, 2013



Figure 7. Crater as Viewed from the West on April 25, 2013

Some of the firefighting apparatuses were still present on the scene when ABS Consulting engineers had access to the site on April 23rd, 2013. The pump truck was located to the

southeast of the crater and is shown below in Figure 8 and the door from the pump truck, which was projected by the explosion to the east, is shown below in Figure 9. The pump truck was heavily damaged by the explosion overpressure and debris. A water truck was located on Jerry Mashek drive and is shown below in Figure 10.

The pump truck in Figure 8 was probably moved a short distance by the blast overpressure. A close investigation of the fire truck could not be performed by ABS Consulting engineers; however, a large piece of farm equipment located to the south of the production building toward the scale house, shown below in Figure 11, was moved about a six inches to the south by the blast wave. This is evident by the marks left on the ground by the equipment from displacement during the explosion, as seen in Figure 12. This farm implement was located much further from the blast than the pump truck. In addition, there was a rail car loaded with Ammonium Nitrate located to the north of the production building and crater and can be seen underneath the tarp in Figure 6 above. The rail car, shown below in Figure 13, was overturned and heavily damaged by the explosion. The farm equipment and the rail car are referenced here in relation to the fire equipment to show the severity of the blast environment on the West Fertilizer property where the first responders were located.



Figure 8. Pump Truck Southeast of Crater on April 23, 2013



Figure 9. Door from Pump Truck (Pump Truck in the Background)



Figure 10. Water Tank Truck on Jerry Mashek Drive



Figure 11. Farm Equipment South of Crater Near the Scale House



Figure 12. Ground Mark from Displacement of Farm Equipment from Blast Overpressure



Figure 13. Rail Car Loaded with AN Overturned by Explosion

The Scale House, shown below in Figure 14, was completely destroyed by the explosion. The walls on all four facades are failed, the roof had failed and there was a significant amount of structural and non-structural debris inside the scale house.



Figure 14. Scale House

The Chemical Storage / Office Building located to the East of the Production Building was destroyed by the blast and ensuing fire as shown below in Figure 15. The pre-engineered metal building was so completely devastated, all that remained was a stack of metal debris where the building once stood.



Figure 15. Remains of Chemical Storage / Office Building (Behind Crater in Photo)

The Corn Silo located north of the Fertilizer Production Building was also destroyed by the explosion, spilling the contents of the Silo as shown below in Figure 16. The Corn Silo structure was displaced to the North, away from the Production Building crater, as would be expected from an explosion located at the crater. There was no evidence observed, such as Corn Silo debris being thrown in all directions, of the corn silo contributing to the event.



Figure 16. Corn Silo Damage (Composite of Two Photographs)

The above ground liquid storage tanks were also heavily damaged by the blast as shown below in Figure 17 and Figure 18. In Figure 17 the liquid level in the tank to the left that was present during the explosion is clearly visible by the crease at the top of the tank where the deformation begins. The tank on the right in Figure 17 clearly shows a large debris impact that folded and crushed the tank. Figure 18 is a composite of three pictures taken from just south of the crater. The anhydrous ammonia tanks can be seen in the background just behind the liquid storage tanks.



Figure 17. Liquid Fertilizer Tank Damage



Figure 18. Liquid Fertilizer Tank Damage (Composite of three photographs)

3.1.1 Anhydrous Ammonia Tanks

The liquid anhydrous ammonia tanks contained ammonia at the time of the explosion. A detailed survey of the tanks and the pressure relief valves was conducted on May 28, 2013. Figure 19 shows the tanks as photographed by the CSB on April 19, 2013 and the PRV at the West end of the north Anhydrous Ammonia tank can be seen along with the PRVs in the middle of the South tank. The PRVs on the north tank still had their weather caps on and consequently did not relieve. The PRVs in the middle tank were missing the weather caps. A close up photo of the PRVs from the southern tank taken on May 28, 2013 is shown in Figure 20. There is no evidence of the caps melting in the photograph nor is there evidence that these valves had been hit by a piece of debris. It is unknown if the missing caps were recovered by the BATF during site cleanup; however, it is not known if this set of pressure relief valves may have opened at some point during the fire prior to or after the explosion. The Anhydrous Ammonia tanks were manufactured in 1963 by Delta Southern Co. of Baton Rouge, LA. The tank label is provided below in Figure 21 and provided the following specifications concerning the tanks:

Maximum Allowable Working Pressure	250 psi
Maximum Allowable Temperature	650 F
HSB No.	452
National Board No.	258
Water Capacity	12,000 Gallons
Shell Thickness	0.5625"
Head Thickness	0.323"
Outside Diameter	82.5625"
Overall Length	46'-8.5625"
Year Built	1963

One of the pressure relief valves from the west end of the north Anhydrous Ammonia tanks was knocked off during the site cleanup effort. It is presumed that this occurred when the crane and lift bucket were operating in the area. This occurred prior to the site inspection on May 28, 2013; however, the pressure relief valve that was knocked off of the tank was located on the ground directly adjacent to its original position on the tank. The pressure relief valve markings were photographed as shown below in Figure 22.



Figure 19. Anhydrous Ammonia Tanks Photo of PRVs (CSB Photo 04-19-2013)



Figure 20. PRV Valve from Southern Anhydrous Ammonia Tank (Photo 05-28-13)



Figure 21. Plate on Anhydrous Ammonia Tank



Figure 22. Pressure Relief Valve Markings

3.2 Community Structures and Facilities

Several community facilities were in close proximity to the explosion at West Fertilizer and were surveyed in the field to ascertain the level of damage. These facilities, highlighted below in Figure 23 included:

- Apartment Complex
- Nursing Home
- Playground
- West Intermediate School
- West High School
- West Middle School

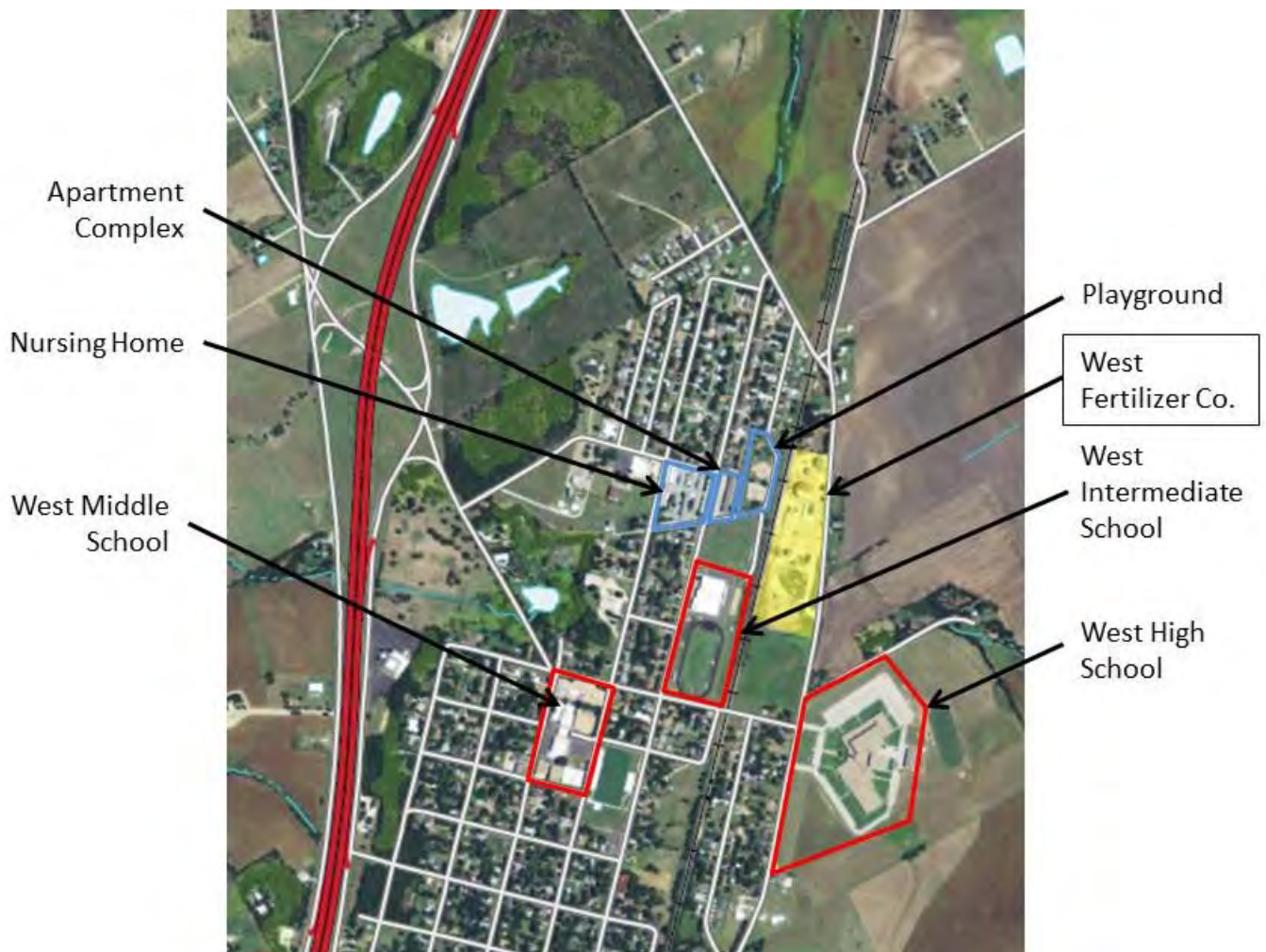


Figure 23. Community Facilities in West, TX

3.2.1 Rest Haven Nursing Home

The Rest Haven Nursing Home, 300 W. Haven St., was located at the corner of N. Reagan and W. Haven streets and was approximately 650 ft. to the west of the crater and is shown below in Figure 24. ABS Consulting surveyed Rest Haven Nursing home on the 24th and 25th of April, 2013. The nursing home was constructed of load bearing wood stud walls with brick veneer and wood trusses which spanned across the wings from exterior wall to exterior wall. A copy of the emergency exit plan which shows the floor plan and room layout of the Nursing Home is shown below in Figure 25. The eastern most corridor of the nursing home was the most heavily damaged by the explosion. The roof trusses collapsed and the east wall was failed by the explosion as shown below in Figure 26 through Figure 28. The eastern rooms were heavily damaged and subjected to flying wall debris, window fragments and failing drywall, insulation and light fixtures from the ceiling. A photo inside a bedroom from the East hallway is shown below in Figure 29. The glazing hazards were high with glass shards penetrating the wall opposite the windows. Ceilings, insulation and interior contents of rooms were lying on beds, blocking doorways and would have presented hazards to occupants of these rooms. Additionally there would have been air blast infiltration into the rooms through the failed windows. It is important to note that this photo was taken after search and rescue operations in the nursing home. Rescuers undoubtedly conducted a room by room search, moving debris, to ensure that there were no victims present.



Figure 24. Rest Haven Nursing Home



Figure 25. Nursing Home Emergency Exit Floor Plan



Figure 26. East Façade of Rest Haven Nursing Home



Figure 27. Damage to Reagan St. Entry of Rest Haven Nursing Home



Figure 28. East Façade of North Wing Rooms at Rest Haven Nursing Home



Figure 29. East Façade Bedroom in Rest Haven Nursing Home (After FEMA USAR Operations)

There was also significant damage to the western portion of the nursing home and the great rooms, such as the lobby, which were damaged particularly heavily due to the large spans of the overhead trusses that failed and were held up by furniture, as shown in Figure 30. In addition, hallways in this area (see Figure 31) presented many hazards including hanging light fixtures, failed ceiling joists and collapsed drywall and insulation on the floors.



Figure 30. West Lobby of Rest Haven Nursing Home

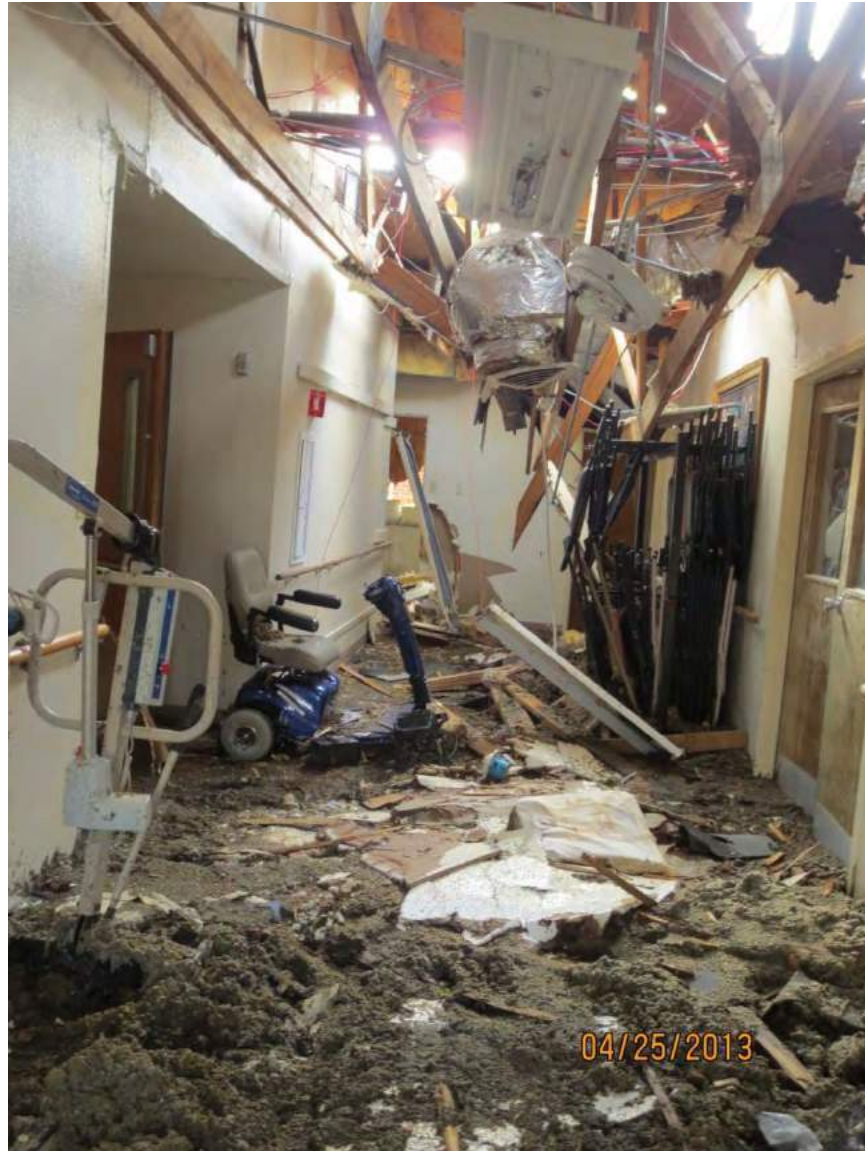


Figure 31. Hallway in Western Portion of Rest Haven Nursing Home Outside of the Chapel

The Rest Haven Nursing home was within the debris field for secondary fragments from the West Fertilizer Production Building and the crater ejecta, which was constituted of massive pieces of concrete from the fertilizer plant foundation and significant masses of earth. Figure 32 clearly shows numerous debris impacts to the roof of the Nursing Home. A large piece of the fertilizer plant foundation measuring 16 inches wide by 16 inches tall and 36 inches long, shown below in Figure 33, was observed to have impacted room 79, travelling through the roof and the exterior wall. The piece of debris was calculated to have weighed approximately 800 pounds and had sufficient momentum that after exiting the nursing home and striking the ground the fragment travelled an additional 60 feet and came to rest just to the west of N. Davis St.



Figure 32. Post Incident Aerial View of Rest Haven Nursing Home (Debris Impacts)



Figure 33. Concrete Crater Debris (West Fertilizer Foundation) that Impacted Nursing Home

A simple observation made by the entry team including the CSB, Atlas Engineers, and ABS Consulting, was that we walked on glass with almost every step that was taken inside of the nursing home, with the exception of the hallway corridors that were shielded from windows by interior partitions. The great rooms, lobby and patient rooms were subjected to significant glazing hazards as can be seen below in Figure 34 and Figure 35.



Figure 34. Typical Glass Fragments on Floor and Into Rooms of Rest haven Nursing Home



Figure 35. Typical High Glazing Hazards in Rest Haven Nursing Home

There was one fatality involving an occupant of the Nursing home who passed away at a hospital post incident. Evidence of injury to occupants was observed in the facility on chairs and hand rails within the Nursing Home.

3.2.2 Park

The playground area of a local park, located directly to the west of the West Fertilizer property, is shown below in Figure 36. The equipment on the playground was destroyed by the blast as shown below in Figure 37. Two items of note were observed in this area. The first was the damage to the basketball goal posts on the basketball court. These items were utilized as blast damage indicators and are discussed in further detail in Section 5.1.2. In addition, the trees in the vicinity of the park showed evidence of scorching as highlighted below in Figure 39. The scope of work^[3] did not include making a determination whether these trees were scorched from the fire or from another source but it is noted as an item of interest^[46]. The trees are directly downwind of the anhydrous ammonia tanks as shown in Figure 40. The trees were not located within the smoke plume from the fire. Pre-explosion video of the fire shows the smoke travelling with the wind but crossing the playground equipment to the north of the basketball courts. A screen shot from one of the videos is provided below in Figure 41.



Figure 36. Playground

⁴⁶ Letter to Ms. Kelly Wilson, "Report regarding video analysis of 'Explosion Video of West.mp4'", Forensic Media Services, Denver, Co., September 3, 2013.



Figure 37. Playground equipment



Figure 38. Damaged Basketball Goal Post on Basketball Court



Figure 39. Tree Adjacent to Basketball Court



Figure 40. Map Showing Location of Tree Adjacent to Basketball Court Downwind of Anhydrous Ammonia Tanks

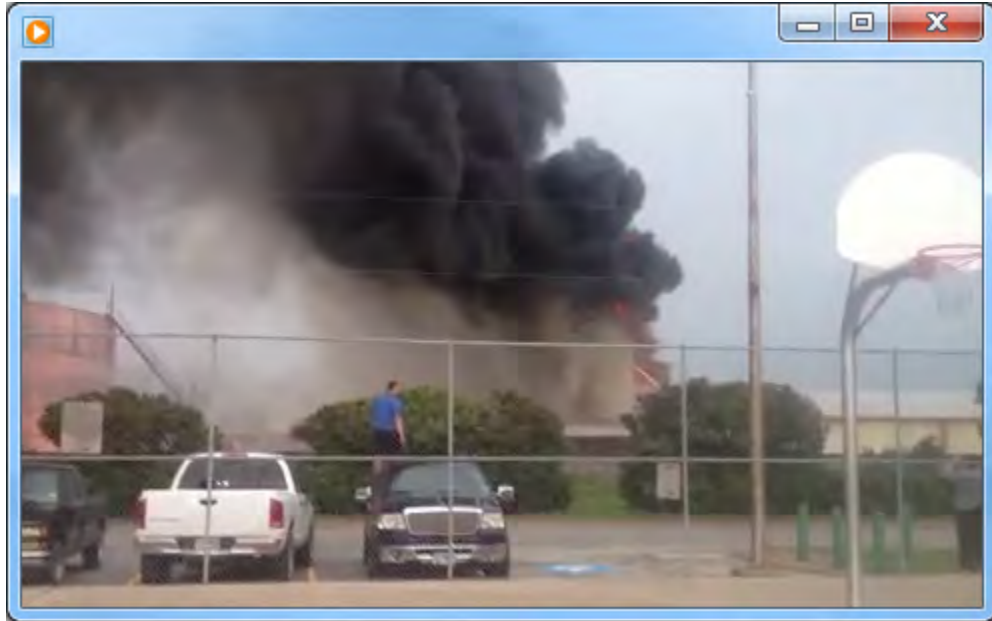


Figure 41. Pre-Explosion Smoke Plume from the Fire (Passing North of Basketball Courts)

3.2.3 West Intermediate School

ABS Consulting and Atlas Engineering made entry into West Intermediate School on May 29th in order to record the damage to the school. The original school was a pre-engineered metal building consisting of lightweight steel frames, cold formed girts and purlins supporting lightweight metal decks. The Gymnasium and Cafeteria were also pre-engineered metal buildings. The remainder of the school, highlighted in yellow in Figure 42 below, was constructed of precast concrete tilt up load bearing walls that supported open webbed steel joists and a metal roof deck with a built up roof. The building room layout taken from the school evacuation plan is provided below in Figure 43 and an aerial view taken prior to the explosion is provided below in Figure 44.



Figure 42. West Intermediate School Building Sections

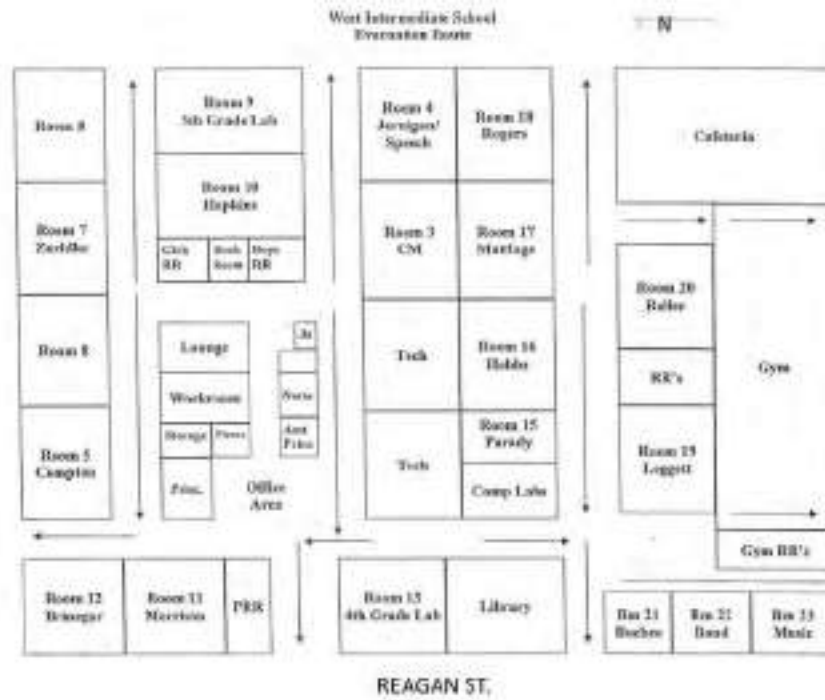


Figure 43. West Intermediate School Room Layout from Evacuation Plan



Figure 44. West Intermediate School Aerial Photograph (Prior to Event)

The roof of the northwest portion of the school above Room 12 is shown below in Figure 45. Figure 46 shows the amount of debris in the hallway outside of Rooms 11 and 12 (photo is looking North towards the exit). An interior door frame was blocking the hallway, the acoustic ceiling was down and there are numerous obstacles that would have made exiting the building difficult for students and staff. In addition, the original metal school building just to the south of this location was involved in a fire so there would have been smoke and heat to contend with as well. Figure 47 shows the interior of Classroom 12. The acoustic ceiling, light fixtures and other debris have been thrown onto all of the desks. In addition, the window on the North façade failed violently and a large shard of glass approximately 3 inches long was observed embedded in the assignment poster on the south wall of the classroom as shown in Figure 48.



Figure 45. West Intermediate School – Northwest Wing Roof



Figure 46. West Intermediate School- North Hallway Looking Toward Northeast Exit Door



Figure 47. West Intermediate School Classroom 12



Figure 48. West Intermediate School Glazing Hazard Room 12

The pre-engineered portion of the school in the northeast corner was heavily damaged by blast overpressure and was also fully involved in a fire. Damage to this portion of the building could not be evaluated due to the magnitude and heat associated with the fire. An aerial view of the roof is shown below in Figure 49 and a view looking East down the hallway of this portion of the School is shown below in Figure 50.



Figure 49. West Intermediate School – Original School Northeast Wing Roof



Figure 50. West Intermediate School Interior of Northeast Section that Burned

The Intermediate School gymnasium, shown from above in Figure 51, was heavily damaged by the explosion at West Fertilizer. There is evidence that some of the built up roof over the gymnasium burned; however the level of heat damage to the roof was minor compared to the damage from blast overpressure. It is clearly evident in Figure 51 that the north half of the Gymnasium roof has failed. A view of the gymnasium from the interior is shown below in Figure 52 and Figure 53. The pre-engineered frames are heavily damaged by the blast and are unstable as a result. The roof purlins are moderately deformed with the exception of where they have failed on the north half of the frame spans. In addition, the windows from the south façade of the gymnasium have failed and been propelled over the south bleachers onto the gym floor by the overpressure. The roof in the cafeteria to the south of the gymnasium was also heavily damaged by the explosion as shown below in Figure 54. At the time this photograph was taken, significant cleanup and debris removal in this space had already begun.



Figure 51. West Intermediate School – Gymnasium Roof



Figure 52. West Intermediate School Gymnasium



Figure 53. West Intermediate School Gymnasium Roof Failure



Figure 54. West Intermediate School Cafeteria (Insulate has been picked up and stacked)

The classrooms in the heart of the school were heavily damaged by the explosion. The interior of Classroom 20 is shown below in Figure 55. The acoustic ceiling, light fixtures and insulation have been blown down onto the floor from a combination of the roof motion and air blast entering through the HVAC duct after the roof top air conditioner was displaced by the

explosion. The complete contents of the ceiling plenum are located on top of the desks. Any persons present in the room would have been covered in this debris and would have had to climb their way through to reach the exit. In addition, there was evidence of overpressure having entered the room through the HVAC opening of sufficient magnitude to fail the door latch as shown below in Figure 56. Although it is possible that first responders may have forced the door open, it is noted that school was not in session during the explosion, there were no tool marks on the door or other evidence of forceful entry from the exterior, and the debris inside the room was undisturbed and had not been moved for a thorough search of the room.



Figure 55. West Intermediate School – Classroom 20 Nonstructural Debris



Figure 56. West Intermediate School – Typical Failed Classroom Door Latch

Damage to the Intermediate school reduced as the distance from the explosion source increased from the northeast to the southwest. For reference, the interior of the Library is shown below in Figure 57 and the Band Hall in Room 22 is shown below in Figure 58. The Library was in the process of having the books and other contents recovered so workers had shored the failed Joist Girder (Figure 57) and stacked insulation and removed a significant portion of the debris in the library. Significant glazing hazards can be observed from the glass fragments on the floor a great distance from the windows in Room 22 shown in Figure 58. As in the Library, clean up and recovery activities had begun and the debris stacked in the center of the room.

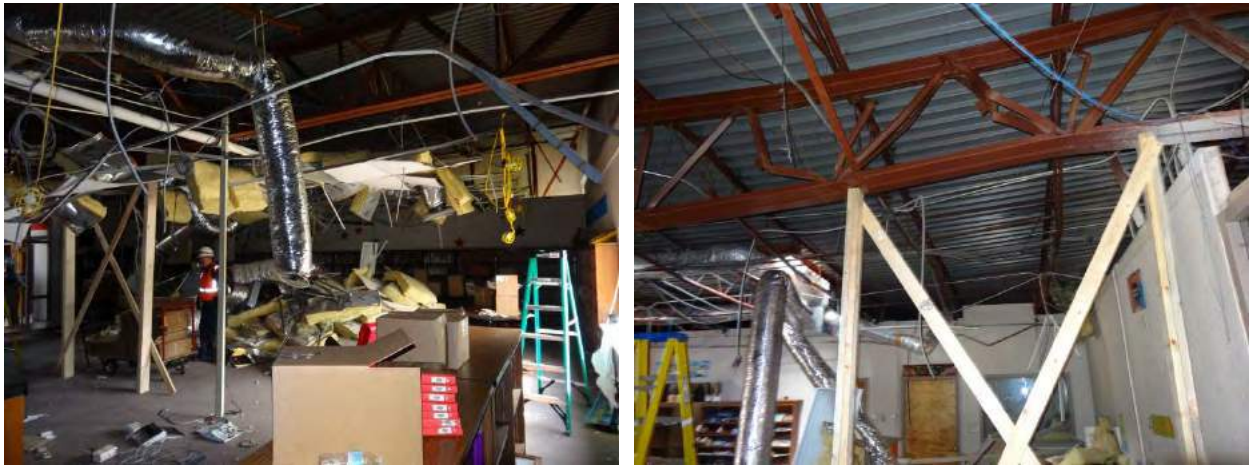


Figure 57. West Intermediate School Library after Shoring and Debris Removal



Figure 58. West Intermediate School Room 22 Interior after Moderate Cleanup

3.2.4 West High School

ABS Consulting surveyed West High School on April 25th along with Atlas Engineering in order to record the damage to the school. The high school was constructed of concrete masonry unit (CMU) walls supporting open webbed steel joists and a metal deck with built up roofing and gravel ballast. The building room layout taken from the school evacuation plan is provided below in Figure 59 and an aerial view taken prior to the explosion is provided below in Figure 60. The school was organized into two wings. The north wing contained the activities area including two gymnasiums, two weight rooms, the boys athletics locker room, the girls athletics locker room, and the band hall. The south wing contained the class rooms as well as a large lecture hall, which was utilized by the responding agencies to conduct daily morning and evening briefings about the investigation and recovery efforts. Between the two wings was the entry hall, administrative offices, the commons area, kitchen, and to the rear was the auditorium. A pre-engineered maintenance building was located directly behind the school to the east.



Figure 59. West High School Evacuation Map and Floor Plan



Figure 60. West High School Aerial Photo

The Auditorium of the High School was a steel frame structure with masonry infill walls. Some of the masonry veneer on the exterior was loose near the northeast corner. Inside the auditorium, large areas of the hanging ceiling were unstable and the supporting structure was compromised especially the area of the ceiling between the seating and the stage which was near collapse due to the failed hanger connections. Evidence of damage to the ceiling from underneath was observable at light fixtures and evidence of cracking and separation near the walls as shown below in Figure 61 was also observed. However, the severity of the damage and compromise to the ceiling hangers became evident when inspected from the catwalks above as shown in Figure 62.

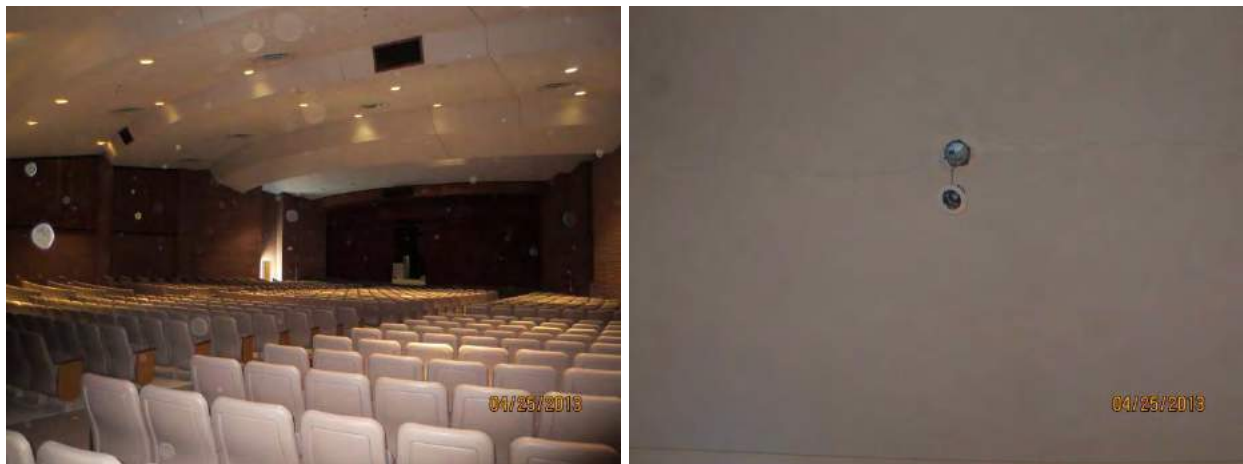


Figure 61. High School Auditorium as Ceiling as Viewed from Below



Figure 62. Auditorium Ceiling Hanger Damage

The Commons area outside of the auditorium is shown below in Figure 63. Partial collapse of the acoustic ceiling and light fixtures hanging from their conduits were observed. Structural damage to the ceiling joist could not be observed due to obstruction by the acoustic ceiling.



Figure 63. Commons Area Ceiling Damage

Similarly, the Band Rooms, shown below in Figure 64, also exhibited partial collapse of ceiling assemblies and hanging light fixtures.



Figure 64. West High School Band Hall

Gymnasium 2, which is the northern most of the two gymnasiums, across the hall from the band hall, was heavily damaged by the explosion and the roof structure, was unstable, and near collapse. Severe damage to the main roof trusses, as highlighted below in Figure 65, was observed. The joist girders appear to have been damaged by a combination of out-of-plane blast load on the roof and the in-plane loading resulting from the masonry wall reaction into the roof diaphragm. The damage to the joist girders was more pronounced in the middle of the room than near the side walls, which was consistent with the point of maximum deformation of the masonry wall resulting in the point of highest in plane loading in the diaphragm. The bolts fastening the joist girder cross-bracing were also failed as shown below in Figure 66. A large number of fasteners were found on the gymnasium floor. In addition, the open webbed steel joists that spanned roughly north to south between the joist girders were buckled out of plane, as shown below in Figure 67. It is clear that the gymnasium was subjected to significant racking. In addition, the columns, see Figure 68, were separated from the masonry infill and may have been deformed and the roof was subject to ponding and potential overload.

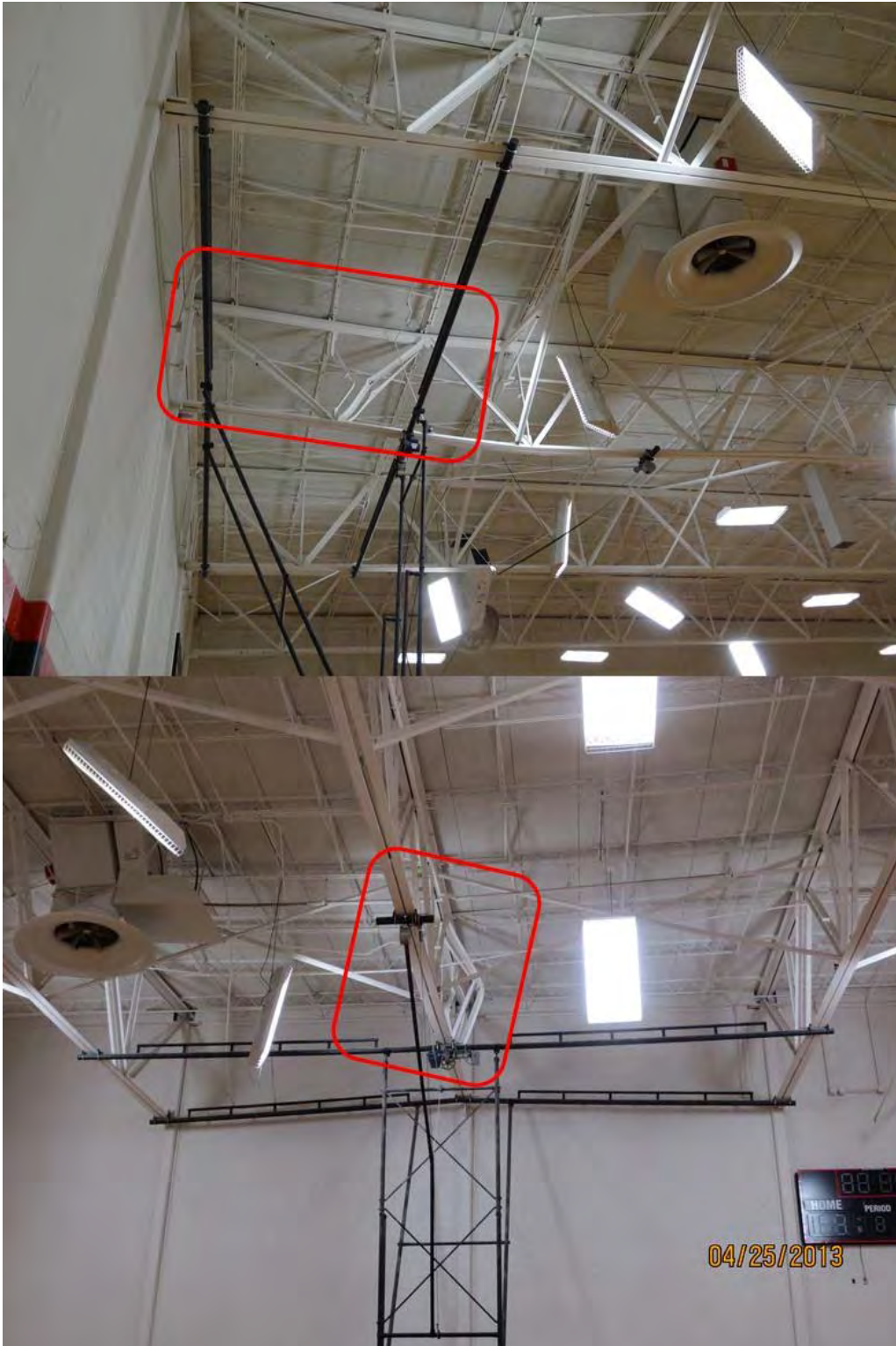


Figure 65. Joist Girder Damage in Gymnasium 2



Figure 66. Failed Cross-Bracing Fasteners Gymnasium 2



Figure 67. Buckled OWSJs in Gymnasium 2



Figure 68. West Wall of Gymnasium 2

The roof structure of Gymnasium 1 was more severely damaged than Gymnasium 2 and had collapsed onto the gymnasium floor. The opening in the roof from the collapse can be seen in Figure 69. The collapse as viewed from the south bleachers is provided in Figure 70 and the collapse viewed from the east gymnasium entry is provided in Figure 71. The Gymnasium 1 roof had failed by the same mechanisms that were observed to have damaged the Gymnasium 2 roof, which had yet to collapse. Gymnasium 1 was larger than Gymnasium 2 in plan and therefore was subjected to higher diaphragm loads than Gymnasium 2. Damage to the Gymnasium 1 joist girders are shown below in Figure 72. The potential for injury to occupants of the gymnasium floor underneath the collapsed section of roof would have been high.



Figure 69. Aerial View of West High School Roof



Figure 70. West High School Gymnasium 1 Roof Collapse from South Bleachers

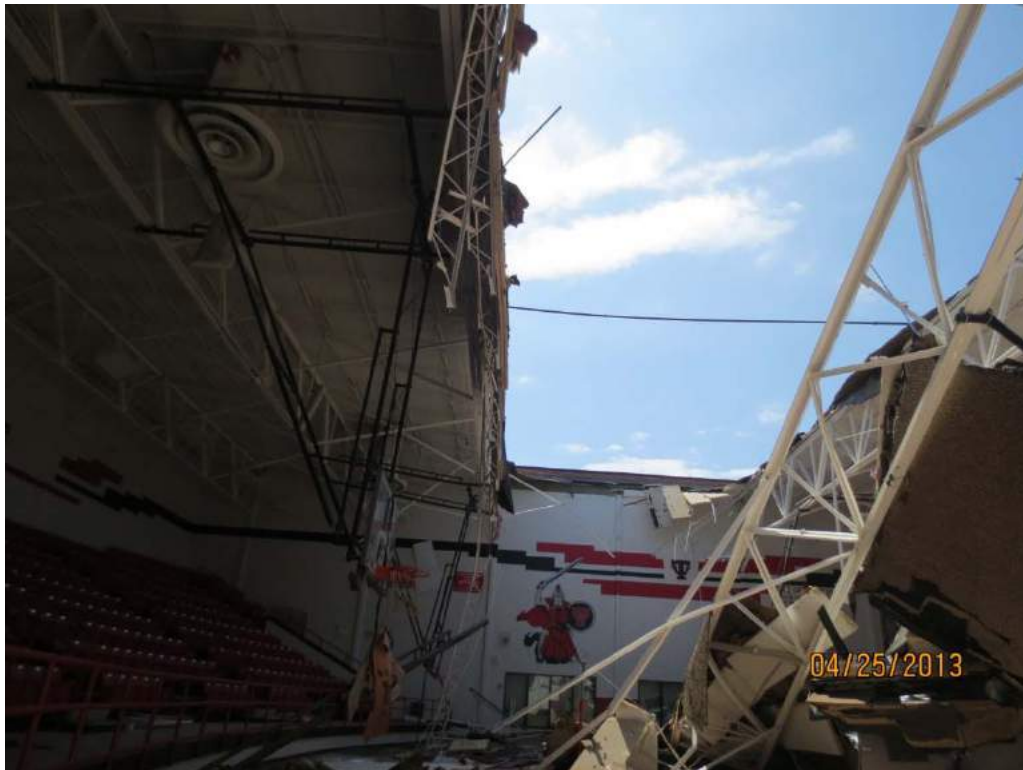


Figure 71. West high School Gymnasium1 Roof Collapse Viewed from Gymnasium Floor Entry



Figure 72. Joist Girder Damage in Gymnasium 1

The entrance lobby of West High School experienced almost complete collapse of the acoustic ceiling and there were multiple overhead hanging hazards. In addition, the open webbed steel joists supporting the roof were deformed laterally out of plane. Deformation of the lobby roof was evident when viewed from above.



Figure 73. West High School Entrance Lobby

The south wing of West High School was occupied by the responding agencies and utilized for organizing investigation efforts. In general evidence of roof motion could be observed by displacement of the acoustic ceilings which leads to suspicion of possible permanent displacement of roof joists and damage to structural connections in the roof structure. The Library ceiling was still intact but showed evidence of motion, as shown below in Figure 74. The ceiling in the hallway to the east of Room 411 which leads to the Counselors Office, shown in Figure 75, was collapsed on to the floor.



Figure 74. West High School Library



Figure 75. West High School Hallway Outside Room 411

3.2.5 West Middle School

West Middle School was located approximately 2,000 feet from the explosion epicenter at 406 W. Shook St and is highlighted below in Figure 76. The Middle School is located at the site of the original West High School that was constructed in 1923. In addition, the athletic field located to the east of the Middle School was the location of the triage and evacuation of the wounded after the explosion. The campus is shown below in Figure 77. The Practice Gym, which was a lightweight pre-engineered metal building with a brick façade, is shown below in Figure 78. Pre-engineered frames were buckled by the explosion, as shown below in Figure 79, and there was a small permanent deformation of the roof purlins observed. The roof purlins and frames were damaged by the overpressure as shown below in Figure 79.

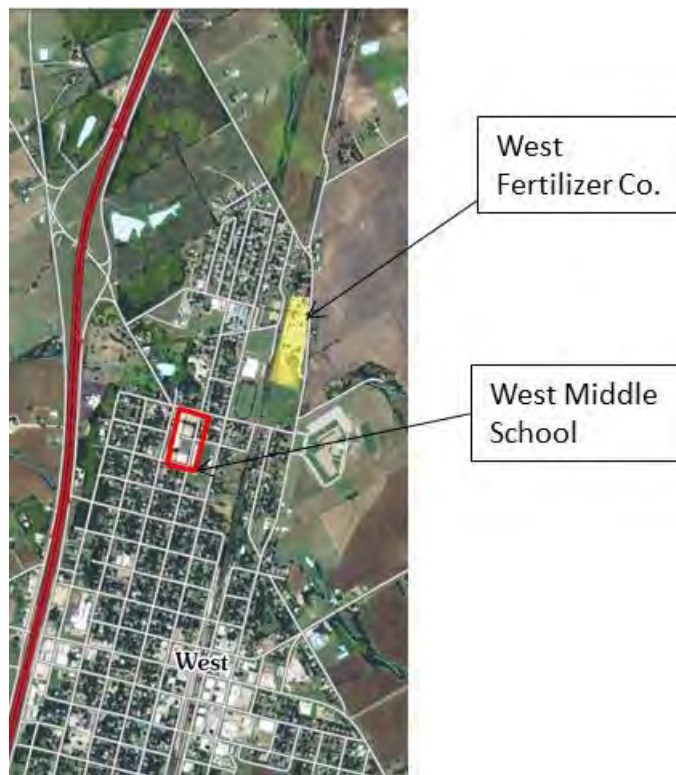


Figure 76. West Middle School Location

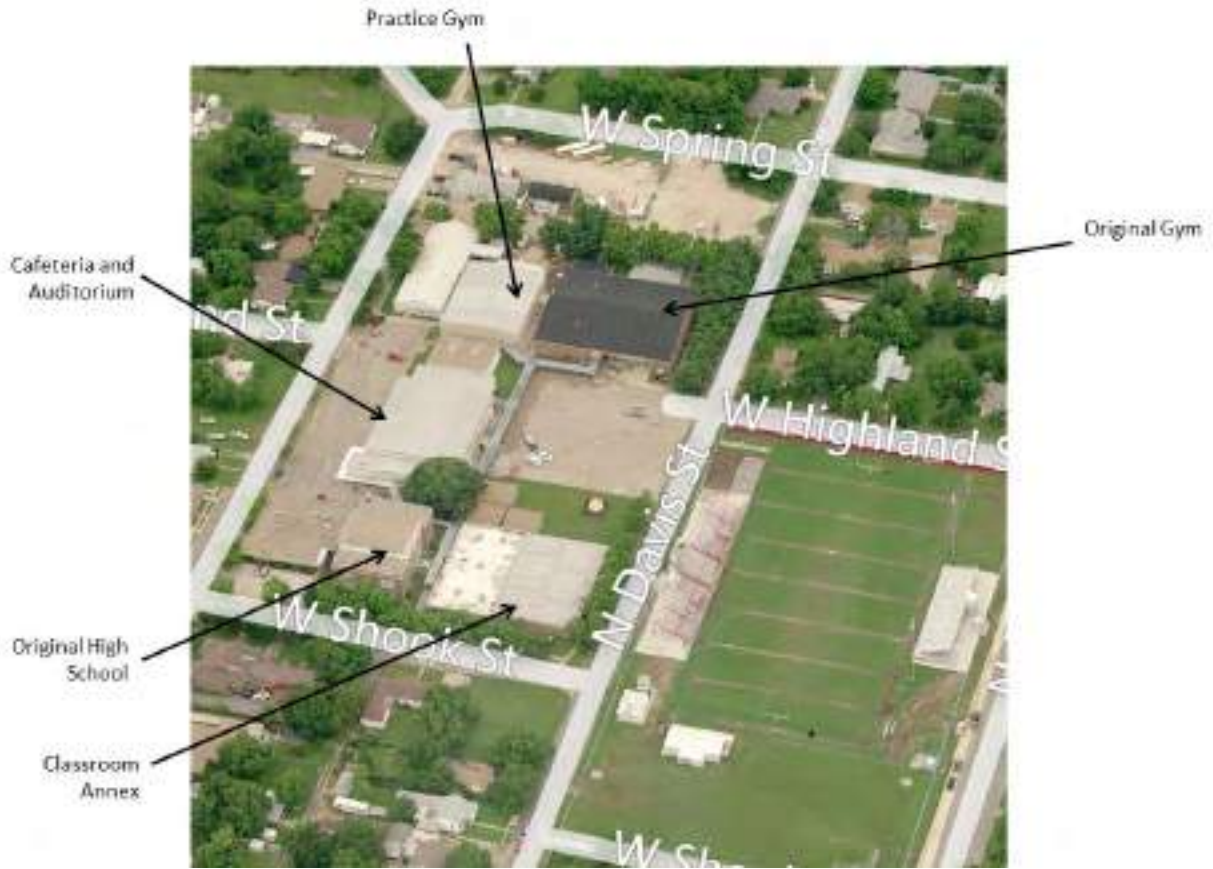


Figure 77. Middle School Campus



Figure 78. West Middle School Practice Gym



Figure 79. West Middle School Practice Gym Buckled Frame

A limited entry into the Cafeteria and Auditorium building was made. The structural components above the ceiling were not readily accessible for inspection and little was known about the condition of the roof; therefore, the team decided that what little data may be available in this particular structure to advance our goal of determining the net explosive weight of the explosion was not worth the potential hazards posed by the high ceiling and unknown conditions. However, the limited observable damage to the building included damage to the ceiling components. As can be seen below in Figure 80, many of the windows on the west façade were unbroken.



Figure 80. West Middle School Cafeteria / Auditorium

The original High School classroom building at West Middle School was constructed in 1923 and is shown below in Figure 81. The windows facing the north towards West Fertilizer were broken and only some of the remaining windows had failed. The building was originally not air-conditioned and had a high tin ceiling. At some point a drop ceiling was installed to allow the building to be conditioned with central air. Upon entry the new drop ceiling had failed; however the original tin ceiling was still in place and some of the windows were broken as shown below in Figure 82. Window hazards were low to moderate and the damage to the building appeared to be superficial; however, observation of the roof framing from underneath was not possible.



Figure 81. West Middle School – Old High School Classroom Building

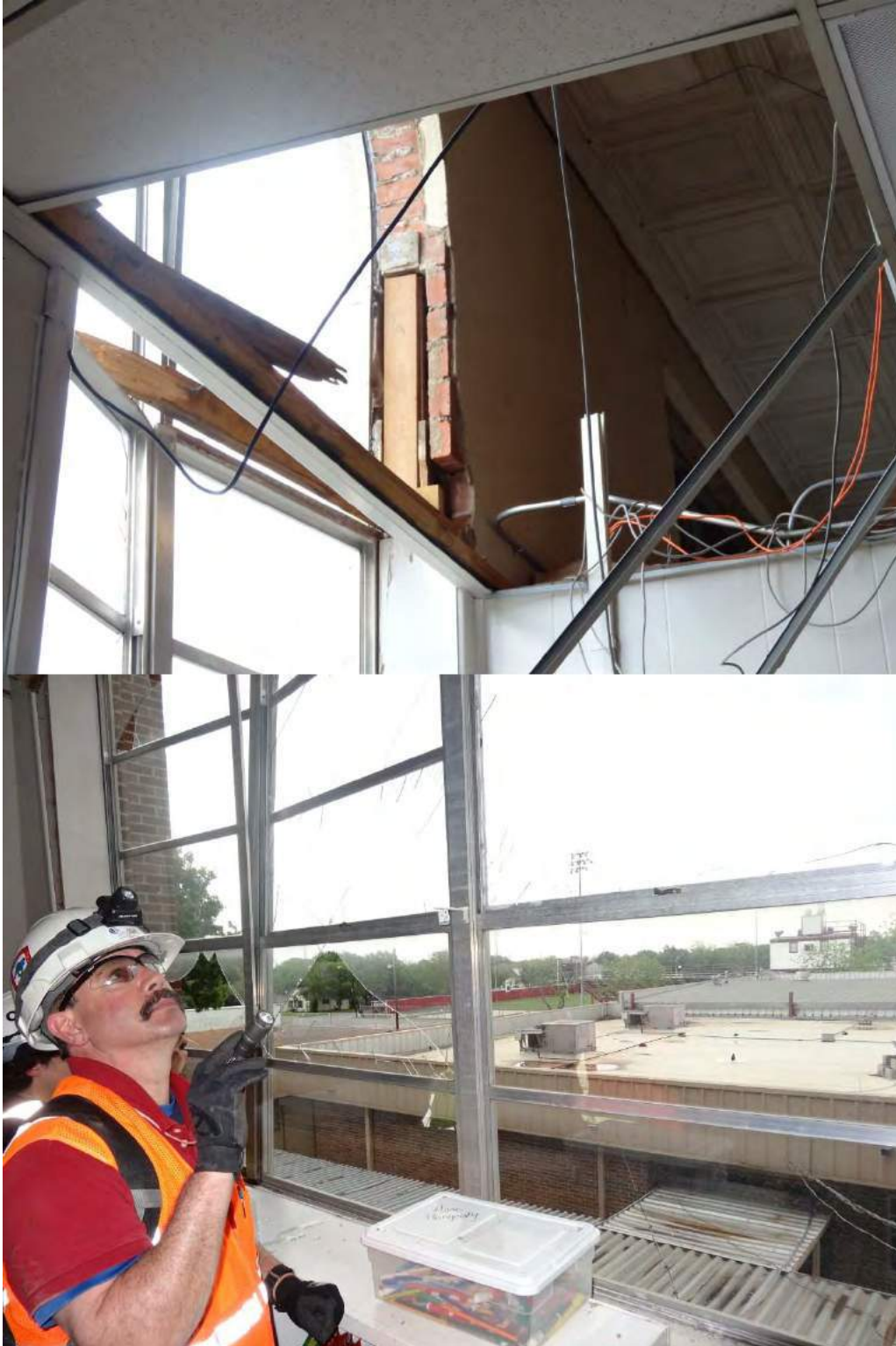


Figure 82. West Middle School Original Classroom Building Superficial Damage

Entry was also made into the classroom annex located in the southeast corner of the campus. The annex classroom building roof structures were open web steel joists supporting a built up roof on metal deck. There was no observable damage to the roof structure. The suspended ceiling was failed from the motion of the roof, as shown below in Figure 83.



Figure 83. Classroom Annex Interior Hallway and Ceiling Damage

3.3 Residences

Residential structures within the surrounding community of West included both single family residences and the Apartment complex. Damage observations for each are summarized in the following sections.

3.3.1 Single Family Residences

A total of 190 single family residential buildings were assessed by ABS Consulting within a radius of 3,500-feet from the identified crater location, as depicted in Figure 84; however, it is noted that damage occurred beyond this distance. Window breakage, façade damage, and non-structural and structural component failure (i.e. wall, roof system) were documented.

Fragment travel of broken glazing was used to quantify the window performance condition in accordance with the ASTM- F1642^[47], adopted by the General Services Administration (GSA). The matrix of hazards used to quantify and classify glazing performance conditions are summarized in Table 7. A graphic description of the table is shown in Figure 85, illustrating fragment impact locations and their corresponding hazard level.

Since deformations cannot be measured for brittle members such as wood stud walls and wood roof trusses, qualitative building damage levels were assigned to each residential building based on the overall structural condition observed on the field. Assignment was performed based on both damage descriptions contained in the ABS Consulting building damage levels (BDL) definitions and the Engineer Technical Letter (ETL) 1110-3-495^[48] building damage categories. Damage descriptions for ABS Consulting and ETL 110-3-495 are shown in Table 8 and Table 9, respectively.

⁴⁷ ASTM F1642-12, Standard Test Method for Glazing and Glazing Systems Subject to Airblast Loadings.

⁴⁸ Department of the Army, “Estimating Damage to Structures from Terrorist Bombs Field Operation Guide“, Engineer Technical Letter 1110-3-495. U.S. Army Corps of Engineers, Washington, DC 20314-1000, 14 July 1999 (FOUO).

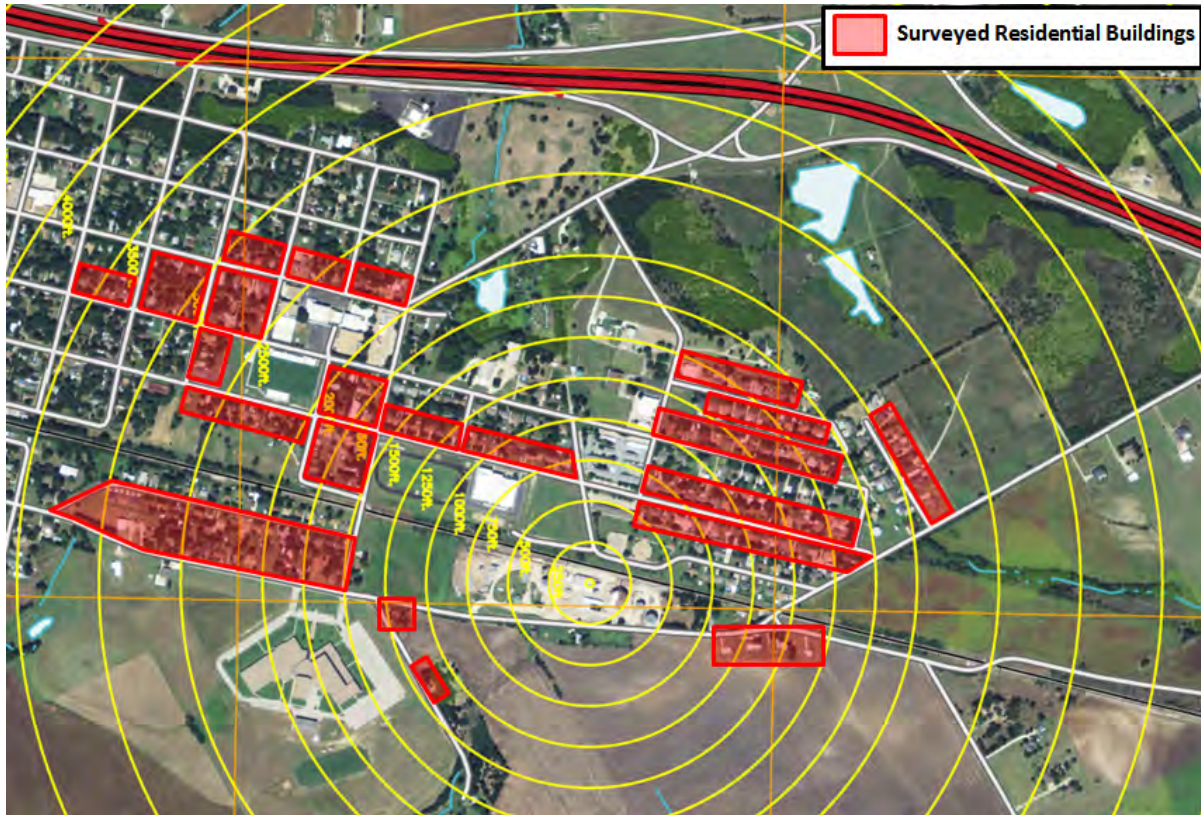


Figure 84. Extent of Surveyed Residential Building

Table 7. GSA Hazards Classification System

GSA Performance Condition	Hazard Level	Description of Window Glazing Response
1	None	Glazing does not break. No visible damage to glazing or frame.
2	None	Glazing cracks but is retained by the frame. Dusting or very small fragments near sill or on floor acceptable.
3a	Very Low	Glazing cracks. Fragments enter space and land on floor no further than 3.3-ft from the window.
3b	Low	Glazing cracks. Fragments enter space and land on floor no further than 10-ft from the window.
4	Medium	Glazing cracks. Fragments enter space and land on floor and impact a vertical witness panel at a distance of no more than 10-ft from the window at a height no greater than 2-ft above the floor.
5	High	Glazing cracks and window system fails catastrophically. Fragments enter space impacting a vertical witness panel at a distance of no more than 10-ft from the window at a height of no more than 2-ft above the floor.

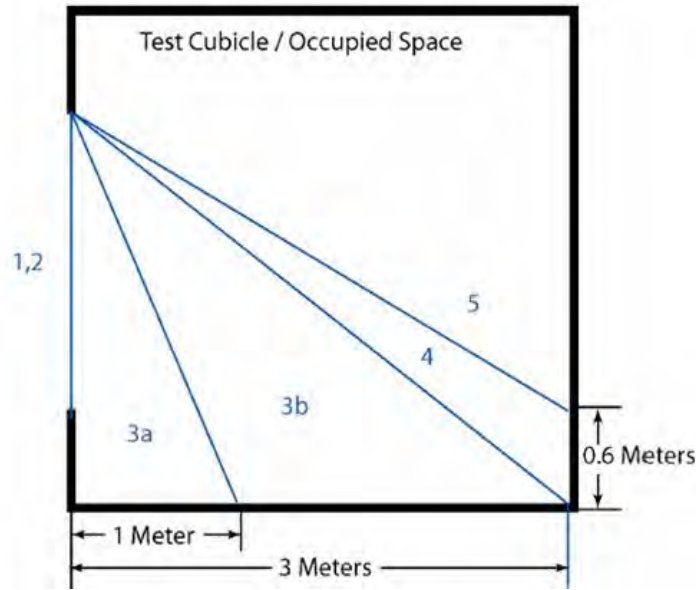


Figure 85. GSA Hazards Classification Diagram

Table 8. Building Damage Level Definition – ABS Consulting

Building Damage Level	Damage Description
1	No permanent deformations. The building is immediately usable.
2	Onset of visible damage to reflected wall of building. Space in and around damaged area can be used and is fully functional after cleanup and repairs.
3	Reflected wall components sustain permanent damage requiring replacement, other walls and roof have visible damage that is generally repairable. Progressive collapse will not occur. Space in and around damaged area is unusable.
4	Reflected wall components are collapsed or very severely damaged. Other walls and roof have permanent damage requiring replacement. Progressive collapse possible. Space in and around damaged area is unusable.
5	Reflected wall has collapsed. Other walls and roof have substantial plastic deformation that may be approaching incipient collapse.
6	Complete failure of the building roof and substantial area of walls.

Table 9. Building Damage Categories – ETL 1110-3-495

[REDACTED]	[REDACTED]	[REDACTED]	[REDACTED]
[REDACTED]	[REDACTED]	[REDACTED]	[REDACTED]
[REDACTED]	[REDACTED]	[REDACTED]	[REDACTED]
[REDACTED]	[REDACTED]	[REDACTED]	[REDACTED]
[REDACTED]	[REDACTED]	[REDACTED]	[REDACTED]
[REDACTED]	[REDACTED]	[REDACTED]	[REDACTED]

A broad spectrum of damage levels ranging from ABS BDL 1/ETL Minimal to ABS BDL 5/ETL Severe were identified throughout the evaluated area.

Damage assessment was performed in the majority of the cases by inspection of the perimeter of the property. Access to the home interior was usually restricted because the owner was not present or unwilling to grant access. Hence, assigned residential buildings damage levels could have an inherent uncertainty level, especially for lower building damage levels (i.e. member damaged but no failures were observable).

3.3.2 Apartment Complex

An apartment complex was located approximately 450 feet from the explosion center directly west of the epicenter. The apartment building was heavily damaged by the explosion with failure of all walls and the roof as shown below in Figure 86 and Figure 87. There were two fatalities reported, one occupying the Apartment Complex and one individual on the east side of the apartment complex who was observing the fire.



Figure 86. Apartment Complex East Façade



Figure 87. Apartment Complex after USAR Operations

4 Computational Fluid Dynamics Simulation

Explosion consequence modeling involved analysis of high explosive detonations to predict blast overpressures and compare to the damage observed to buildings. Evaluation of those scenarios included:

- 1) Determining an explosive size (weight);
- 2) Developing a 3D solid model for analysis,
- 3) CFD modeling of an explosion for the selected size to predict blast pressure and impulse applied to nearby buildings;
- 4) Prediction of damage to buildings due to predicted blast loads and compare to observed damage (analyzed in Section 5).

4.1 Computational Fluid Dynamics

Computational Fluid Dynamics (CFD) is a numerical technique to solve complex equations for fluid interactions. CEBAM is a CFD simulation tool developed specifically to assess blast load interaction with structures and objects. CEBAM can model condensed phase explosions using a simplified energy source term (i.e., the explosion kinetics inside the charge are not modeled but the charge is idealized as a time dependent energy release source representative of a TNT explosion.) CEBAM uses CFD methods that grid the 3D domain and solves fundamental equations. It tracks blast propagation in air and interaction with surfaces, capturing details of shock interaction with objects (e.g., reflections, channeling, or rarefactions).

4.2 CFD vs. Blast Curve Analysis

Blast propagation within urban settings is complex because of reflections, shielding and channeling. These effects limit the accuracy of simple analytical methods which rely on empirical data. In environments where analytical methods become inaccurate, CFD offers a method to accurately model blast wave propagation which includes these effects. In simpler settings, CFD compares very well with analytical methods. This is seen in Figure 88 where CFD simulations for an open field condition are compared to curve fits of test data (K-B).

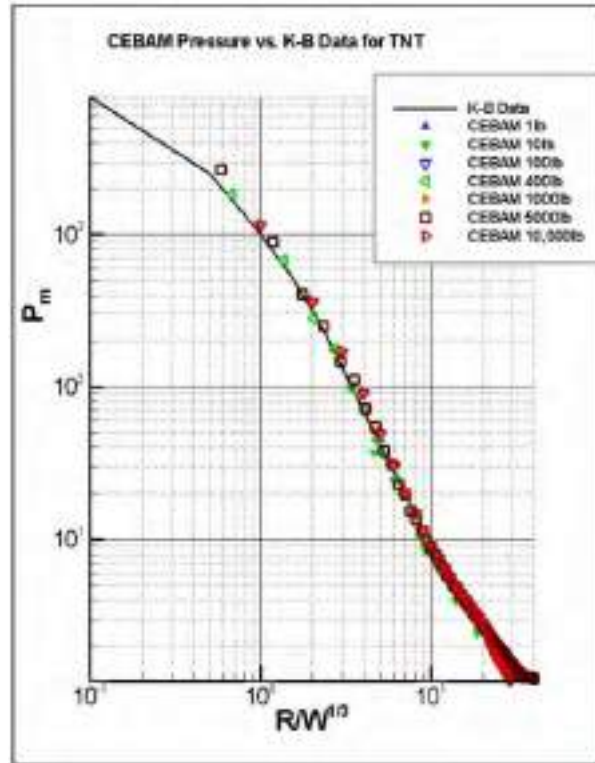


Figure 88. Peak Pressure vs. Scaled Distance for Multiple CFD (CEBAM) Simulations and Kingery-Bulmash Curve^[49]

⁴⁹ J. Keith Clutter, Ph.D., James T. Mathis, and Michael Stahl, "Modeling Environmental Effects in the Simulation of Explosion Events"

4.3 Computer Aided Design (CAD) Representation of West

The area near the blast site was modeled in AutoCAD® for the purpose of importing into a CFD computer code (CEBAM). Figure 89 and Figure 90 show the blast site outlined in red and some of the community surrounding the blast site.

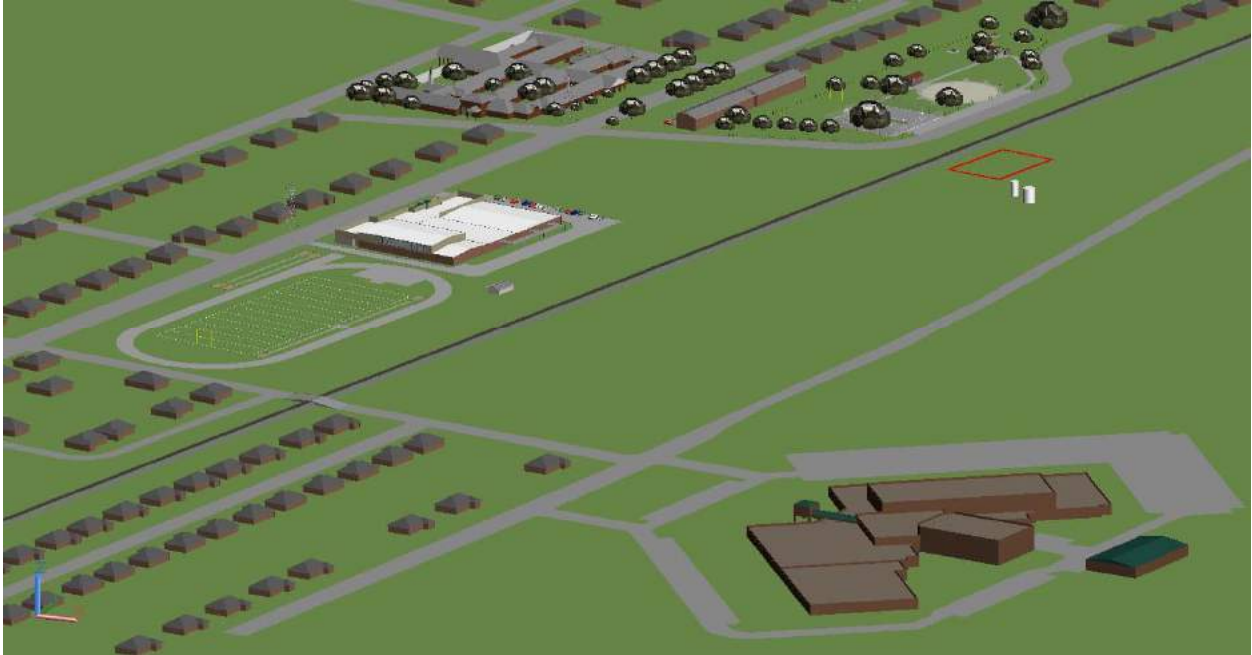


Figure 89. CAD Model of the Area Near the Blast Site (viewed from the Southeast)



Figure 90. A View of the Blast Site from the Northwest

The 3D model object data was imported into the CFD model as shown below in Figure 93 and analyzed. A computational grid was established and a grid refinement study was conducted to determine the required mesh density for accurate results. The results of the grid study are shown below in Figure 91 for peak free-field pressure and Figure 92 for peak free-field scaled impulse. The pressure and impulse values at selected points are shown for each grid size and for the Kingery-Bullmash test data. The results show that the CFD model compares well with Kingery-Bullmash data for peak pressure but over predicts impulse by about 30% in the far field. While a smaller grid size (larger mesh density) would be expected to produce blast impulse values closer to the Kingery-Bulmash data as presented in Figure 88 from the CEBAM validation, the selected grid size produces a reasonable approximation in the free-field given the large domain and the required computational effort. Run time for the model was still lengthy even with the grid approximation utilized; therefore, the large size of the domain utilized in this analysis necessitates some compromise on the grid size in order to accommodate manageable run times.

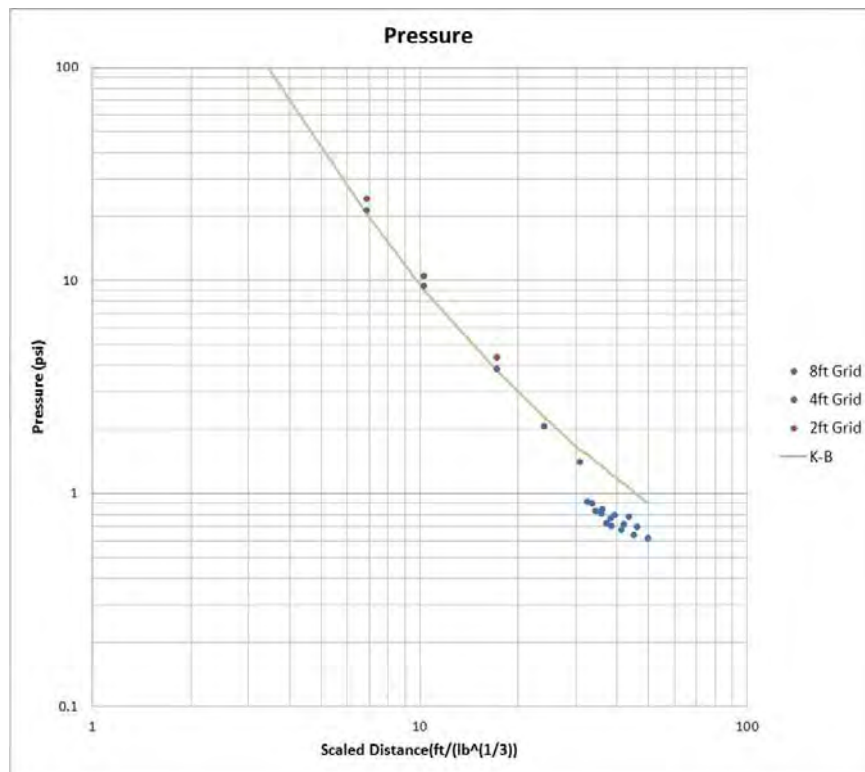


Figure 91. Grid Study Results – Peak Free-Field Pressure

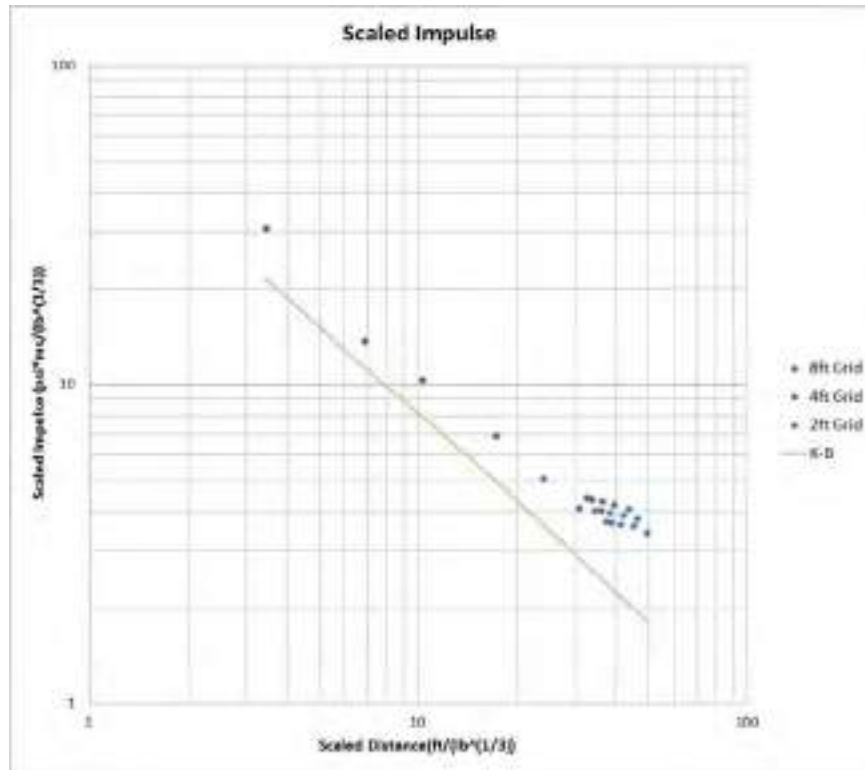


Figure 92. Grid Study Results – Peak Free-Field Scaled Impulse

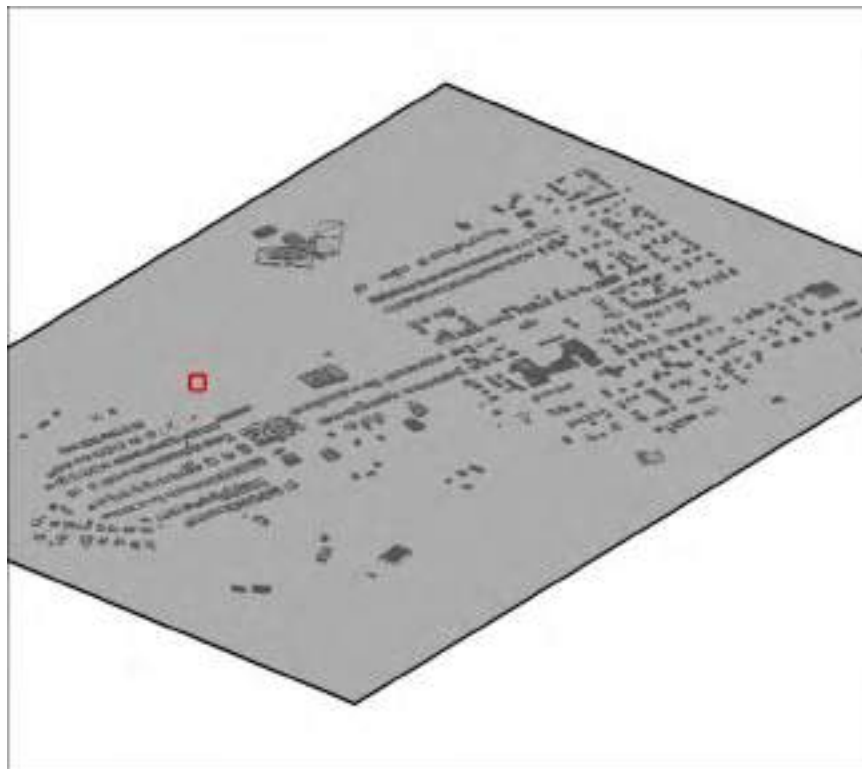


Figure 93. Objects modeled in CEBAM

4.4 Computational Explosion & Blast Assessment Model (CEBAM)

CFD analysis was used to perform a detailed evaluation of the High Explosive using CEBAM [50,51,52] developed by SciRisq. CEBAM is a CFD simulation tool developed specifically to assess blast load interaction with structures and objects. CEBAM can model condensed phase explosions using a simplified energy source term (i.e., the explosion kinetics inside the charge are not modeled but the charge is idealized as a time dependent energy release source representative of a TNT explosion.) CEBAM uses CFD methods that grid the 3D domain and solves fundamental equations for continuity, momentum and energy. Blast propagation in air and interaction with surfaces is also tracked which allows for the capture of shock interaction details with objects (e.g., reflections, channeling, or rarefactions).

Geometries of houses, buildings, and other objects deemed important to the domain of interest are included in the CEBAM model. This includes objects that will affect the propagation of the blast or are objects of special interest (such as public buildings.) The size and location of the explosive source is specified in the model.

The code uses first-principle calculations to produce a time accurate prediction of the event. Phenomena key in determining the hazard severity such as blast focusing, shielding, and diffraction are resolved.

Field data and probes are used to determine pressure and impulse characteristics. In the case of field data, the maximum pressure and impulse of the entire event can be predicted. Specific time dependent traces for pressure and impulse are recorded by probes.

4.5 Explosive Size

The purpose of this analysis was to determine an estimate of the explosive yield by analyzing the damage caused by the overpressure from a high explosive event and comparing to damage predicted by blast load predictions for selected explosives weights. The analysis iterates explosive size to find overpressure that most closely matches damage to surrounding structures observed in the West event.

⁵⁰ CEBAM, Computational Explosion & Blast Assessment Model, ACENG, San Antonio, TX 2005.

⁵¹ J. Keith Clutter (a), Robert T. Luckritz (b), "Comparison of a reduced explosion model to blast curve and experimental data," Journal of Hazardous Materials A79 2000 41–61, a) Analytical and Computational Engineering, Inc., P.O. Box 809, Helotes, TX 78023, USA b) QAnalytics, Mountain Lakes, NJ, USA, Elsevier Press, accepted 16 February 2000.

⁵² J. Keith Clutter (a), Mark G. Whitney (b), "Use of computational modeling to identify the cause of vapor cloud explosion incidents," a) College of Engineering, University of Texas at San Antonio, 6900 North Loop 1604 West, San Antonio, TX 78249, USA b) EQE International, Inc., San Antonio, TX, USA, Journal of Loss Prevention in the Process Industries 14 (2001) 337–347, Elsevier Press, 2001.

Table 10. Scenarios Modeled

Scenario Number	TNT Equivalent (x1000 lb)
1	20,000
2	22,500
3	25,000
4	27,500
5	30,000

4.6 Modeling Explosion

During the modeling of the individual explosions, overpressures at varying locations in all directions from the blast site were evaluated. The overpressures calculated for each structure were then compared to the field data. Prior to contact with structures, the pressure wave appears circular (as with non-CFD methods) as shown below in Figure 94. However, once the pressure wave comes in contact with structures and other site geometry, the pressure wave will become distorted due to phenomena such as shock reflections, and channeling.



Figure 94. An Example of Overpressures Along the Ground

The data produced is three-dimensional, and therefore overpressures on all surfaces (e.g., wall, roofs) can be assessed. Figure 95 shows a three-dimensional pressure wave in the process of propagating away from the blast site.

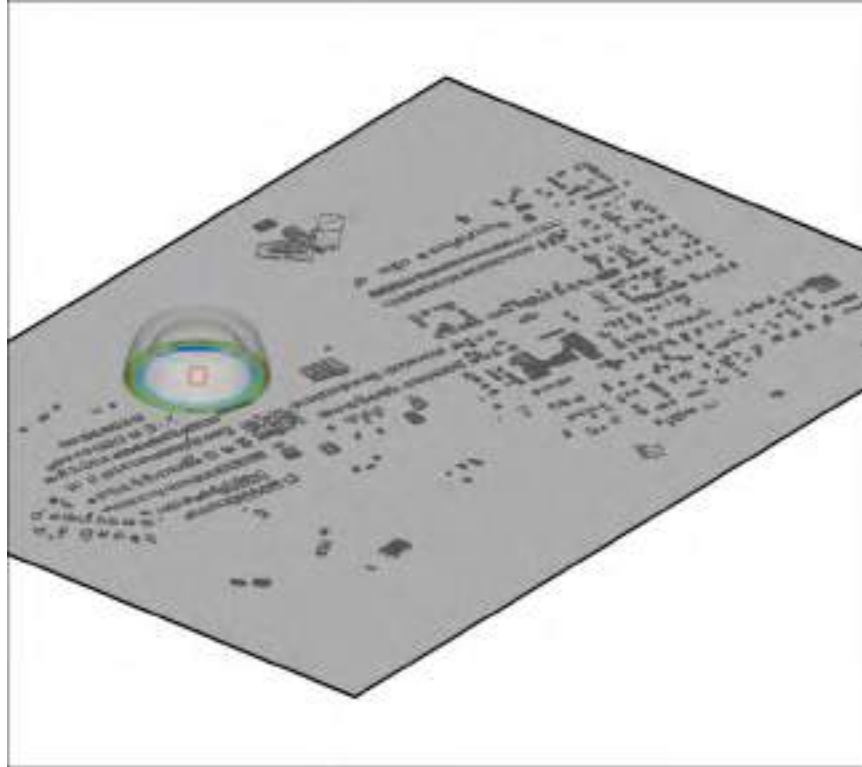


Figure 95. Example of Three-Dimensional Field Data

5 Blast Damage Indicator Analysis

The estimation of TNT equivalent net explosive weight (NEW) for the West Fertilizer explosion was performed in phases. First, preliminary upper and lower bounds of the NEW were estimated. The minimum threshold (lower bound) to cause the observed damage was estimated by analysis of the observed damage to lightweight metal buildings. The upper bound of the expected explosive yield of the West Fertilizer explosion was estimated by analyzing damage due to drag load loads from the blast wave on posts at the basketball court as well as analysis of damage to the nursing home and apartment complex. The building structure analysis utilized a Corps of Engineers guideline, “Estimating Damage to Structures from Terrorist Bombs Field Operations Guide”.^[53] Finally, a three dimensional model was constructed of the West community which included single family residences and community structures. This model was used to predict blast over pressure time histories from various charges weights to determine structural damage and determine the charge weight that best explained the observed damage.

5.1 Preliminary Estimate of Explosive Yield

The preliminary estimated range of TNT equivalent charge weights that are consistent with the observed damage to lightweight metal buildings, the basketball goals, the Apartment Complex and Nursing home was found to be between 20,000 lb_{TNT} and 40,000 lb_{TNT} as discussed in the following sections.

5.1.1 Lightweight Metal Buildings

Twenty different metal buildings were surveyed during the site inspection and permanent deformations of building components were documented. The measured permanent deflections of the structural components were analyzed to determine the minimum charge weight necessary to cause the observed damage.

Structural indicators can be components of a building such as a beam, wall panel, girt, purlin, or plates. Permanent plastic deformations of structural members were collected. The best load indicators are those with minimal permanent deformations, such that the response mode can be identified and modeled. Heavily damaged or totally failed components often have response modes that cannot be easily modeled to allow load prediction.

⁵³ ETL 1110-3-495, “Estimating Damage to Structures from Terrorist Bombs Field Operations Guide”, U.S. Army Corps of Engineers, 14 July 1999.

Attention was paid during data collection to details that could influence the structural conditions or the loading used in analysis. Examples include assessment or definition of the following:

- Support conditions (simple, fixed, continuous, flexible support, slip at connections, etc.)
- Modes of response (bending, membrane, one-way, two-way, flexible supports, etc.)
- Dimensional information (span, spacing, etc.)
- Dimensions required to calculate section properties
- Loaded area supported by the member
- Material type (steel, aluminum, etc.)
- Distance between damaged indicator and explosion location
- Orientation to the explosion source
- Proximity to nearby reflecting surfaces

A dynamic elastic-plastic single-degree-of-freedom (SDOF) analysis was performed on each damaged component that was surveyed using the SBEDS^[54] computer program. The damaged element's structural properties such as cross-section, span, material properties and supported mass are inputs to the program. The component is then analyzed for an equivalent TNT charge weight at a given standoff and orientation (angle of incidence) to compute the structural response.

For each component, a standoff distance is measured to its centerline from the scaled aerial map. Using the standoff and angle of incidence, the charge weight is varied in an iterative analysis until the predicted deformation matches the observed deformation. The permanent deformation of a given member is obtained from the resistance-deflection curve as shown in Figure 96. Deformations measured in the field were all permanent plastic deformation which occurred after the member undergoes elastic recovery and any plastic rebound. This procedure was repeated for each component and a minimum TNT charge weight required to cause the measured damage was obtained.

⁵⁴ Single-Degree-of-Freedom Blast Effects Design Spreadsheets (SBEDS), V5.0, December 2012.

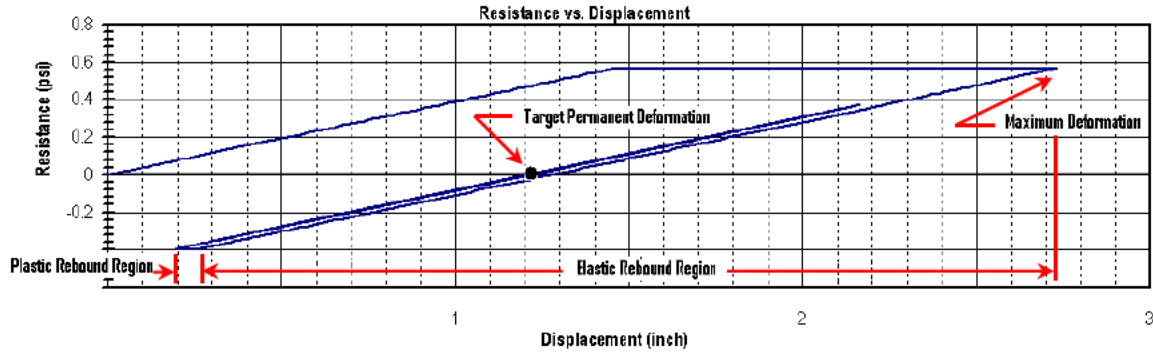


Figure 96. Typical Resistance-Deflection Curve

The shape of a blast wave, from detonations or High Explosives (HE) such as TNT, is a sudden rise in pressure which decays exponentially followed by a negative pressure with a much smaller magnitude. A typical detonation blast wave shape is shown in Figure 97. An initial analysis of all measured damage indicators was performed using only the positive phase of the blast wave.

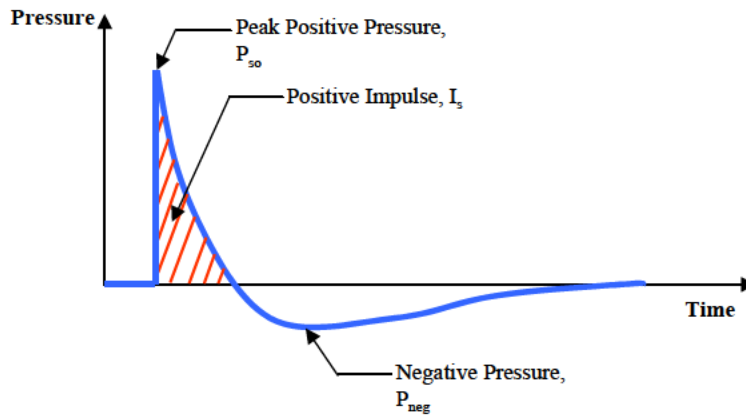


Figure 97. Typical Blast Load for High Explosives

5.1.1.1 Observed Damage

Figure 98 depicts the location of the surveyed metal buildings and Table 11 summarizes the type of field observation for each one of the metal buildings identified in Figure 98.



Figure 98. Surveyed Metal Buildings

Table 11. Metal Building Damage Assessment

Building ID	Location		Survey Date	Measured Damage
	Street No.	Street Name		
MB-01	630	Grady Calvary Dr.	4/26/2013	South wall deflection
MB-02	---	Grady Calvary Dr.	4/26/2013	South wall deflection
MB-03	369	Trlica Rd.	4/26/2013	N/A
MB-04	520	Trlica Rd.	4/26/2013	South wall deflection
MB-05	620	Trlica Rd.	4/26/2013	South wall deflection
MB-06	622	Trlica Rd.	4/26/2013	N/A
MB-07	694 <i>West Lodge 475</i>	Jerry Mashek Rd.	4/26/2013	N/A
MB-08	695	Jerry Mashek Rd.	4/26/2013	N/A
MB-09	<i>Football Field Booth</i>	N Reagan St.	4/24/2013	N/A
MB-10	1008 <i>Webre Hower Service</i>	N Reagan St.	4/26/2013	Roof purlin deflection
				North wall girt deflection
				North wall buckled (no deflection)
MB-11	1203	N Davis St.	4/26/2013	North wall deflection
				Roof purlin deflection
MB-12	1276	Marble St.	4/26/2013	North wall east end deflection
MB-13	<i>Private garage</i>	Haven St.	4/26/2013	Roof purlin deflection (local buckling)
MB-14	411 <i>West Hospital Authority Heliport</i>	Meadow Dr.	4/25/2013	North wall girt deflection
MB-15	411 <i>Storage Building</i>	Meadow Dr.	4/25/2013	N/A
MB-16	412 <i>Office Building & Warehouse</i>	Meadow Dr.	4/25/2013	N/A
MB-17	1502	Stillmeadow Dr.	4/26/2013	N/A
MB-18	1515	N Reagan St.	4/26/2013	South wall deflection
MB-19	---	N I-35 Frontage Rd.	4/26/2013	Roof panel
MB-20	---	N I-35 Frontage Rd.		N/A

Analysis of undamaged indicators established a very high maximum charge weight due to their location in the far field at a great distance from the production building (source location). Undamaged indicators locations (i.e. building locations) are depicted in Figure 99.



Figure 99. Undamaged Metal Buildings Indicators

The information collected in the field was used to estimate the charge weight in pounds of TNT to causing the component damage documented during the surveyed of each metal building. Statistical analysis performed on data set yielded an average charge weight of 20,000-lb_{TNT}. The metal building data has a very large standard deviation and is considered an approximation. Factors affecting the data include (but are not limited to) blast load infiltration into the structure, boundary condition approximations, presence of tension membrane, multiple energy dissipation mechanisms, and clearing of reflected blast loads.

5.1.2 Basketball Goals

The basketball court goal posts presented a noticeable deformation. The observed damage indicated that blast overpressures acting on the basketball backboard and drag forces acting on the hoop posts generated a significant lateral deflection of the system. A substantial amount of crater ejecta and Production Building debris was also identified.

A total of four basketball goal posts were surveyed. Characteristics of each system such as post length, diameter, board dimension and lateral displacement were collected. Approximate standoff distances from the blast source were also determined.

A general plan view of the playground and basketball court, before and after the event, is shown in Figure 100. Surveyed basketball goals are depicted in Figure 101 through Figure 103.



Figure 100. Playground & Basketball Court Plan View – Before and After



Figure 101. Identified Basketball Goal Locations



Basketball Goal #1



Basketball Goal #2

Figure 102. Surveyed Basketball Hoops 1 & 2



Basketball Goal #3



Basketball Goal #4

Figure 103. Surveyed Basketball Goals 3 & 4

Impulse-Momentum and Work-Energy principles were used to predict the response of the structural system, idealized as an equivalent SDOF system, to transient blast loads. The developed model was used to relate blast impulse to the measured post lateral deflection (and post rotation angle). Basic assumptions/approximations used in the analytical formulation were:

- Duration of the blast load was assumed to be relatively short compared to the response time of the system; hence the solution was obtained using impulse/momentum and work/energy principles as opposed to a traditional equivalent SDOF transient time history analysis
- Only positive phase HE blast load was considered; negative phase blast load was ignored
- A rigid-plastic material model for the post was used
- Backboards were assumed to remain attached to the post for sufficient amount of time to transfer the full positive phase blast impulse to the post

Figure 104 describes analytical assumptions model used for the analysis.

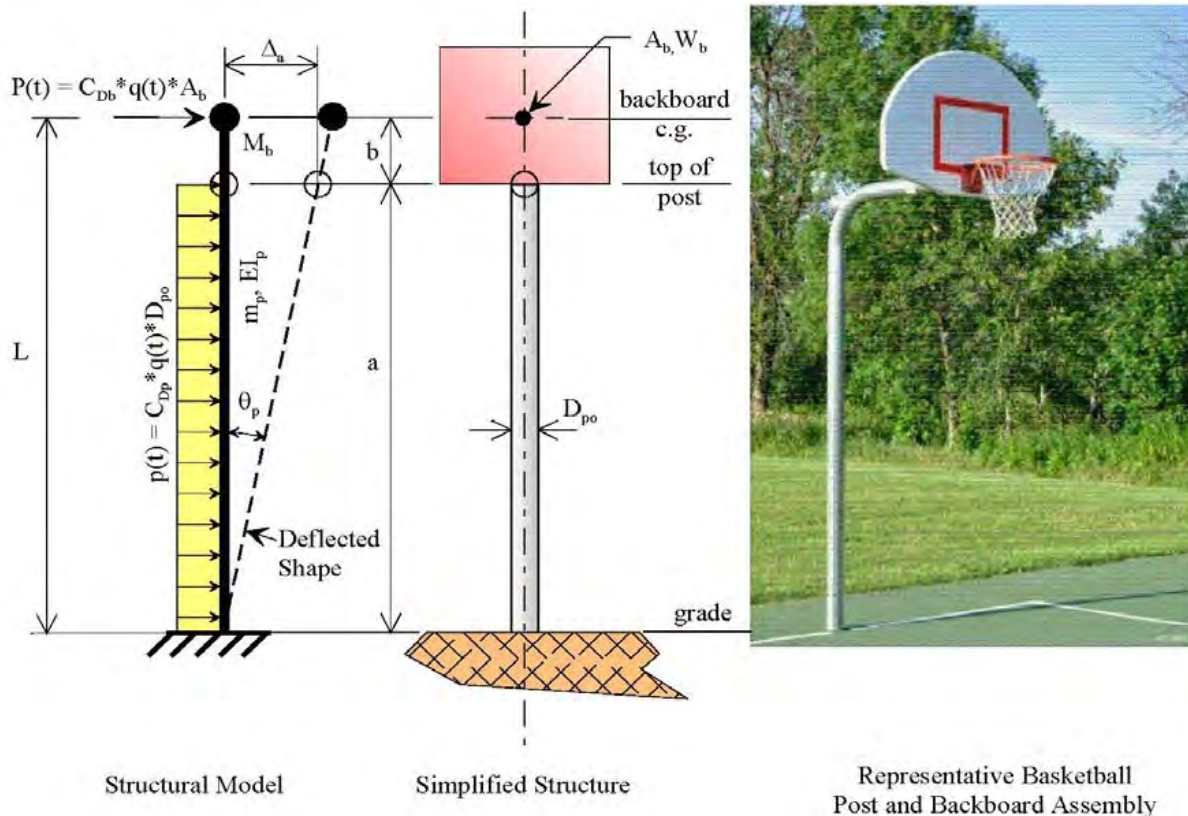


Figure 104. Basketball Goal Structural Model Analysis

Analysis results indicated an average charge weight of approximately 51,000-lb_{TNT}. However, this estimate is known to be high due to the presence of a significant amount of crater ejecta and secondary debris from the Production Building on the basketball court, which can be seen in Figure 102 and Figure 103. Therefore, the damage to the basketball goals was caused by a combination of air blast and debris loading of the goal posts and backboards by the significant amount of secondary debris from the explosion crater and Production Building. The analysis neglects this additional loading and attributes the damage caused by the impact of the crater ejecta erroneously to air blast and thus over predicts the charge weight.

Table 12. Basketball Goal Analysis – TNT_{Eq} Charge Weight

Basketball Hoop ID	Approximate Range (ft)	Permanent Displacement (in)	Calculated TNT _{Eq} Charge Weight (lb)
1	255	44.5	53,600
2	270	46.0	59,500
3	360	10.5	41,600
4	372	15.0	50,700

5.1.3 Apartment Complex and Nursing Home

The Apartment Complex was a two-story timber construction. The building perimeter was constructed of wood stud walls with brick veneer. The roof was constructed of a wood truss system.

Site inspection of the structure indicated the large deformation of the structural members, roof collapse, partial collapse of perimeter walls and major non-structural component damage. The structure was unstable and required shoring for search and rescue efforts. Photos of the damaged Apartment Complex structure are presented in Figure 105 through Figure 107.

A building damage level of [REDACTED] was assigned to the structure based on the observed damage. The definition of [REDACTED] is highlighted below in [REDACTED]. The east façade of the Apartment Complex was at a range of approximately 450 ft. from ground zero. Since [REDACTED] is an area between the charge weight standoff plots shown in [REDACTED] the potential range of charges that could have resulted in the observed damage to the Apartment Complex is [REDACTED] lb_{TNT}.



Figure 105. Apartment Complex Damage



Figure 106. Apartment Complex Damage



Figure 107. Apartment Complex Damage

The Nursing Home was a single story wood framed structure with brick veneer supporting a wood truss roof. [REDACTED] most closely resembles the construction of the Nursing Home even though the Nursing Home is only one story.

Observed field damage of this structure is described in Section 3 of this report; however, the damage to the east façade is shown below in Figure 109 for reference. The east wall is collapsed and the roof trusses have failed.

[REDACTED]^[53] was assigned to the structure based on the observed damage. The definition of [REDACTED] is highlighted below in [REDACTED]

[REDACTED] The east façade of the Nursing was at a range of approximately 650 ft. from ground zero. Since [REDACTED] is an area between the charge weight standoff plots shown below in [REDACTED], the potential range of charges that could have resulted in the observed damage to the Nursing Home is [REDACTED] lb_{TNT}.



Figure 109. Rest Haven Nursing Home East Façade Damage

5.2 3-D Model of West Community

The range of potential explosive yields in TNT has been determined to be between 20,000 lb_{TNT} and 40,000 lb_{TNT} by evaluating the damage to the lightweight metal buildings in the West community as well as performing some field damage estimates of the Nursing Home and Apartment complex in conjunction with the analysis of the basketball court goal posts. In order to further determine a specific charge weight that is most consistent with all of the observed damage a three dimensional model of the West Community, shown below in Figure 111, was constructed. ABS Consulting software FACET3D was utilized to build the virtual model in order to evaluate potential explosion yields with the observed damage to the single family residences and the community structures including the Intermediate School and High School. In addition, the extents of the observed window breakage in West were also evaluated.

5.2.1 Model Methodology

FACET3D is a bespoke software tool developed by ABS Consulting for the analysis and response of buildings and their components to the effects of blast loads from both high explosives and vapor cloud explosions. FACET3D provides a graphical user interface utilizing 3D graphics to draw buildings and display analysis results, often in the form of blast load and damage contour plots.

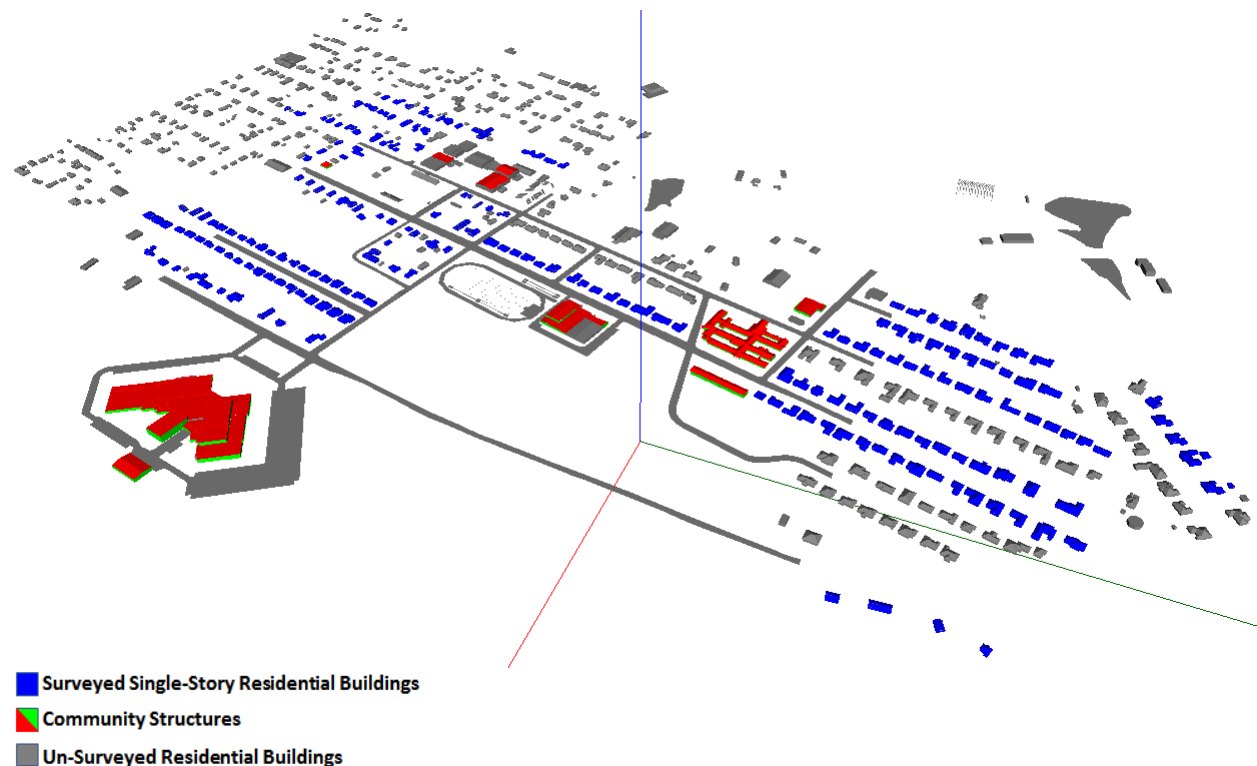


Figure 111. Rendering of the West FACET3D Model

FACET3D was built on the methodology from TM 5-855⁵⁵ which was incorporated into many of the blast prediction tools developed by the US Department of Defense (DOD) such as ConWep, AT Planner, and BEEM. The software allows the user to define threat locations and predicts the peak pressure and impulse applied to each surface defined in the model. As an alternative, blast loads calculated using more advance tools such as computational fluid dynamic (CFD) simulations can be imported into the model. This option was utilized in this specific analysis.

CFD analyses were performed with the software CEBAM as discussed previously in Section 4 and the resulting pressure and impulses were mapped into FACET3D in order to perform the damage assessment to the community. Utilization of CFD provides a more accurate depiction of the shock wave as it wraps around structures and other obstacles, and it also more accurately predicts the total positive impulse on a building face including local reflections, clearing and other blast load phenomena.

Typical construction members (i.e. walls, roof) were analyzed using the single-degree-of-freedom (SDOF) method. The strength and geometric properties of the components were used to determine the SDOF system properties including mass (M), stiffness (K), and force (F). John M. Biggs⁵⁶, *Introduction to Structural Dynamics*, contains a more detailed discussion of the equivalent SDOF technique.

Damage functions (P-I diagrams) were developed to determine structural response, or damage, to walls and roof system components utilizing the response limits and damage level definitions developed by the U.S. Army Corps of Engineers in PDC-TR-06-08⁵⁷. The component damage levels (CDLs) as defined by PDC-TR-06-08 are provided in Table 13 below. The SDOF models were run iteratively for various loads to develop Pressure-impulse (P-I) diagrams. A P-I diagram as shown in Figure 112, is an iso-response curve (each pressure-impulse pair results in the same response in the structure) for a structural member loaded with a particular blast load history shape. Each P-I curve in the set divides the plot into two regions: loads in the area above and to the right of a curve are predicted to produce greater response/damage while loads in the area below and to the left of the curve are predicted to produce less response/damage than loads on the P-I curve. This allows P-I curves to be compared to multiple blast loads and quickly determine the expected damage to a building component. As can be seen below in Figure 112, the four P-I diagrams derived from the PDC-TR-06-08 component damage level definitions in

⁵⁵ Departments of the Army, Air Force, and Navy and the Defense Special Weapons Agency, "Design and Analysis of Hardened Structures to Conventional Weapons Effects", TM 5-855. Washington, DC, Headquarters, Departments of the Army, Air Force, and Navy and the Defense Special Weapons Agency, August 1998.

⁵⁶ Biggs J.M., *Introduction to Structural Dynamics*. New York: McGraw-Hill Book Company. 1964.

⁵⁷ PDC-TR-06-08, "Single Degree of Freedom Structural Response Limits for Antiterrorism Design", U.S. Army Corps of Engineers PDC, Rev. 1, Jan 2008.

Table 13 divide the chart into five distinct damage regions, each corresponding to the PDC component damage levels.

Table 13. Component Damage Level Definitions^[57]

Component Damage Level		Description
1	Superficial Damage	Component has no visible permanent damage
2	Moderate Damage	Component has some permanent deflection. It is generally repairable, if necessary, although replacement may be more economical and aesthetic
3	Heavy Damage	Component has not failed, but it has significant permanent deflections causing it to be unrepairable
4	Hazardous Failure	Component has failed, and debris velocities range from insignificant to very significant
5	Blowout	Component is overwhelmed by the blast load causing debris with significant velocities

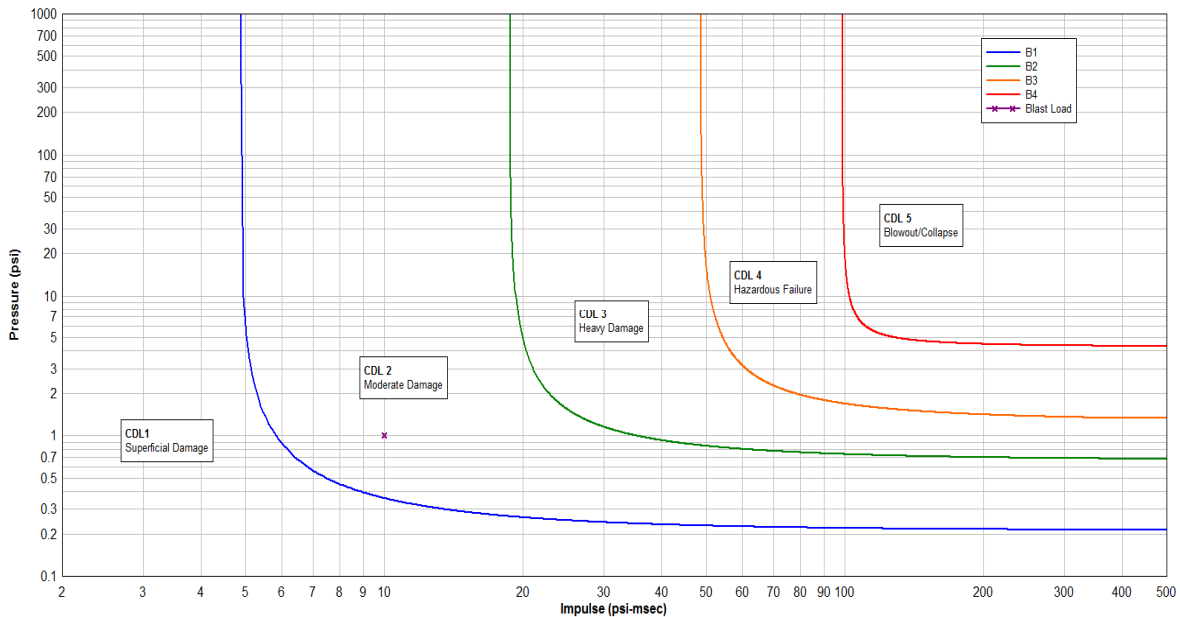


Figure 112. P-I Diagram Example

The structural damage indicators incorporated into the blast model are discussed in the following sections.

5.2.2 Single Family Residences

A graphical map showing the building damage levels assigned to the single family residences are provided in Figure 113 through Figure 114. Damage levels are as defined by ABS Consulting damage methodology as defined in Section 3.3.1 and Table 8.

Overall extent of observed window breakage as observed in the field is shown below in Figure 115. These extents do not mean that windows were not broken outside of this distance. Field observations were made of windows broken well outside of this range; however, this boundary represents the extents of consistent window breakage within the residential community.



Figure 113. Qualitative Building Damage ABS BDL Levels of Surveyed Structures [1/2]



Figure 114. Qualitative Building Damage ABS BDL Levels of Surveyed Structures [2/2]

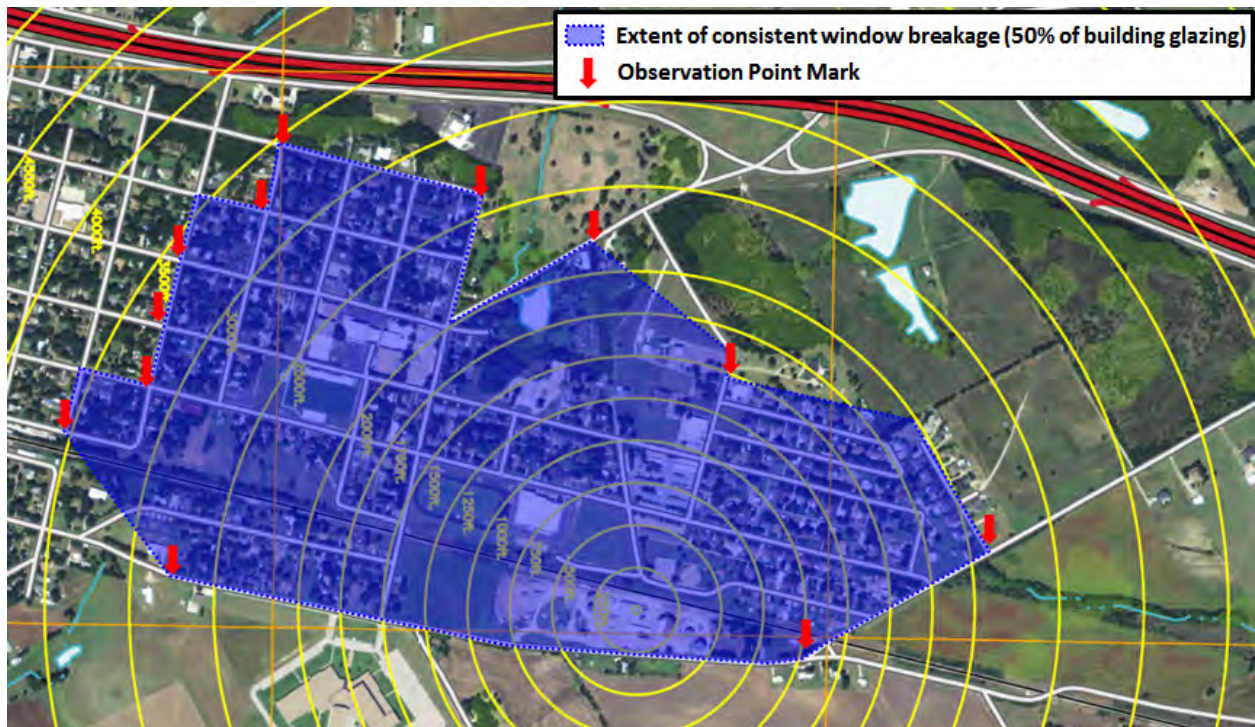


Figure 115. Extent of Observed Window Breakage

P-I curves corresponding to structural components (i.e. walls, roof) were developed utilizing the software tool SBEDS. SBEDS is an Excel© based tool developed for the US Army Corps of Engineers used for the design and analysis of structural components subjected to dynamic loads, such as air blast from explosives, using SDOF methodology. SBEDS is based on Army TM 5-1300 (also designated as NAVFAC P-397 and AFR 88-22, currently UFC 3-340-02⁵⁸). The P-I diagrams are provided for reference in Figure 116 through Figure 118 for the single family residences.

Glazing P-I curves corresponding to the identified window configuration were developed using WINGARD PE Version 6.0. This code determines window system performance subjected to blast loads. The code was developed by the General Services Administration (GSA) based on a combination of analytical techniques and validated by test data.

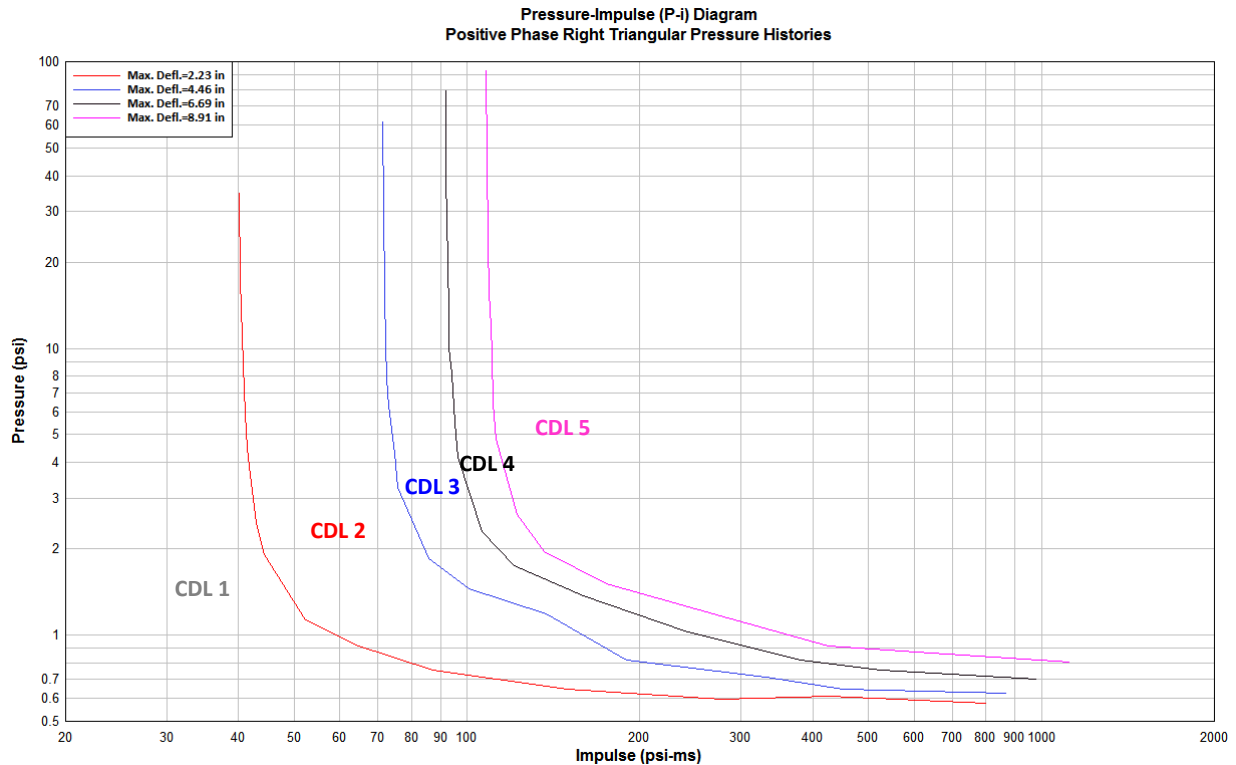


Figure 116. Residential Building Analysis: Wood Stud Wall with Brick Veneer P-I Diagram

⁵⁸ Departments of the Army, the Navy, and the Air Force, “Structure to Resist the Effects of Accidental Explosions,” United Facilities Criteria (UFC) 3-340-02, 5 December 2008.

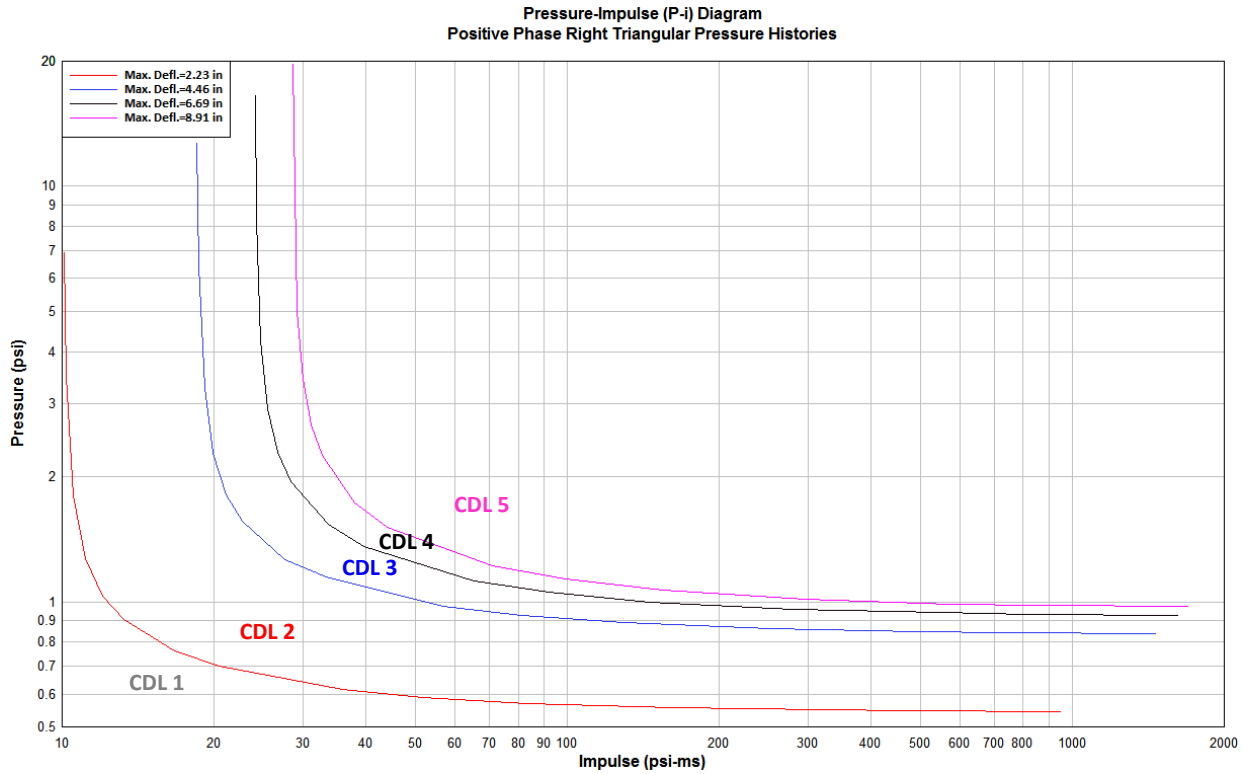


Figure 117. Residential Building Analysis: Wood Stud Wall with Wood Siding P-I Diagram

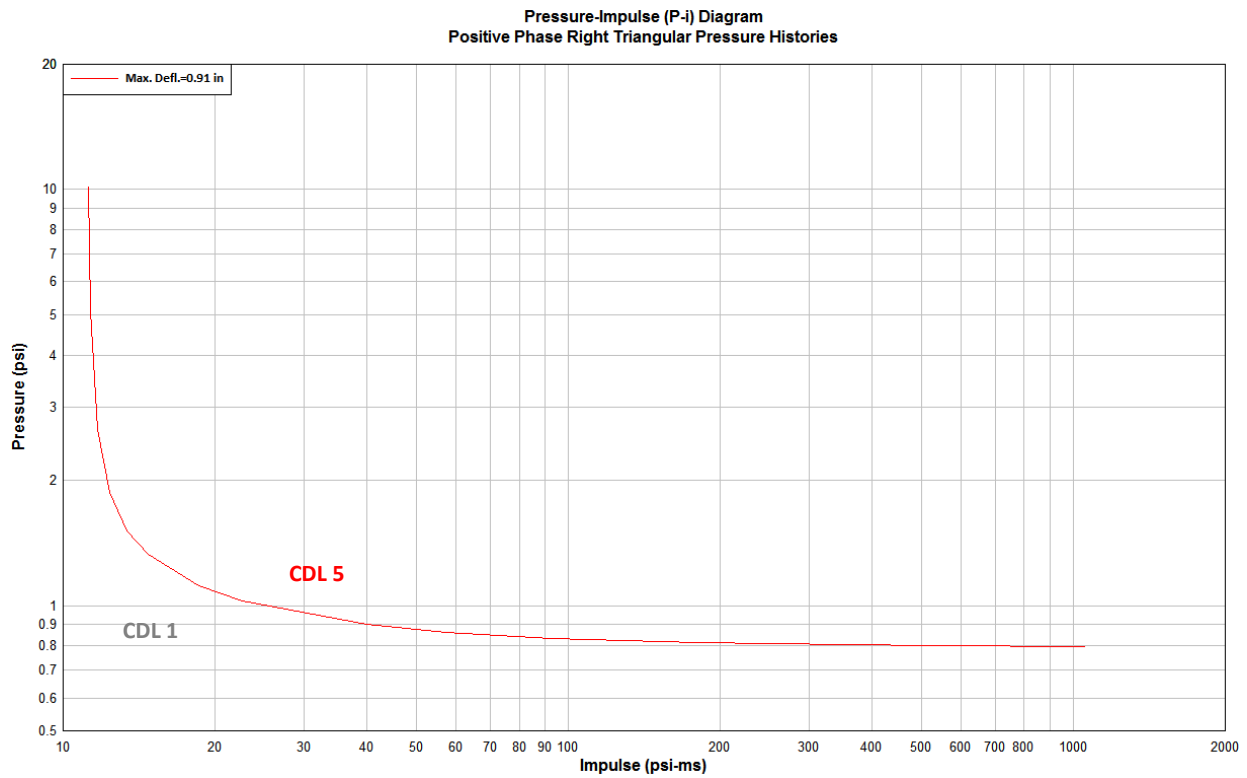


Figure 118. Residential Building Analysis: Roof Wood Truss

5.2.3 Community Structures

Five community structures were assessed during the West, TX site inspection. However, damage functions for the following three structures were incorporated into the West Fertilizer FACET3D model:

- West Intermediate School
- West High School
- West Middle School

Typical construction system, component characteristics and post-event structural condition were document for each facility. Collected data and performed analysis details are described below for each aforementioned structure.

5.2.3.1 West Intermediate School

A detail assessment of the West Intermediate School was conducted by ABS Consulting on May 29, 2013. General construction characteristics, building section and observed damage were documented (refer to Section 3.2.3). Special attention was paid to the identification of qualitative damaged load indicators that could be used to validate the energy of the explosion (i.e. TNT_{Eq} charge weight). Figure 119 through Figure 122 illustrate some of the documented damage indicators.



Figure 119. Roof Purlin Deformation at Gymnasium



Figure 120. Roof Beam & Purlin Deformation at Cafeteria



Figure 121. Deflection of OWSJ at Room 18



Figure 122. Joist Girder Deformation at Library

A structural plan of the West Intermediate School roof system was generated based on the data collected during the facility assessment, as depicted in Appendix A. It is noted here that although the open webbed steel joists were intact, they were heavily damaged (Reference Figure 121 and Figure 122) and were observed have undergone significant deformation which may have generated load redistribution mechanisms in the joist which are not included in the structural models used herein.

P-I curves corresponding to structural components were developed utilizing the software tool SBEDS. A typical P-I curve example is shown in Figure 123.

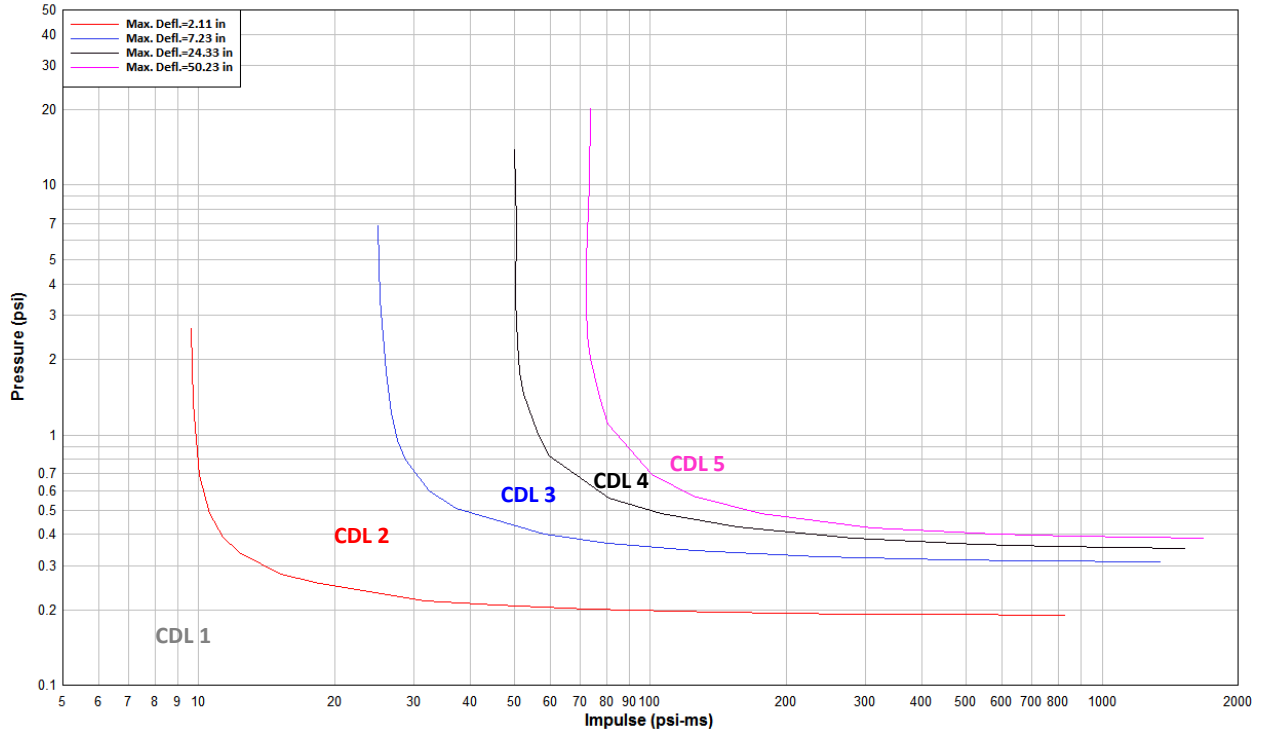


Figure 123. West Intermediate School: Gymnasium Roof Purlin P-I Diagram

5.2.3.2 West High School

Concrete masonry unit (CMU) walls supporting open webbed steel joists and a metal deck with built up roofing and gravel ballast represent the typical construction system of the West High School.

Observed field damage of this structure is described in Section 3.2.4 of this report.

Roof component damage was identified and structural models of the open web steel joists supporting the roof deck and gravel ballast were generated. P-I diagram representative of the High School open web steel joist roof components is provided below in Figure 124.

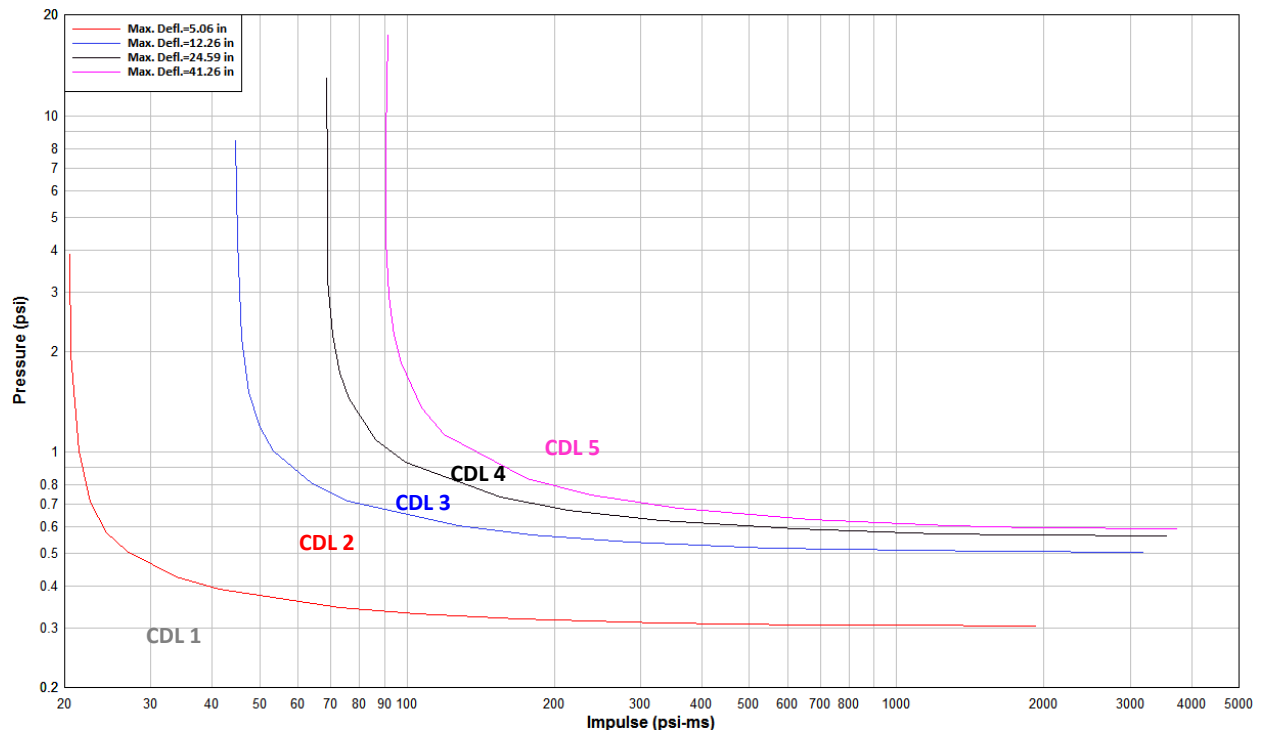


Figure 124. West High School: Example OWSJ P-I Diagram

5.2.3.3 West Middle School

Damage assessment of the West Middle School campus is described in Section 3.2.5. Damage indicators from the Middle School included the Practice Gymnasium roof purlins and Classroom Annex roof joists. Permanent deformations were observed in the Practice gymnasium roof and the Classroom Annex roof was undamaged. P-I diagrams for the practice gymnasium roof purlins and classroom annex OWSJs are provide below in Figure 125 and Figure 126, respectively.

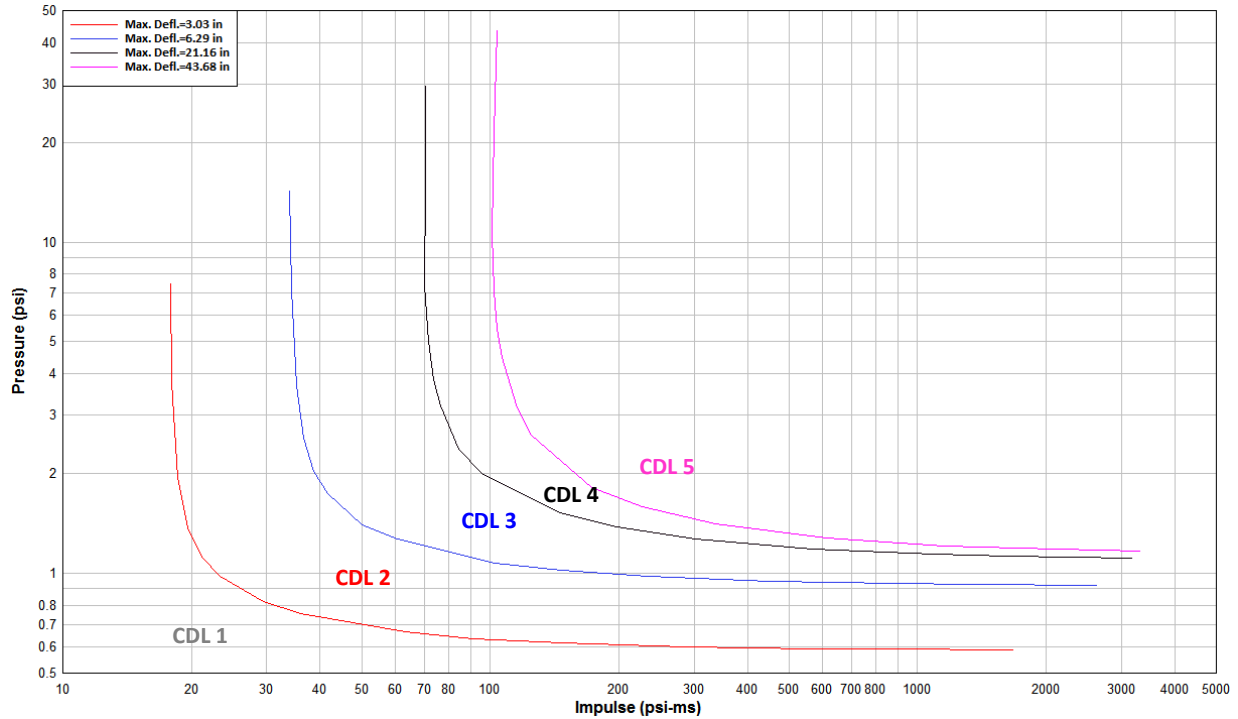


Figure 125. West Middle School: Gymnasium Roof Purlin P-I Diagram

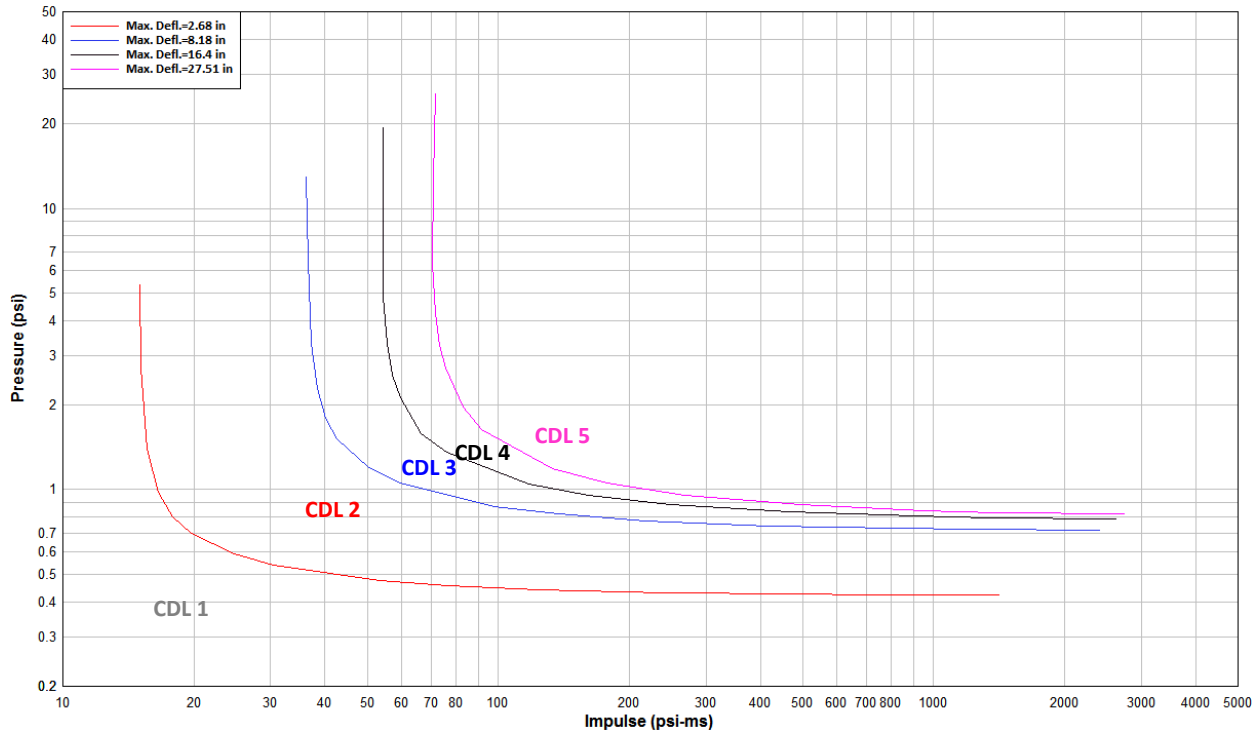


Figure 126. West Middle School: Classroom Annex OWSJ P-I Diagram

5.3 Final Estimate of Explosive Yield Utilizing 3D Model of West

Seven simulations were run in the CFD analysis described in Section 4 in order to develop loads in the West community so that the structural damage could be evaluated for each charge weight and the yield of the West Fertilizer explosion most consistent with the observed damage determined. The charge weights selected based upon the preliminary yield estimate discussed in Section 5.1 were: 20,000 lb_{TNT}, 22,500 lb_{TNT}, 25,000 lb_{TNT}, 27,500 lb_{TNT}, 30,000 lb_{TNT}, 32,500 lb_{TNT}, 35,000 lb_{TNT}. Initial evaluation of the results made it clear that charge weights above 30,000 lb_{TNT} resulted in damage that was not consistent with damage observations to the High School and residential structures. Therefore, a detailed evaluation of the damage for charge weights ranging from 20,000 lb_{TNT} up to 30,000 lb_{TNT} was performed.

Component damage level percentages corresponding to wall surfaces modeled in FACET3D were calculated for the five different charge weights and correlated to the observed BDLs based upon the structural models of the residences discussed in Section 5.2.2. A correlation of expected wall component damage, based upon a percent of the wall surface area, and the Building Damage level was developed based upon the BDL definitions and is presented below in Table 14.

Table 14. Approximate Residential Wall CDL Percentages by ABS Consulting BDL

Building Damage Level	Damage Description	Approximate Percent of Wall Damage by CDL				
		CDL 1	CDL 2	CDL 3	CDL 4	CDL 5
1	No permanent deformations. The building is immediately usable.	100%	-	-	-	-
2	Onset of visible damage to reflected wall of building. Space in and around damaged area can be used and is fully functional after cleanup and repairs.	0% up to 75%	25% up to 100%	-	-	-
3	Reflected wall components sustain permanent damage requiring replacement, other walls and roof have visible damage that is generally repairable. Progressive collapse will not occur. Space in and around damaged area is unusable.	75%		25%	-	-
4	Reflected wall components are collapsed or very severely damaged. Other walls and roof have permanent damage requiring replacement. Progressive collapse possible. Space in and around damaged area is unusable.	75%			25%	
5	Reflected wall has collapsed. Other walls and roof have substantial plastic deformation that may be approaching incipient collapse.	0% – 25%			75% - 100%	

The single family residences from the 1100 to the 1500 block of N. Reagan were selected for BDL evaluation due to the proximity of the homes to the explosion center, as well as the array of observed BDLs. The observed BDLs ranged from a BDL of 5, in the vicinity of the Rest Haven Nursing Home, to a BDL of 2 at 1100 N. Reagan. The residences were divided into two groups based on their location with respect to the approximate explosion source: 1400 & 1500 Blocks of N. Reagan St. the North of W. Haven, and the 1100 & 1200 blocks of N. Reagan Street, to the south of W. Haven. Charge weights that best explained the observe BDLS to these single family residences were determined for homes grouped by building damage level. The results for the 1100-1200 block of N. Reagan are presented below in Figure 127 and the results for the 1400-1500 block of N. Reagan are presented below in Figure 128.

BDL 4: Reflected wall components are collapsed or very severely damaged. Other walls and roof have permanent damage requiring replacement. Progressive collapse possible.

TNT _{Eq}	CDL1	CDL2	CDL3	CDL4	CDL5	Total
20,000-lb	4%	40%	25%	12%	19%	100%
22,500-lb	4%	32%	24%	13%	27%	100%
25,000-lb	3%	24%	24%	14%	34%	100%
27,500-lb	4%	9%	25%	18%	44%	100%
30,000-lb	3%	7%	21%	19%	50%	100%

BDL 3: Reflected wall components sustain permanent damage requiring replacement, other walls and roof have visible damage that is generally repairable.

TNT _{Eq}	CDL1	CDL2	CDL3	CDL4	CDL5	Total
20,000-lb	16%	63%	19%	1%	2%	100%
22,500-lb	11%	59%	22%	6%	2%	100%
25,000-lb	8%	56%	20%	11%	5%	100%
27,500-lb	8%	41%	24%	13%	14%	100%
30,000-lb	8%	33%	26%	12%	22%	100%

BDL 2: Onset of visible damage to reflected wall of building.

TNT _{Eq}	CDL1	CDL2	CDL3	CDL4	CDL5	Total
20,000-lb	55%	45%	0%	0%	0%	100%
22,500-lb	41%	59%	0%	0%	0%	100%
25,000-lb	26%	74%	0%	0%	0%	100%
27,500-lb	8%	92%	0%	0%	0%	100%
30,000-lb	7%	91%	2%	0%	0%	100%

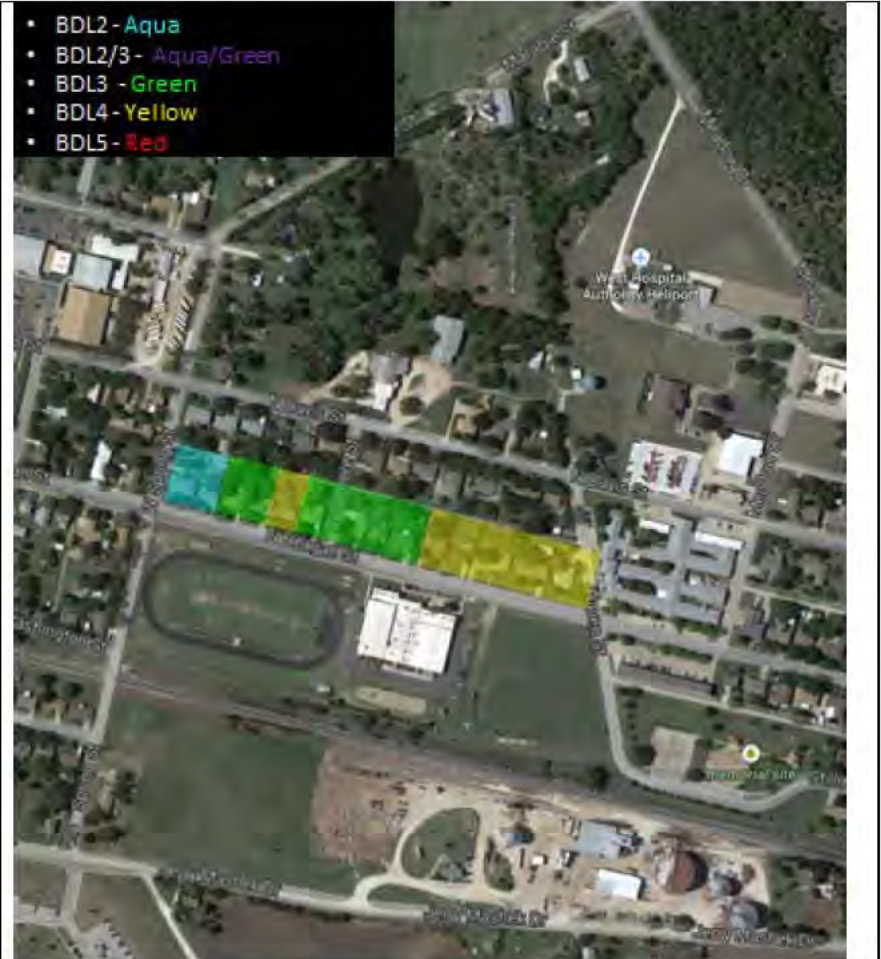


Figure 127. 1100 - 1200 Blocks of N. Reagan St. Observed Single Family Dwelling BDLs

BDL 5: Reflected wall has collapsed. Other walls and roof have substantial plastic deformation that may be approaching incipient collapse.

TNT _{Eq}	CDL1	CDL2	CDL3	CDL4	CDL5	Total
20,000-lb	6%	20%	22%	16%	36%	100%
22,500-lb	6%	12%	20%	19%	43%	100%
25,000-lb	6%	8%	18%	13%	55%	100%
27,500-lb	6%	2%	11%	16%	64%	100%
30,000-lb	5%	2%	10%	12%	72%	100%

BDL 4: Reflected wall components are collapsed or very severely damaged. Other walls and roof have permanent damage requiring replacement.

TNT _{Eq}	CDL1	CDL2	CDL3	CDL4	CDL5	Total
20,000-lb	8%	66%	20%	5%	0%	100%
22,500-lb	5%	59%	23%	11%	2%	100%
25,000-lb	3%	51%	27%	14%	6%	100%
27,500-lb	2%	38%	28%	14%	17%	100%
30,000-lb	2%	28%	30%	18%	22%	100%

BDL 3: Reflected wall components sustain permanent damage requiring replacement, other walls and roof have visible damage that is generally repairable.

TNT _{Eq}	CDL1	CDL2	CDL3	CDL4	CDL5	Total
20,000-lb	30%	69%	1%	0%	0%	100%
22,500-lb	20%	78%	2%	0%	0%	100%
25,000-lb	10%	84%	6%	0%	0%	100%
27,500-lb	2%	86%	10%	1%	0%	100%
30,000-lb	0%	81%	16%	3%	0%	100%



Figure 128. 1400 - 1500 Block of N. Reagan St. Observed Single Family Dwelling BDLs

The results of the residential BDL assessment are summarized in Table 15 below. The charge weight that most consistently explained the observed damage to the single family residences on N. Reagan Street was clearly 25,000 lb_{TNT}.

Table 15. Summary of Yield Assessment based upon N. Reagan Street Single Family Residence Damage

1100 - 1200 Block of N. Reagan St.					
BDL	20,000-lb	22,500-lb	25,000-lb	27,500-lb	30,000-lb
2	•	•	•		
3		•	•		
4		•	•		
1400 - 1500 Block of N. Reagan St.					
3			•	•	•
4			•	•	
5		•	•	•	

The damage to the Intermediate School roof was heavy as observed by ABS Consulting and discussed in Section 3.2.3. Also, as previously discussed, although the open webbed steel joists were intact, they were heavily damaged (Reference Figure 139 and Figure 140) and were observed have undergone significant deformation which may have generated load redistribution mechanisms in the joist which are not included in the structural models used herein. FACET3D analysis indicated that modeled roof components reached a response level equivalent to CDL 5 for each evaluated charge weight, a response that differs from the observed damage in the field. Analysis outcome is due in part due to:

- Limitation of the model to capture the interaction of internal and external loading acting on roof systems as consequence of blast wave penetration of the building envelop.
- Load redistribution in the OWSJs after formation of a failure mechanism including development of tension membrane forces in the top cord of the joists.
- Joists contacting and transferring load to non-bearing internal metal stud partition walls was also observed.

Therefore, although the damage to the Intermediate School predicted by the 25,000 lb_{TNT} simulation is higher than observed, the differences between the observed damage and the predicted damage can be explained.

As discussed previously in Section 3.2.4 and 5.2.3.2, the West High School roof sustained light to moderate damage from the explosion. The failure of the roof over the Gymnasium was caused by a combination of out-of-plane blast loading and in-plane diaphragm loading from the wall blast reaction. The model utilized does not account for the significant in-plane loading of the gymnasium roof; therefore, the gymnasium joist girders were not modelled, only the OWSJs. The damage to the High School predicted by the FACED3D simulation for 20,000 lb_{TNT}, 25,000 lb_{TNT} and 30,000 lb_{TNT} are presented below in Figure 129, Figure 130 and Figure 131, respectively. FACET3D results for 20,000 lb_{TNT} and the 25,000 lb_{TNT} CEBAM simulation and the , shown below in Figure 129 and Figure 130, show that the predicted damage to the roof of the north wing of the High School more closely resembles the deformations that were observed. The results for the 30,000 lb_{TNT} simulations shown below in Figure 131 appear to over predict the damage to the High School. Therefore, the 25,000 lb_{TNT} yield that is consistent with the damage to the single family residences is also most consistent with the observed damage to the High School. It is noted that the High School is located far from the explosion source and near the domain boundaries and that the impulse predictions at this location of the model are affected by these gridding and domain approximations.

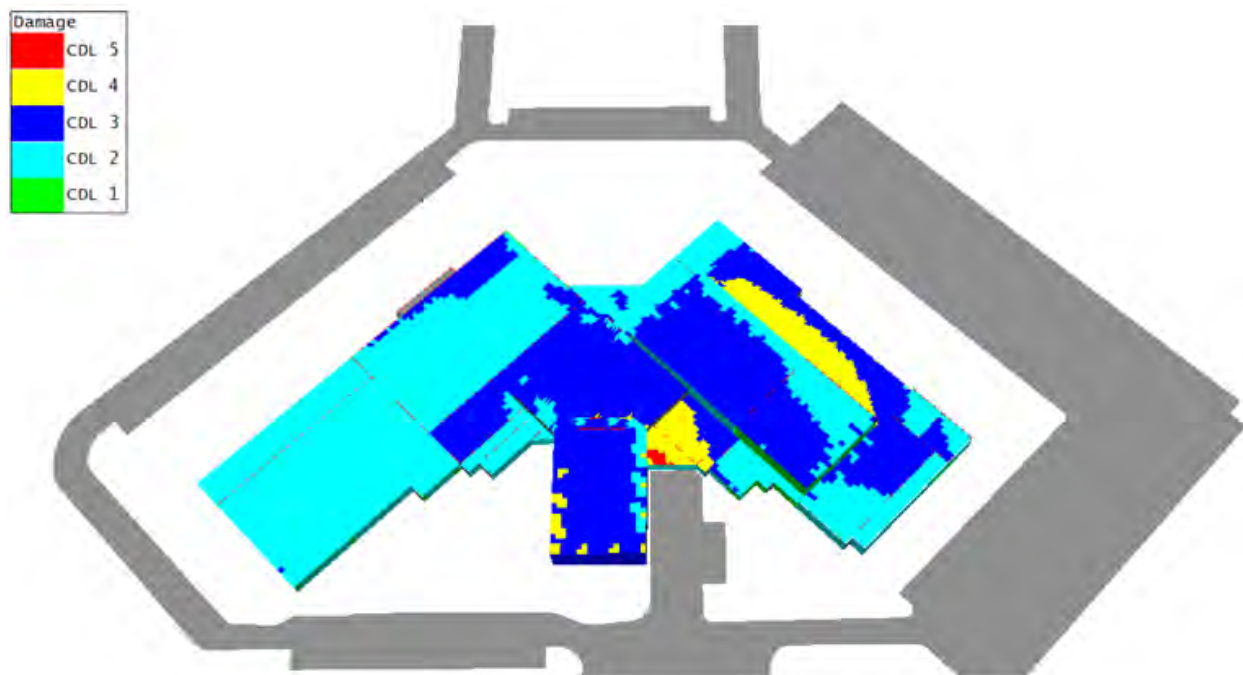


Figure 129. High School FACET3D Model Response – 20,000-lb_{TNT}

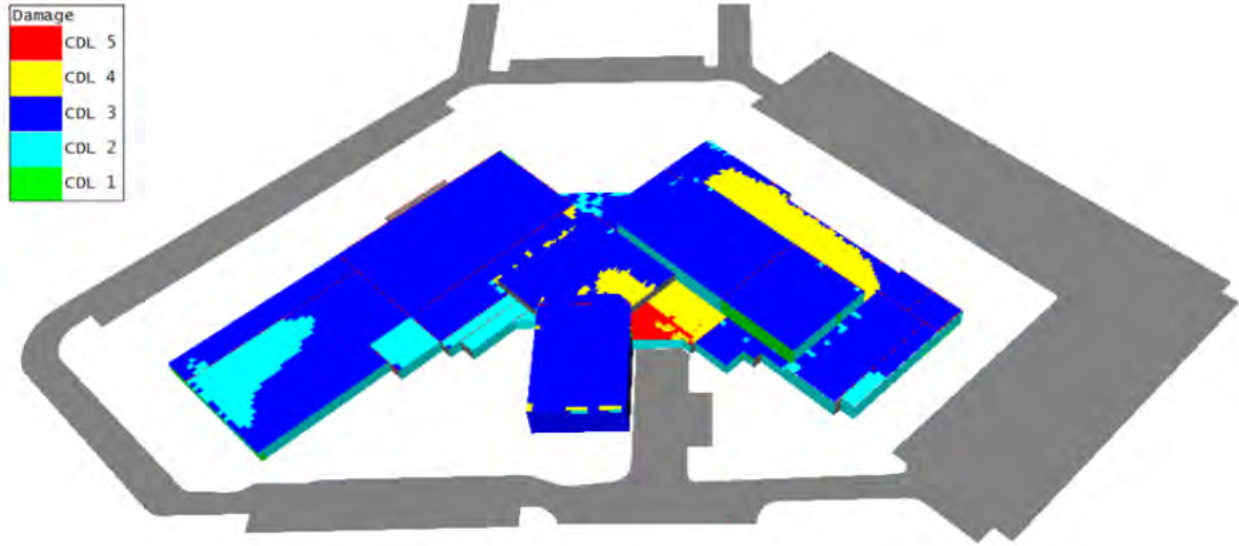


Figure 130. High School FACET3D Model Response – 25,000-lb_{TNT}

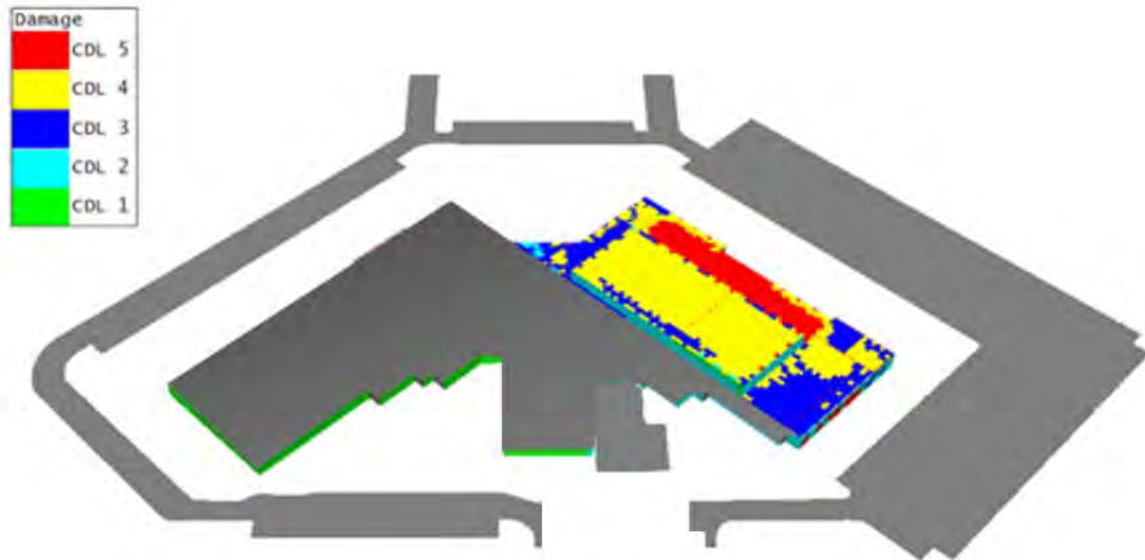


Figure 131. High School FACET3D Model Response – 30,000-lb_{TNT}

6 Findings

ABS Consulting Inc. was contracted by the U.S. Chemical Safety Board (CSB) to perform a site survey, collect data pertaining to structural damage and to estimate the explosion yield and resulting overpressure and impulse contours could be made. The objectives of the ABS Consulting work, the results of which are discussed in the prior sections of this report, included:

1. Provide preliminary opinions of explosion characteristics including but not limited to potential fuel source(s), blast pressures and fuel source configurations.
2. Perform a field investigation in order to document damage to the community and measure structural damage.
3. Conduct a literature review of Ammonium Nitrate (AN) including review of the following information:
 - a. AN- TNT explosive equivalence with various contaminants, physical states, particle size and AN pile geometry.
 - b. Percentage of AN quantity present that would be expected to detonate from review of previous incidents and testing.
4. Perform a Computational Fluid Dynamics (CFD) analysis of the West community to simulate the blast wave expansion and interaction with structures to confirm the estimated Net Explosive Weight (NEW) required to cause the observed damage.
5. Perform a detailed assessment of explosive yield based upon blast damage indicators.

ABS Consulting determined that the explosive energy of the West Fertilizer explosion that is most consistent with the observed damage was 25,000 lb_{TNT}. As discussed in Section 2.3.3.3 of the literature survey, the theoretical maximum TNT_{eq} for AN is 60%. Therefore, the explosive yield of AN would be predicted to be 25,000 lb_{TNT} / 0.6 = ~42,000 lb_{AN} based upon the maximum reported TNT equivalence of 60%. In addition, the suggested U.S. Army Field Manual TNT_{eq} of 23% would result in a yield of ammonium nitrate of approximately 109,000 lb_{AN}. Clearly the TNT_{eq} of 23% reported by the field manual is too low based upon the observed damage to the community by the event shock wave. The stack in the main AN bin was estimated to be 30 tons, which results in a TNT_{eq} of 42% based upon the 25,000 lb_{TNT} yield determined in the damage indicator assessment. In addition, since it was not determined how much AN was consumed in the fire prior to exploding, the yield, or efficiency, is ultimately indeterminate.

Pressure and Impulse contours for the community of west, based upon the predicted 25,000 lb_{TNT} equivalent explosive yield, are presented below in Figure 132 and Figure 133 below. Applied pressures predicted for: the High School are presented below in Figure 134, for the Intermediate School are presented in Figure 135, Rest Haven Nursing Home in Figure 136, and for the Apartment Complex in Figure 137.



Figure 132. West Fertilizer Explosion Free-Field K-B Pressure Contours for 25,000 lb_{TNT}

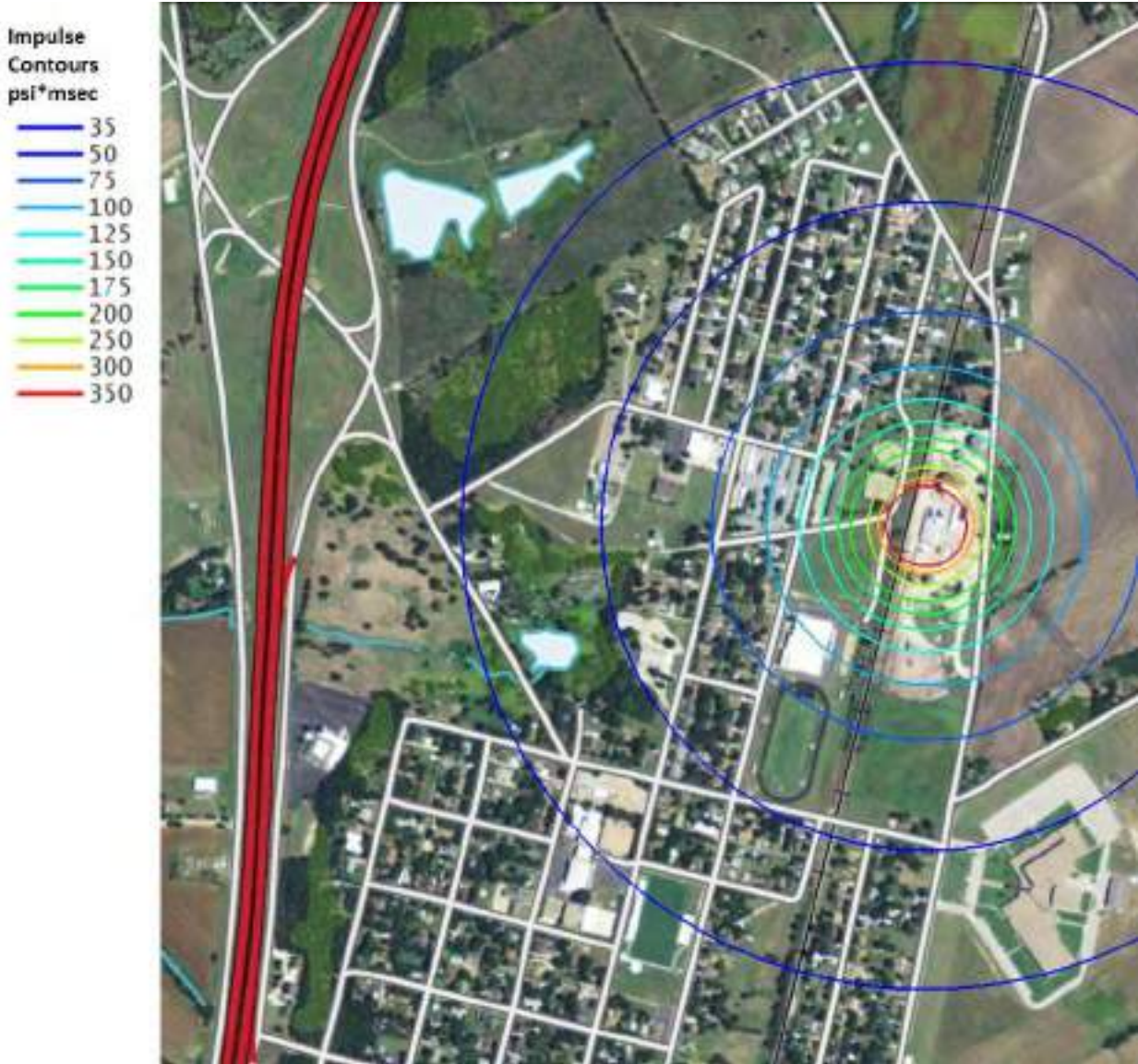


Figure 133. West Fertilizer Explosion Free-Field K-B Impulse Contours for 25,000 lb_{TNT}

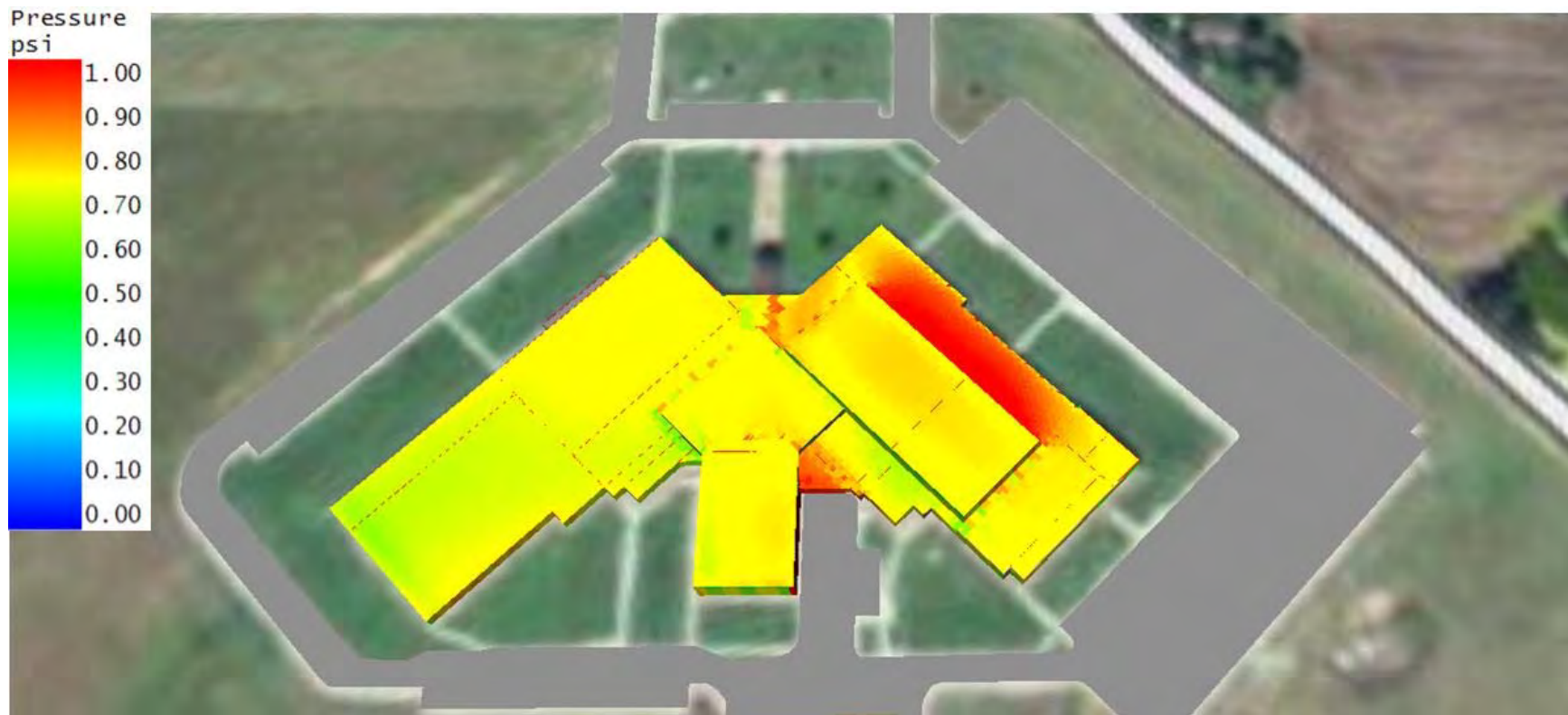


Figure 134. West High School Applied Pressures (CFD)

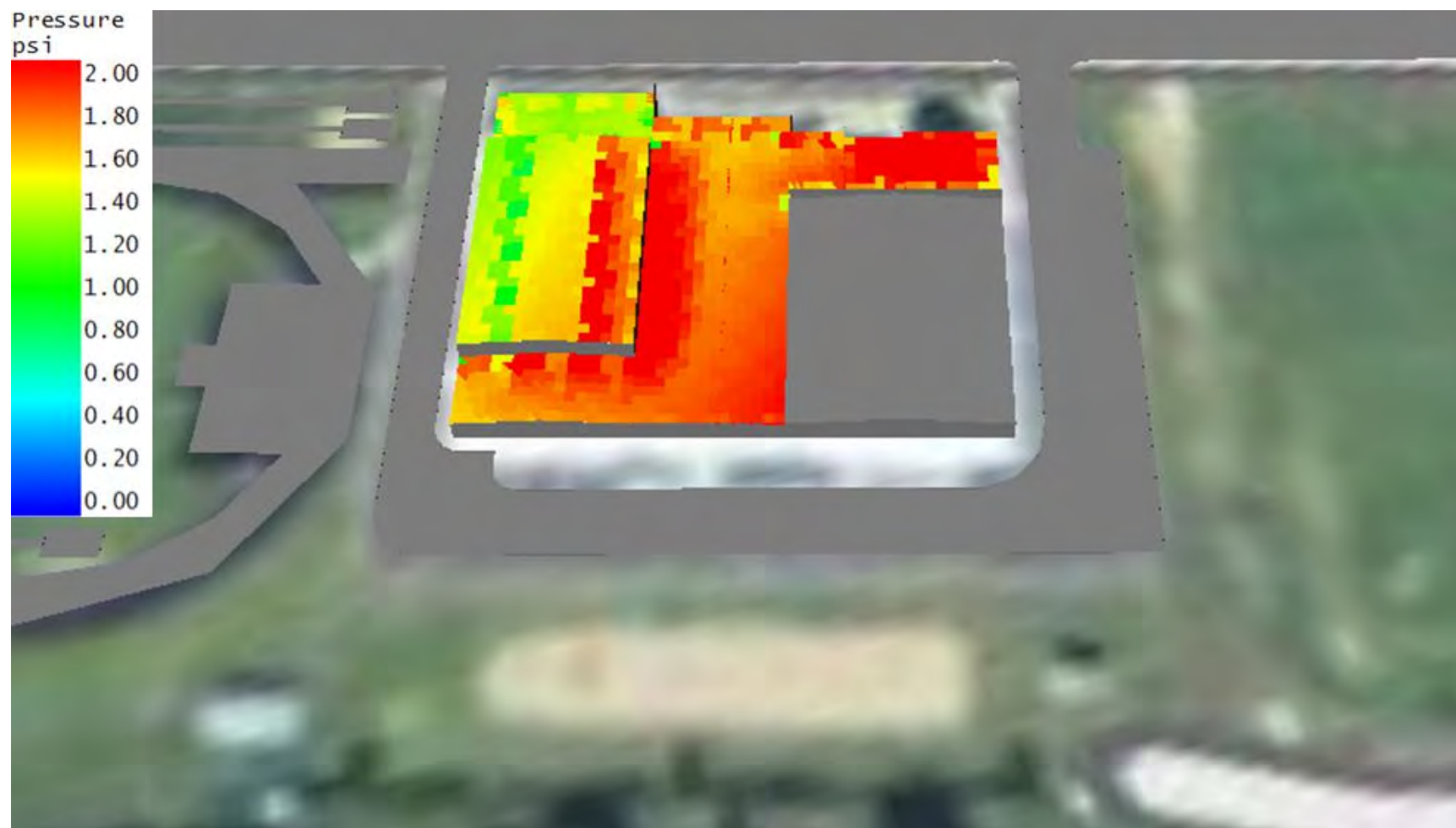


Figure 135. West Intermediate School Applied Pressures (CFD - Portion that Burned not Included)

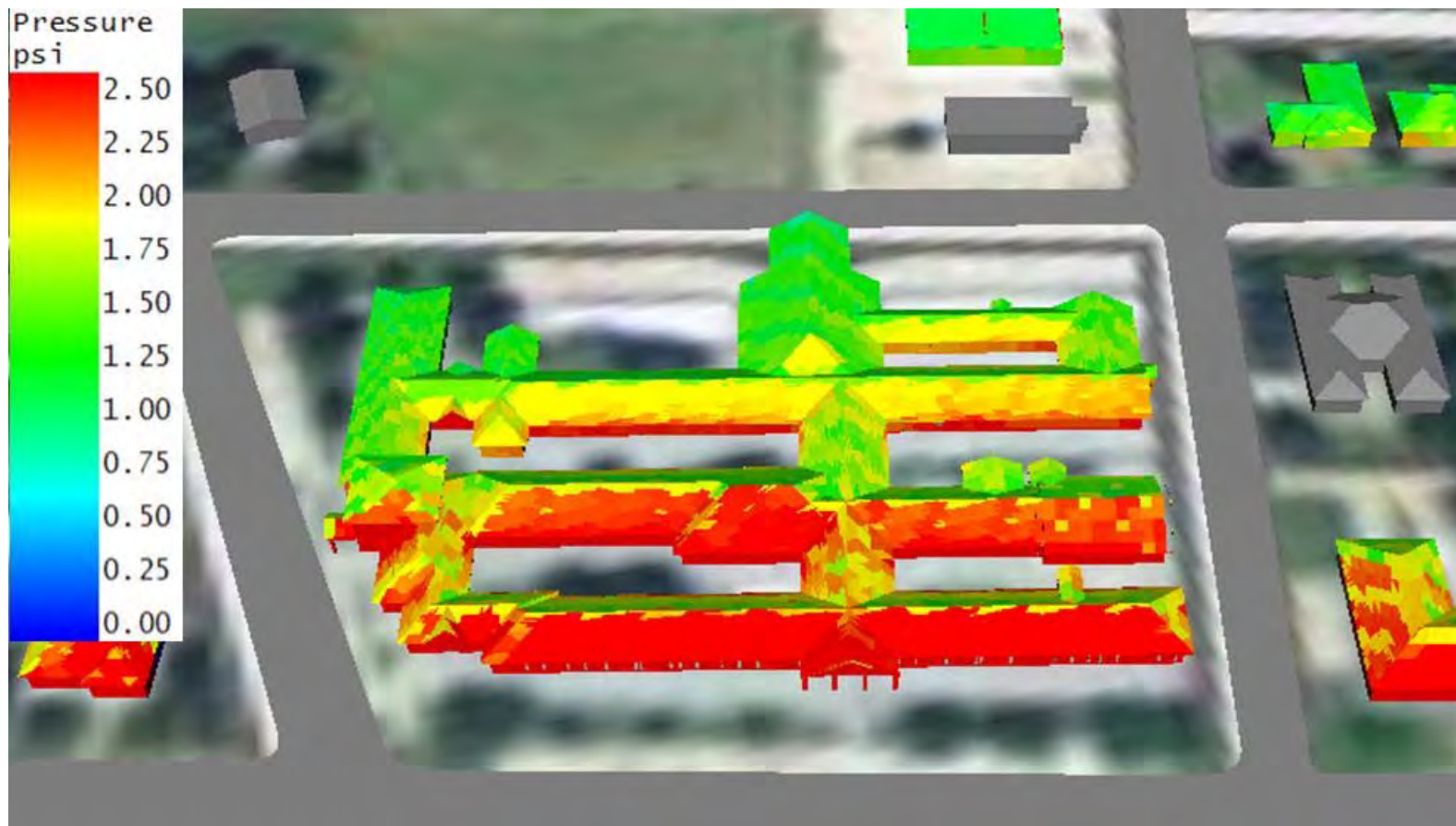


Figure 136. Rest haven Nursing Home Applied Pressures (CFD)

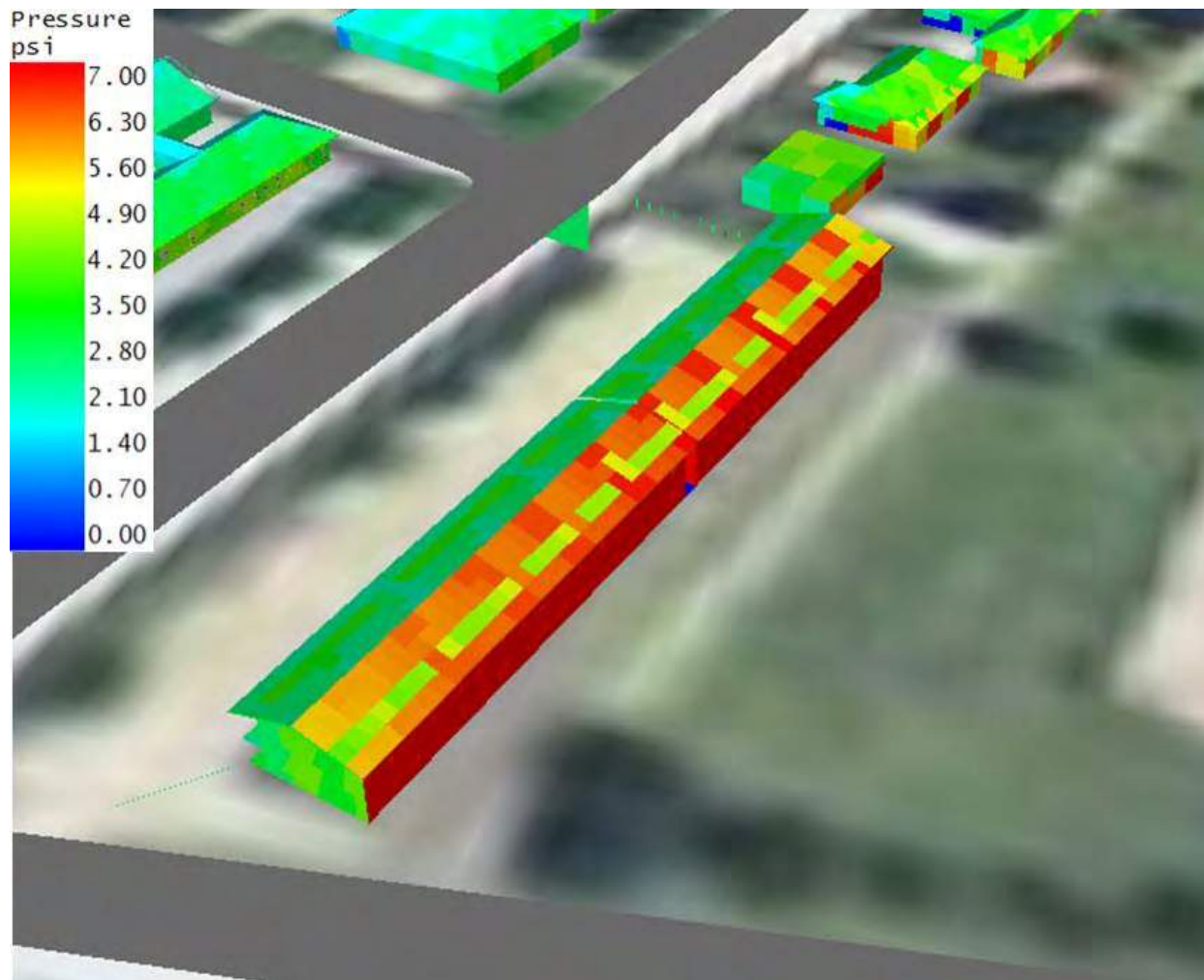


Figure 137. Apartment Complex Applied Pressures (CFD)

7 References

- 1 CSB Contract CSB-13-022, GSA order number GS—10F-0242L. 04/19/2013.
- 2 CSB Contract CSB-13-025, GSA order number GS—10F-0242L, 04/23/2013.
- 3 CSB Contract CSB-13-026, GSA order number GS—10F-0242L, 08/19/2013.
- 4 Chemical MSDSs and Spec Sheets, received from CSB via e-mail on 10-30-2013.
- 5 Production Process and Materials of Construction, received from CSB via e-mail on 10-30-2013.
- 6 Clancey, V.J., The Explosive and fire hazard characteristics of ammonium nitrate fertilizers: Part 1. Introduction and critical literature survey. 1963.
- 7 Biasutti, G.S., History of Accidents in the Explosives Industry. 1985: Corbaz.
- 8 Khan, F.I. and S.A. Abbasi, Major accidents in process industries and an analysis of causes and consequences. Journal of Loss Prevention in the Process Industries, 1999. 12(5): p. 361-378.
- 9 Oxley, J.C., et al., Ammonium nitrate: thermal stability and explosivity modifiers. Thermochemica Acta, 2002. 384(1–2): p. 23-45.
- 10 Munroe, C.E., The Explosivity of Ammonium nitrate. Chemical & Metallurgical Engineering, 1922. 26: p. 535-542.
- 11 Greiner, M., Ammonium Nitrate Fertilizer--exploding the myth. Ammonia Plant Safety (Environmental Sciences & Pollution Management), 1985. 25: p. 1-8.
- 12 Marlair, G. and M.-A. Kordek, Safety and security issues relating to low capacity storage of AN-based fertilizers. Journal of Hazardous Materials, 2005. 123(1–3): p. 13-28.
- 13 Ivanov, Y.A., Fire and Explosion Hazards of Ammonium Nitrate. Foreign Technology Division, 1990: p. 7.
- 14 Thomas, M.J., TERRA CHEMICAL ACCIDENT INVESTIGATION REPORT. U.S. Environmental Protection Agency, 1996: p. 114.
15. Hengel, E.I.V.v.d., et al., Ammonium nitrate behavior in a fire. Loss Prevention Bulletin, 2008(202): p. 19.
16. Dechy, N., et al., First lessons of the Toulouse ammonium nitrate disaster, 21st September 2001, AZF plant, France. Journal of Hazardous Materials, 2004. 111(1–3): p. 131-138.
- 17 Mainiero, R.J. and J.H. Rowland, A review of recent accidents involving explosives transport. 2008: National Institute for Occupational Safety and Health.

- 18 Fedoroff, B.T., *The Encyclopedia of Explosives and Related Items*. Picatinny Arsenal, 1960. 1: p. A311-A340.
- 19 Shaffer, H.B., *Studies in comparative detonation sensitivities*. Fertilizer research, 1987. 14(3): p. 265-273.
- 20 Izato, Y.-i., A. Miyake, and S. Date, *Combustion Characteristics of Ammonium Nitrate and Carbon Mixtures Based on a Thermal Decomposition Mechanism*. *Propellants, Explosives, Pyrotechnics*, 2013. 38(1): p. 129-135.
- 21 Dolah, R.W.V., *Explosion Hazards of ammonium nitrate under fire exposure*. U.S. Dept. of Interior, Bureau of Mines, 1966: p. 79.
- 22 Nygaard, E.C., *Large scale testing of ammonium nitrate*. *The 4th EFEE World Conf. of Explosives and Blasting*, 2007. 4(1).
- 23 King, D.A.W., *Threshold Shock Initiation Parameters of Liquid Phase Ammonium Nitrate*. 2008: p. 26.
- 24 Winning, C.H., *Detonation characteristics of prilled ammonium nitrate*. *Fire Technology*, 1965. 1(1): p. 23-31.
- 25 Miyake, A., et al., *Detonation characteristics of ammonium nitrate and activated carbon mixtures*. *Journal of Loss Prevention in the Process Industries*, 2007. 20(4–6): p. 584-588.
- 26 Marshall, A., *Explosibility of ammonium nitrate*. *Nature*, 1949. 164(4165): p. 348-349.
- 27 Ermolaev, B.S., et al., *Initial stage of the explosion of ammonium nitrate and its powder mixtures*. *Russian Journal of Physical Chemistry B*, 2010. 5(4): p. 640-649.
- 28 Ottoson, K.G., *Investigation of Sensitivity of fertilizer grade ammonium nitrate to explosion*. *Explosibility of Cal-Nitro and uraform-ammonium nitrate fertilizers*. Picatinny arsenal Technical Division, 1948: p. 8.
- 29 Macy, P.F., *Investigation of Sensitivity of Fertilizer Grade Ammonium Nitrate to Explosion*. Picatinny arsenal Technical Division Chemical Branch, 1947(1658): p. 1-49.
- 30 Verrato, P., *Investigation of Sensitivity of Fertilizer Grade Ammonium nitrate to Explosion-Relative sensitivity of pure, Wax-Coated and Fertilizer Grade Ammonium Nitrate*. Picatinny arsenal Technical Division, 1949(1720): p. 26.
- 31 Clancey, V.J., *The Explosive and fire hazard characteristics of ammonium nitrate fertilizers: Part 2 Assessment of the fire hazard*. Royal Armament Research and Development Establishment, 1966. *Explosives Division*(1/66).
- 32 Oommen, C. and S.R. Jain, *Ammonium nitrate: a promising rocket propellant oxidizer*. *Journal of Hazardous Materials*, 1999. 67(3): p. 253-281.

- 33 Ettouney, R.S. and M.A. El-Rifai, Explosion of ammonium nitrate solutions, two case studies. *Process Safety and Environmental Protection*, 2012. 90(1): p. 1-7.
- 34 Sinditskii, V.P., et al., Ammonium Nitrate: Combustion Mechanism and the Role of Additives. *Propellants, Explosives, Pyrotechnics*, 2005. 30(4): p. 269-280.
- 35 Jahrestagung, F.-I.f.C.T.I., et al., *Energetic Materials : Performance and Safety: 36th International Annual Conference of ICT & 32nd International Pyrotechnics Seminar : June 28- July 1, 2005, Karlsruhe, Federal Republic of Germany. 2005: Fraunhofer-Institut für Chemische Technologie.*
- 36 Turcotte, R., et al., Thermal hazard assessment of AN and AN-based explosives. *Journal of Hazardous Materials*, 2003. 101(1): p. 1-27.
- 37 Little, A.D., *Study of Ammonium Nitrate Materials. 1952: p. 1-49.*
- 38 Munroe, C.E., *The Explosivity of Ammonium nitrate. Chemical & Metallurgical Engineering, 1922. 26: p. 535-542.*
- 39 Presles, H.-N., P. Vidal, and B. Khasainov, Experimental study of the detonation of technical grade ammonium nitrate. *Comptes Rendus Mécanique*, 2009. 337(11–12): p. 755-760.
- 40 Cooper, P.W., *Explosives Engineering. 2009: John Wiley & Sons, Incorporated.*
- 41 United States. Headquarters, D.o.t.a., *Explosives and demolitions: FM 5-25. 1994: Paladin Press.*
- 42 Shvedov, K.K., A.I. Kazakov, and Y.I. Rubtsov, Shock-wave sensitivity and self-propagating explosive processes in binary mixtures on the basis of ammonium nitrate with exo- and endothermic transformations of the components. *Russian Journal of Physical Chemistry B*, 2007. 1(6): p. 553-562.
- 43 Keshavarz, M.H., Simple correlation for predicting detonation velocity of ideal and non-ideal explosives. *Journal of Hazardous Materials*, 2009. 166(2–3): p. 762-769.
- 44 Akst, I., *EXPLOSIVE PERFORMANCE MODIFICATION BY COSOLIDIFICATION OF AMMONIUM NITRATE WITH FUELS. US ARMY Picatinny Arsenal, 1976(4987): p. 59.*
- 45 Miyake, A., et al., Influence of physical properties of ammonium nitrate on the detonation behavior of ANFO. *Journal of Loss Prevention in the Process Industries*, 2001. 14(6): p. 533-538.
- 47 ASTM F1642-12, *Standard Test Method for Glazing and Glazing Systems Subject to Airblast Loadings.*
- 48 Department of the Army, “Estimating Damage to Structures from Terrorist Bombs Field Operation Guide”, Engineer Technical Letter 1110-3-495. U.S. Army Corps of Engineers, Washington, DC 20314-1000, 14 July 1999.

- 50 CEBAM, Computational Explosion & Blast Assessment Model, ACENG, San Antonio, TX 2005
- 51 J. Keith Clutter (a), Robert T. Luckritz (b), “Comparison of a reduced explosion model to blast curve and experimental data,” Journal of Hazardous Materials A79 2000 41–61, a) Analytical and Computational Engineering, Inc., P.O. Box 809, Helotes, TX 78023, USA b) QAnalytics, Mountain Lakes, NJ, USA, Elsevier Press, accepted 16 February 2000.
- 52 J. Keith Clutter (a), Mark G. Whitney (b), “Use of computational modeling to identify the cause of vapor cloud explosion incidents,” a) College of Engineering, University of Texas at San Antonio, 6900 North Loop 1604 West, San Antonio, TX 78249, USA b) EQE International, Inc., San Antonio, TX, USA, Journal of Loss Prevention in the Process Industries 14 (2001) 337–347, Elsevier Press, 2001.
- 53 ETL 1110-3-495, “Estimating Damage to Structures from Terrorist Bombs Field Operations Guide”, U.S. Army Corps of Engineers, 14 July 1999.
- 54 Single-Degree-of-Freedom Blast Effects Design Spreadsheets (SBEDS), V5.0, December 2012.
- 55 Departments of the Army, Air Force, and Navy and the Defense Special Weapons Agency, "Design and Analysis of Hardened Structures to Conventional Weapons Effects", TM 5-855. Washington, DC, Headquarters, Departments of the Army, Air Force, and Navy and the Defense Special Weapons Agency, August 1998.
- 56 Biggs J.M., Introduction to Structural Dynamics. New York: McGraw-Hill Book Company. 1964.
- 58 Departments of the Army, the Navy, and the Air Force, “Structure to Resist the Effects of Accidental Explosions,” United Facilities Criteria (UFC) 3-340-02, 5 December 2008.

Appendix A Community Structure Damage Survey Summary

West High School



West Fertilizer Co.

West High School

- **Construction:**

- Walls: load bearing and non-load bearing CMU with a brick veneer.
- Roof: various open web steel joists through out the building that support a built up steel deck.





Damage Assessment

Auditorium



Damage Assessment

Commons



Damage Assessment

Band Rooms



Damage Assessment

Front Foyer



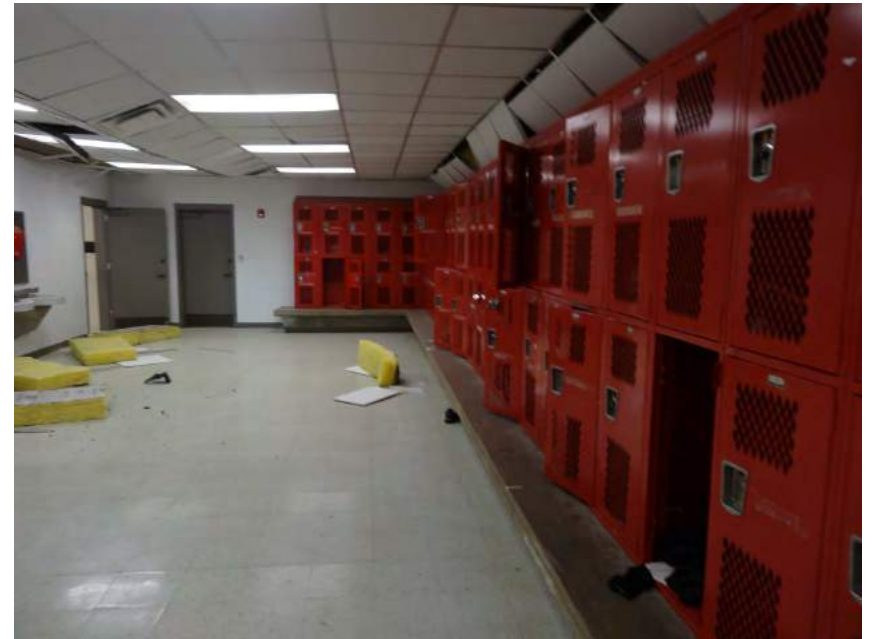
Damage Assessment

Gym #1



Damage Assessment

Main East-West Hallway



Damage Assessment

Gym #2



Damage Assessment

Roof Slope



West Intermediate School



West Fertilizer Co.

West Intermediate School

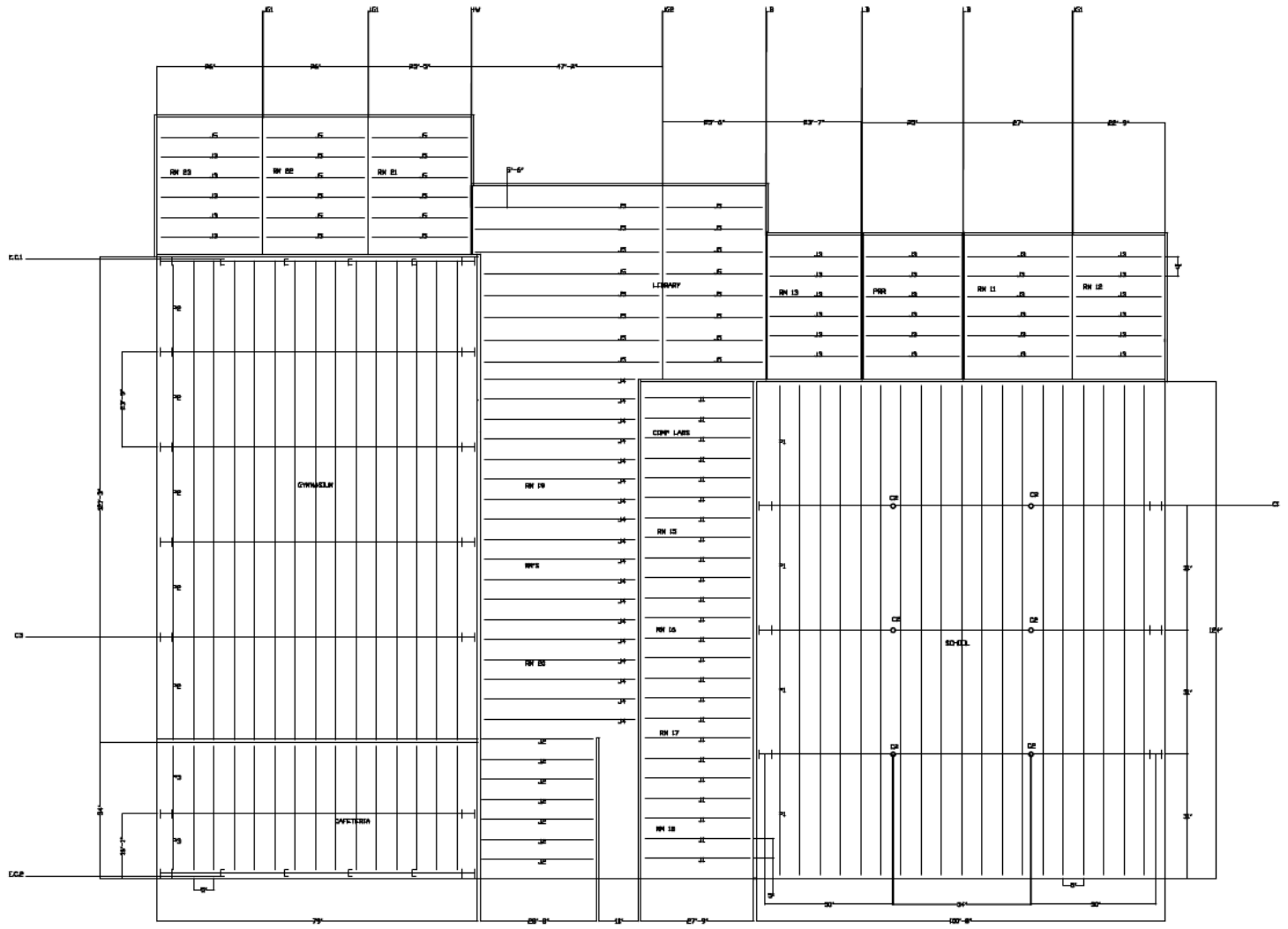
- Construction:

- Walls: load bearing and non-load bearing pre-cast walls.
- Roof: various open web steel joists through out the building that support a built up steel deck.



D-12

NOTES
 FRAME:
 C1 See Attached
 C2 See Attached
 C3 See Attached
 FLOOR:
 F1 SEE PLAN, 10'-0" TO 10'-0" F., RHP-F-8
 F2 SEE PLAN, 10'-0" TO 10'-0" F., RHP-F-8
 F3 SEE PLAN, 10'-0" TO 10'-0" F., RHP-F-8
 GROUND:
 G1 SEE GIBBY, D-80
 JOIST:
 J1 LINDSAY, LINDSAY & CO. INC.
 J2 LINDSAY, LINDSAY & CO. INC.
 J3 LINDSAY, LINDSAY & CO. INC.
 J4 LINDSAY, LINDSAY & CO. INC.
 LOAD BEARING WALL:
 LB
 EXTERIOR COLUMN:
 EC1 COLUMN, 10'-0" DIA.
 EC2 COLUMN, 10'-0" DIA.
 EC3 COLUMN, 10'-0" DIA.



Damage Assessment

Outside



Damage Assessment

Cafeteria



Damage Assessment

Computer Lab 2



Damage Assessment

Existing School



Damage Assessment

Gym



Damage Assessment

Library



Damage Assessment

Office Area



Damage Assessment

Room 11



Damage Assessment

Room 12



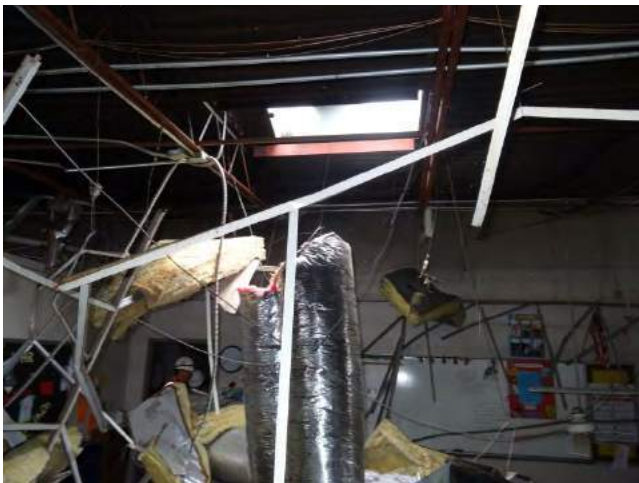
Damage Assessment

Room 13



Damage Assessment

Room 15



Damage Assessment

Room 16



Damage Assessment

Room 17



Damage Assessment

Room 18



Damage Assessment

Room 19



Damage Assessment

Room 20



Damage Assessment

Room 21



Damage Assessment

Room 22



Damage Assessment

Room 23

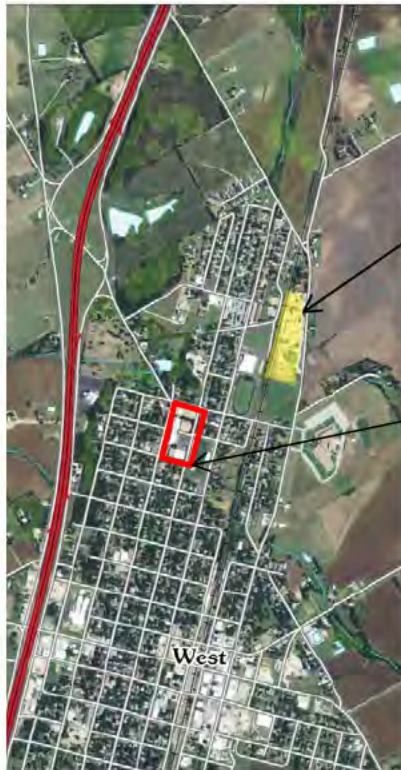


Damage Assessment

Transition Building



West Middle School



West
Fertilizer Co.

West Middle
School

- Construction:

- Walls: load bearing and non-load bearing CM walls with brick veneer.
- Roof: various open web steel joists through out the building that support a built up steel deck.

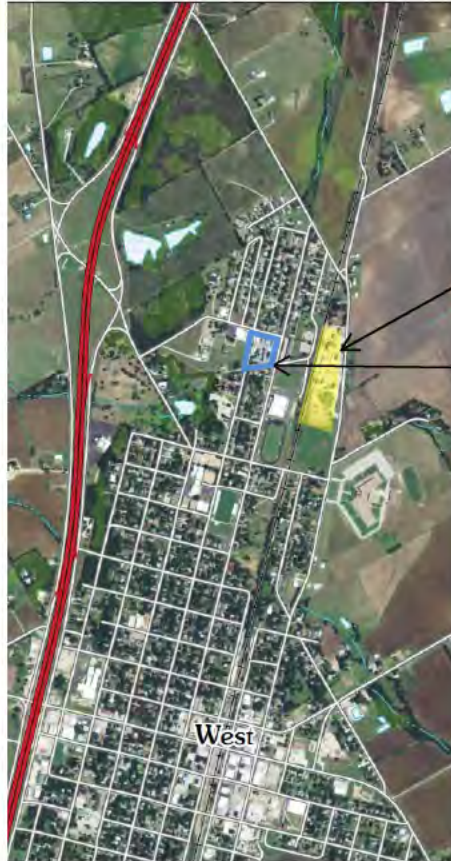


Damage Assessment

Outside Perimeter



West Nursing Home



West
Fertilizer
Co.

Nursing
Home

- Construction:

- Walls: wood stud wall & brick veneer
- Roof: wood roof truss



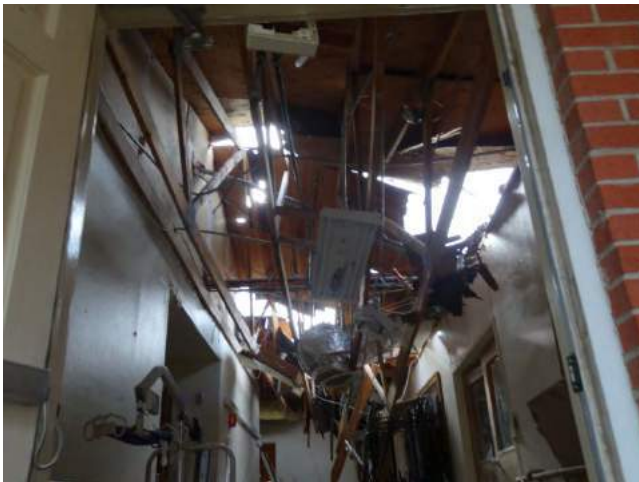
Damage Assessment



Damage Assessment



Damage Assessment



Damage Assessment



Damage Assessment



Emergency Medical Service



West
Fertilizer
Co.

Emergency
Medical
Service

- **Construction:**

- Steel framed building with purlins supporting a metal deck and girts spanning between framed sections.



Damage Assessment



Damage Assessment



Damage Assessment



West Administration Building

West
Fertilizer
Co.

- Construction:
 - Walls: wood stud wall & brick veneer
 - Roof: wood roof truss

Emergency
Medical
Service



Damage Assessment

